Politecnico di Torino

Porto Institutional Repository

[Doctoral thesis] Electric and Hybrid Vehicles With Two Prime Movers

(Article begins on next page)
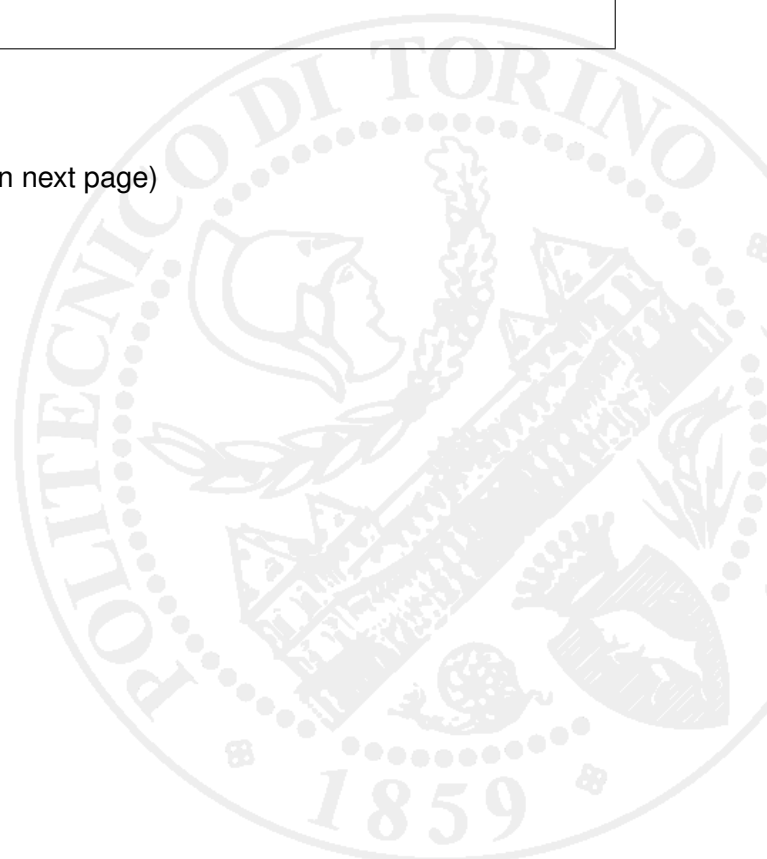
POLITECNICO DI TORINO

SCUOLA DI DOTTORATO
Dottorato in Meccatronica - XXV ciclo

Tesi di Dottorato

Electric and Hybrid Vehicles With Two Prime Movers

Analysis and Torque-Split Strategies for Energy Consumption Optimization

Leonardo Altieri

Tutore	**Coordinatore del corso di dottorato**
Ing. Nicola Amati	Prof. Giancarlo Genta

25 Febbraio 2013

to my parents Silde and Igor and to my grandparents Maria and Gino...

Contents

List of Figures

List of Tables

Acknowledgments

I dedicate this thesis to my parents Silde and Igor and my grandparents Maria and Gino for the teaching and the support during all my studies. Without their help it would have been impossible for me to achieve this target. A particular mention goes to my faculty advisor ing. Nicola Amati and to prof. Andrea Tonoli for their competence and availability during my period at the Mechatronics Lab of the Politecnico di Torino.

Chapter 1

Introduction

1.1 Background

The importance of reducing emissions and energy consumption of the vehicles for individual mobility is continuously growing, particularly considering the increasingly chaotic urban context. The increase of global warming problems due air pollution is determining a dramatic growth of the importance of reducing the CO_2 emissions due to human activities. Furthermore, a significant percentage (20-25%) of them comes from transport [1] and the reduction of world oil resources is leading to a continuous increase of the price of fossil fuels. Therefore the importance of reducing fuel consumption in automotive field is and will be a key factor of the development of the future vehicles. To achieve this target, different solutions start to be adopted and probably will be strongly developed in the next future. Taking into account that the different possible solutions are related to the specific usage of the vehicle, the simplest classification of the different types of passenger vehicles can be based on their average usage:

- Urban vehicles: small and light vehicles specifically designed for urban context. They are required to have low or zero emissions in order to improve the air quality of congested city centers and to guarantee the mobility in case of traffic blocks. On the other hand, the typical usage of this kind of vehicle is the so called systematic transport, mainly the daily journey from house to work. A large amount of statistical analysis about the urban transport demands is available. In [2] the average usage of transportation in Italy is analyzed: the average distance traveled every day to reach the studying or working place is showed to be less than 60 km for 89.7% of the active people, and 86.5% of them use a transport. For these reasons, a limited autonomy of about 100 km can be considered enough for a small urban vehicle. A possible solution might be a small full electric vehicle, which can be generally

recharged during the night, in order to be ready for the next day.

- Traditional vehicles: in this case, a bigger autonomy is needed, in order to allow long extra urban journeys too, without too many stops for refueling. To aim these purposes, an autonomy higher than 400 km is normally required. A possible solution might be an hybrid vehicle, where a traditional internal combustion engine is coupled with an electric motor, in order to maximize the powertrain efficiency and to provide the required autonomy, that a the moment cannot be guaranteed by the available battery technologies in full electric vehicles.

Of course, a minimization of the energy consumption can be reached with an optimization of the whole vehicle, taking into account both the powertrain and all the factors that generates a resistant force to the vehicle motion, like the aerodynamics, the mass, the tires rolling resistance, the mechanical efficiency of the driveline. Furthermore, thanks to the presence of an electric motor, a regenerative braking strategy can be adopted in order to recharge the battery, recovering part of the kinetic energy of the vehicle, rather than dissipating it with the traditional passive brakes. The amount of energy that can be regenerated depends on the driving cycle and can be significant in case of urban driving, with frequent start and stop maneuvers and low average speed.

High fidelity simulation models of the whole vehicle are essential to develop and optimize the driving strategies for both electric and hybrid powertrains, especially taking into account vehicles having two prime movers, where the optimization of the torque-split strategies is fundamental to maximize the global efficiency of the powertrain. Furthermore, the models must be able to take into account all the limitations to the maximum performance of each component of the powertrain. This is required to individuate the most critical components and to drive their optimal sizing. In addition, a reliable evaluation of the efficiencies, dissipation and energy flows through the different components of the powertrain is crucial to evaluate the whole efficiency, in order to setup the optimal control strategies.

In the following chapters, simulation models of both full-electric and hybrid vehicles are presented. The guideline of this thesis is the optimization of the powertrain of two different vehicles, a full-electric (FEV) and an Hybrid-Electric Vehicle (HEV), both using two prime movers, with similar simulation models and methodology.

1.2   Small urban full-electric vehicles

Small electric vehicles seem to be the best solution for individual urban mobility, because the absence of local emissions and the efficiency of the electric motors with

respect to the traditional internal combustion engines. The energy density of fuel (gasoline or diesel oil) is very high (12.7 kWh/kg) if compared to state of the art Li-ion batteries (about 150-220 Wh/kg). In order to achieve enough travel range with affordable weight and cost, a very accurate optimization of the whole EV powertrain system must be performed to maximize the efficiency of the vehicle. Rare earth permanent magnet electric motors are gaining more and more success relative to more conventional asynchronous or reluctance motors because of their higher power and torque density, together with a very high efficiency (about 90%). This comes with a higher cost. The optimization of the powertrain in accordance with the driving cycles is a key issue of EVs design. In fact, a more efficient powertrain means less losses and, therefore, a reduced demand of energy storage, which implies a weight reduction and/or travel range increase.

A number of simulation programs for design and optimization of electric and hybrid powertrains can be found in the literature. One of the most known, called Vehicle Simulation Program (VSP), has been realized by Van Mierlo [3, 17], creating a series of pre-defined Matlab-Simulink components that can be assembled and modified by the final user. Different kinds of batteries and electric motors are available and the respective empirical models are based on experimental data. The vehicle performances, energy consumption and exhaust pollutions can be computed. Successively, an evolution of that model have been realized by Butler [5] with a more flexible software with pre-defined models of the components, based on look-up tables, steady-state or dynamic equations, and the possibility to create personalized components. Different vehicle configurations (ICE, Hybrid and Full-electric) and driving cycles can be considered, comparing the performances of the different solutions. Fellini and Michelena [6] and by Kromer and Heywood [7] investigated the performances, the energy consumption and the emissions of different hybrid powertrains by means of another Matlab-based simulation program dedicated to hybrid vehicles (ADVISOR) [8]. The efficiency of the electric motors has been included more in detail in [9] by mean of empirical look-up tables, as function of the motor speed and torque, including maximum torque and power limitations. Van Mierlo [10, 11] realized an evolution of his VSP, considering the limitation of the powertrain system as maximum torque, angular speed and power, with more sophisticated models used for energy sources and strategies of power splitting between ICE and electric motor for hybrid vehicles. Rizzoni [12, 13, 14] presented some innovative control strategies for energy management in hybrid vehicles, in order to minimize the fuel consumption. Look-up tables are adopted to represent the steady-state efficiency or the ICE and electric motors for the different working conditions.

A new model of a full electric vehicle is presented in the present work, including a model of the electric motor that takes the copper, iron, bearings and winding

losses into account. The parameters of the model and thermal effects on the copper and iron losses have been identified from the data sheet of the motor, in order to match the estimated efficiency map with respect to experimental data, provided by the manufacturer in steady state conditions. Limitations on the peak driving current of the motor, maximum angular speed and temperature have been included in the model. To avoid short circuits of the windings or demagnetisation the motor, temperature is fed back to the motor controller that decreases the current if the temperature gets too high. The power is limited in this way by the thermal dynamic behavior and not by an explicit limitation to the instantaneous, as presented in the literature. This is a more realistic model of the power limitation implemented in drives for traction application that allows to overload the motor for short transient, provided the temperature is in the safe operating area. When the thermal limitation occurs, the continuative power that the motor can generate is exactly the maximum continuative power of the data sheet.

In this thesis, also an motor/s sizing optimization procedure, based on the simulations, is reported. A powertrain with one or two electric motors have been analyzed, with two different strategies for power splitting between them. Another optimization parameter is the transmission ratio between motor and wheel. Simulations have been performed considering different urban cycles, with minimum requirements on hill start and hill traveling capability. Basic performance indexes, such as maximum acceleration and speed, have been included along with the energy consumption. Finally, the configuration that meets all the specifications and minimizes the fuel consumption has been identified. In this first release of optimization procedure, the batteries are not taken into account to explore only the effects of electric motors, torque split strategies and transmission ratio.

1.3 Hybrid vehicles

At the moment, the available battery technologies do not allow to store the required amount of energy, with reasonable cost and weight, to have a full-electric vehicle with the minimum desired autonomy of about 400 km, requested for general-purposes vehicles for urban and extra-urban travels. This limit can be reasonable, considering a typical traditional small citycar optimized for the urban usage, but able to extra-urban travels too. The most promising way to improve the efficiency of the vehicles, minimizing fuel consumption and emissions especially in urban context, seems to be the adoption of an hybrid electric powertrain (HEV), where a traditional Internal Combustion Engine and an Electric Motor can be used together.

In literature, a huge number of different types of hybrid vehicles can be found. The most known and accepted classification [38, 39, 41], related to the coupling

architecture between the internal combustion engine (ICE) and the electric motor, is:

- Series hybrid: is primarily an electric vehicle with an on board battery charger and only the electric motor is mechanically coupled to the transmission and the wheels. The efficiency can be maximized [41] because the engine can work at its maximum efficiency to recharge the battery. But it requires major powertrain modification with respect to the traditional pure-ICE vehicles. In addition, the maximum power of the powertrain is limited by the electric motor and the power of the ICE cannot be added, because it is not mechanically coupled with the transmission.

- Parallel hybrid: both the ICE and the electric motor are mechanically connected to the transmission and the vehicle can be driven with the ICE, the electric motor or both, choosing the torque-split combinations to maximize the powertrain efficiency [44]. The torque-split strategy can be chosen to minimize the fuel consumption or emissions and, in addition, to obtain the maximum vehicle performance adding the torques generated by the two prime movers. It seems to be the most promising solution at reasonable costs. It is used by the Honda Insight with its Integrated Motor Assist (IMA) system, where a 10kW brushless permanent magnet electric motor is integrated with the engine crankshaft and therefore they cannot be decoupled.

- Series/Parallel hybrid: a combination of series and parallel configurations. By means of a more complex mechanical coupling between the prime movers, at any time a series or parallel configuration can be chosen, maximizing the flexibility and the potentialities of the hybrid powertrain. It is used by the famous Toyota Prius [48], where a power-split mechanical device allow to choose the hybrid powertrain configuration. It is an effective solution, but generally more complex and expensive [45, 46, 47] than the other configurations.

Thanks to the power flow control that hybrid vehicles allow, especially the parallel and the more complex series/parallel configurations, it is possible to configure the powertrain and the control strategy to optimize the fuel consumption, emissions, costs or performance [38]. The most promising solution is the usage of a parallel hybrid, with the electric motor directly integrated between the clutch and the gearbox primary shaft (ZF Friedrichschafen AG, Nissan/Ichimura Industrial Award 2012). It requires significant mechanical modifications to the gearbox to allow the coupling with the dedicated electric motor, but the engine can be decoupled simply disengaging the clutch, allowing the full-electric driving mode without the engine resistant torque in over-running mode. Furthermore, another additional classifications of the possible hybridization level of passenger cars [40] is:

- Micro-hybrids: parallel hybrids where the electric motors are not used to move directly the vehicle but are used as generators for regenerative braking, to recharge the battery, and usually employ start&stop strategies in order to switch off the engine during vehicle stops.

- Mild-hybrid: parallel hybrids where the electric motors can be used to move the vehicle but their power and the amount of stored energy is not sufficient to move the vehicle without the traditional ICE. Also regenerative braking and start&stop strategies are implemented.

- Full-hybrid: parallel hybrids with electric motors able to move the car, mainly at low speed and during starting maneuvers, but with a low amount of stored energy into the batteries.

- Series hybrid: actually full electric vehicles with an ICE demanded only to recharge the battery.

The first aim of this project is the analysis and evaluation of the performance that can be achieved with a parallel-hybrid powertrain system on a small urban vehicle, where the coupling between a small electric motor and the traditional ICE must be realized minimizing the structural modifications and costs with respect to the traditional vehicle. For this reason, the traditional alternator was substituted with a motor/alternator, connected to the ICE crankshaft by means of a simple belt transmission, avoiding heavy modifications of the engine and the gearbox. The second aim of the activity is the evaluation of the most critical aspects of this powertrain topology, identifying the possible solutions that can be adopted to improve its performance, mainly in terms of efficiency and fuel consumption on the most commonly used driving cycles.

The optimization of the torque-split strategies and the energy flows and losses between every component of the powertrain are the key factors to minimize the emissions and to maximize the autonomy and the performance of the car. As mentioned in paragraph 1.2, a number of simulation programs for hybrid and electric powertrains are available in literature. Despite this, during this thesis work, a new whole vehicle and powertrain model was realized in Matlab/Simulink environment, in order to model and analyze the vehicle with:

- The maximum flexibility in building the topology of the whole powertrain system: as each typical applied-research activity, different topologies of the powertrain system must be implemented and analyzed.

- No limitations due to the limited types and number of the available components on-the-shelf: usually, the dedicated codes have a huge number of predefined components that can be chosen and connected together to build

the whole vehicle model. But usually, to build self-made components can be demanding, for example for the implementation of the new electric motor model introduced in paragraph 1.2.

- Not in every company all the dedicated codes are available. Instead, generally speaking, Matlab/Simulink is commonly used almost everywhere. Furthermore, during the model and control strategies development, no dedicated toolboxes were used: in this way, the model can be used just with the simplest Matlab/Simulink license.

In this case, differently from the analysis of the full-electric vehicle, also the battery system is modeled in order to evaluate both its state of charge (SOC) and the dissipated energy. The model presented by Tremblay, Dessaint and Dekkiche [35] was chosen and implemented: it is a simple but accurate model, that allows to evaluate both the SOC and energy dissipation and it does not require a huge amount of specific battery data, still not available at this early phase of the project. This is crucial, in parallel with the evaluation of the efficiencies of each component of the hybrid powertrain, in order to define the optimal torque-split strategy between the two prime movers and to evaluate the amount of energy that can be regenerated during the braking phases.

In addition, two different models of the electric motor were implemented and can be selected by the user:

- A simple empiric model: with the static efficiency-map and the maximum driving and braking torque of the motor, implemented by means of look-up tables.

- The analytical model presented in paragraph 1.2, taking into account also the thermal effects on the energy dissipation and efficiency.

In both cases, the electric motor temperature is evaluated and its maximum possible temperature is used as an additional limitation for the motor performance.

The key factor for the optimization of an hybrid powertrain is the torque-split strategy between its prime movers. Different torque-split strategies can determine a strong difference in the usage of the electrical components, with remarkable differences in the electrical energy dissipation and motor temperatures. A number of different torque-split strategies ideas are available in literature [41], based on rules [18], fuzzy logic (conventional [20, 42], adaptive and predictive [43]), optimization based algorithms and so on, for the minimization of the different kinds of typical pollutants generated by a typical automotive ICE, like NO_x, HC, CO, CO_2 and fuel consumption. The aim of this analysis was a preliminary study of the proposed parallel topology, determining the most critical aspects of the whole

system. For this reason, the fuel consumption on the homologation New European Driving Cycle (NEDC) is considered as the reference aspect. The effective, simple and intuitive fuzzy-logic based torque-split strategy concept, presented by Salman, Schouten and Kehir [20] is used as a reference and adapted to the specific case. Its performance are evaluated and compared with other simplified strategies, while the fuel consumption of the same vehicle with a pure ICE powertrain is considered as the reference. Successively, the effects of the main powertrain parameters are quantified, in order to determine the most critical aspects of the proposed topology. A sensitivity analysis of the thermal parameters of the electric motor is realized to better drive the sizing of the motor and the robustness of the strategies to the thermal performance of the motor. Furthermore, the need of a full-electric driving mode and the performance of the strategies on different driving cycles are evaluated. Finally, the most critical aspects of the proposed topology are individuated and some possible improvements are proposed.

Chapter 2

Modeling and powertrain optimization of an urban full-electric vehicle

2.1 Full-electric vehicle model overview

The general structure of the model of a full-electric vehicle that has been adopted is reported in Figure 2.1.1.
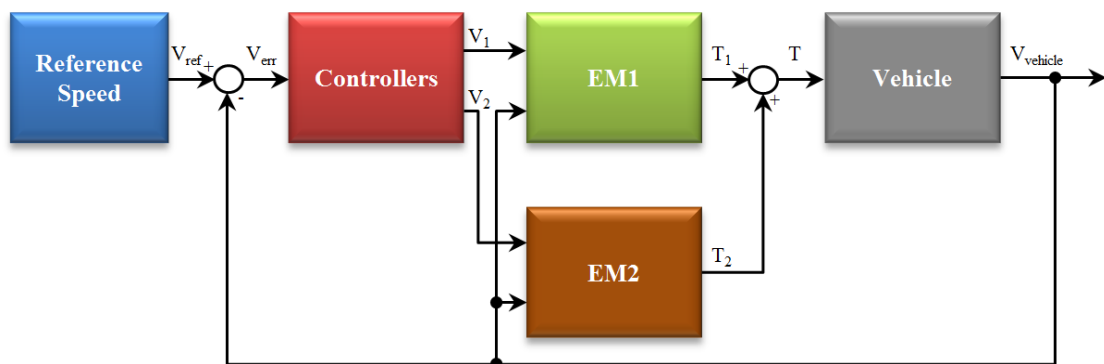
Figure 2.1.1: Model of the full-electric vehicle

The input of the model is the desired vehicle speed profile, like the standard homologation driving cycles commonly used to evaluate fuel consumptions and emissions of internal combustion engine vehicles. A controller drives the electric motors as function of the error between the reference and real speed of the vehicle to follow the desired profile. The electric motors are voltage-driven and the generated torque is provided to the vehicle. Each subsystem model is described in the

9

following paragraphs.

2.2 Vehicle model

The aim of this work is the optimization of the electric powertrain of a small urban vehicle. The vehicle model must therefore represent only longitudinal dynamics, while the lateral ones can be disregarded. The coupling between longitudinal dynamics and vertical and pitching motions is neglected because of the relatively small accelerations involved in most real and homologation driving cycles and the small frequencies involved in cycle tracking. Similarly higher order dynamics related to the powertrain, or the longitudinal behavior of the suspensions is not considered for the same reason. The tires are modeled with their rolling resistance, other effects such as the longitudinal slip and the torsional stiffness are not considered because the small accelerations involved in the driving cycles involve a relatively small longitudinal tire friction coefficients. These effects may be important for maximum acceleration maneuvers in configurations with the highest wheel torque. For this reason the wheel torque is compared with the maximum transmissible torque, including the effect of the load transfer. This simplified approach is motivated by the fact that full throttle acceleration is considered just for a rough estimate of the maximum acceleration, but it will not be included in the energy consumption analysis.
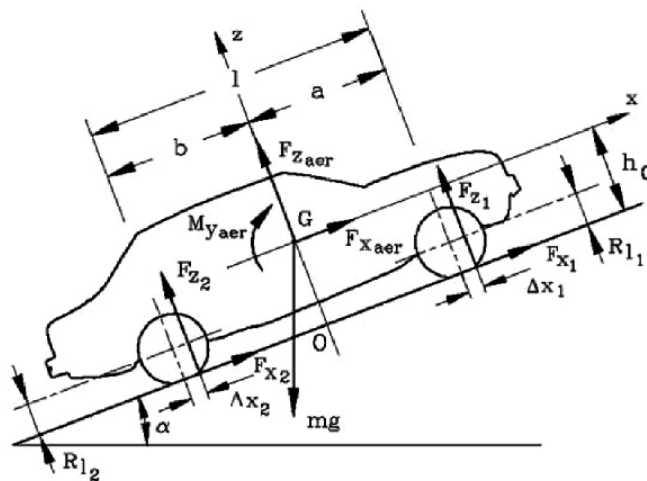
Figure 2.2.1: Forces acting on a vehicle moving on an inclined road

The above assumptions lead to a very simple one-dimensional vehicle model, reported in Figure 2.2.1 including the following effects:

- Inertia force (in terms of a single equivalent mass of the vehicle)

- Aerodynamic drag

- Rolling resistance

- Grading resistance (due to ground slope)

The main parameters of the vehicle are listed in Table 2.2.1 along with the associated symbols. Considering the above assumptions, the equation of motion of the vehicle can be expressed as function of the angular speed of the electric motor:

$$J_{eq}\dot{\omega} = T_{EM} - \frac{r_L}{\tau_T}\left[\omega^2\left(\frac{r_L}{\tau_T}\right)^2\left(\frac{1}{2}\rho C_x S + KMg\cos\alpha\right) + Mg\left(\sin\alpha + f_0\cos\alpha\right)\right]$$
(2.2.1)

Where the equivalent inertia of the vehicle reported to the electric motor shaft is:

$$J_{eq} = J_{ME} + M\left(\frac{r_L}{\tau_T}\right)^2 + 4J_W\frac{1}{\tau_T^2}$$
(2.2.2)

The torque generated by the electric motors (T_{EM}) is computed in the following sections considering the motor electrical and thermal behavior.

	Parameter		Value
M	Whole vehicle mass (with 3 passengers)	$[kg]$	925
J_W	Wheel inertia	$[kgm^2]$	0.31
J_{EM}	Electric motor inertia	$[kgm^2]$	$1.4 \cdot 10^{-2}$
r_L	Wheel loaded rolling radius	$[m]$	0.33
S	Vehicle frontal area	$[m^2]$	2
C_x	Vehicle drag coefficient	$[-]$	0.35
f_0	Tire rolling coefficient	$[-]$	0.013
K	Tire rolling resistance coefficient	$[s^2/m^2]$	$6 \cdot 10^{-6}$
τ_T	Transmission ratio (wheels-electric motor)	$[-]$	T.B.D.

Table 2.2.1: Vehicle parameters

2.3 Electric motor model

Brushless permanent magnet electric motors have been considered in this study. They are one of the most commonly adopted solutions for recent powertrains because their high efficiency, reliability, and better power density in comparison with brushed DC and induction motors. By converse, they cannot be easily defluxed

so for high speeds they require high input voltages. Additionally, their higher cost and the shortage of rare earth materials hinders sometimes their technical advantages.

Several models of permanent magnets synchronous electric motors are available in the literature to describe their behavior in different conditions. The simplest model that can take into account of the motor characteristics has been adopted in the present study: i.e. a mono-phase equivalent, as represented in Figure 2.3.3 [13]. Inductance L_a and resistance R_a represent the inductance and the resistance of the copper winding, L_f and R_f in parallel to the back electromotive force V_{EMF} takes the iron losses into account.

The dynamic equations that regulate the behavior of the electric motor are written in terms of magnetic flux linkages λ_a and λ_f in inductance L_a and L_f. Considering that the back electromotive force is related to the angular speed ω through the motor torque constant $V_{EMF} = K_m\omega$:

$$\begin{cases} \lambda_a &= V_{inv} - R_a\frac{\lambda_a}{L_a} - K_m\omega \\ \lambda_f &= K_m\omega - \frac{R_f}{L_f}\lambda_f \end{cases} \tag{2.3.1}$$

Where V_{inv} is the input voltage. The torque generated by the motor can be expressed as function of the flux linkages as:

$$T_m = K_m i_3 = K_m \left(\frac{\lambda_a}{L_a} - \frac{\lambda_f}{L_f}\right) \tag{2.3.2}$$
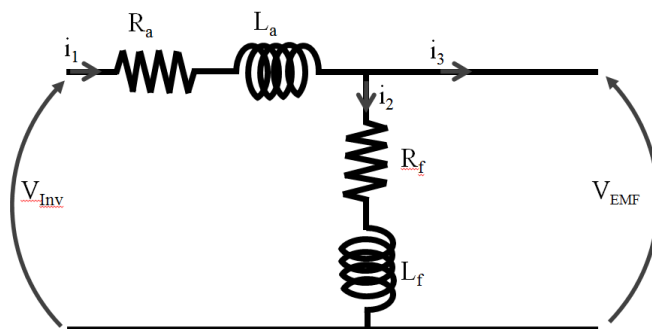
Figure 2.3.1: Electrical model of electric motor

The inputs in the motor subsystem are voltage V_{inv}, supplied by the inverter and the angular speed ω, that is the vehicle output in response to the motor torque.

The heating of the motor due to the dissipated power increases the resistivity of the copper, and hence, resistance R_a. This modifies the motor efficiency in a sort

of internal feedback effect. The temperature increase should be kept under given limits to avoid demagnetisation or short circuits in the winding. This is usually done in industrial applications in a feed-forward approach by limiting the current or, better, the time-current integral (which is related to the energy). This choice does not seem to be very convenient in automotive applications because of the large margins that would be necessary because of the wide range of environmental conditions and mission profiles that characterize such application. An alternative is to have a feed back loop that reacts to excessive temperatures by saturating the current request. This approach gives better possibilities to adapt the powertrain to the driving cycle and operating conditions, without sacrificing too much in terms of weight to torque ratio of the motor.

The importance of the temperature dynamics motivates the inclusion of a thermodynamic model of the motor. The effects of the temperature ϑ on the copper resistance can be approximated with a linear relationship:

$$R_a = R_{a0} \left(1 + \alpha \, \delta\vartheta\right) \tag{2.3.3}$$

where R_{a0} is the resistance at the reference temperature ϑ_0, $\delta\vartheta$ is the difference between the actual and reference temperature, and α is a empirical constant depending on the motor characteristics ($\alpha = 0.00392 \, \Omega/°C$ for the motors considered in the present study).

The variation of the motor resistance due to the thermal effects leads to a parametric variation in the otherwise linear model of Equation 2.3.1. Substituting Equation 2.3.3 in the first of Equation 2.3.1:

$$\lambda_a = V_{inv} - R_{a0}\frac{\lambda_a}{L_a} - V_\vartheta - K_m\omega \tag{2.3.4}$$

voltage drop V_ϑ could be referred to as thermal drift voltage drop that leads to a nonlinear coupling between thermal and electrical dynamics

$$V_\vartheta = \alpha \, \delta\vartheta \, R_{a0}\frac{\lambda_a}{L_a}. \tag{2.3.5}$$

It has been implemented in the block diagram of the electric motor model of Figure 2.3.3 as an additional block named "temperature effects". This block first computes the temperature and then feeds back the related thermal drift voltage V_ϑ, as given by Equation 2.3.5.

The choice of concentrating the nonlinearity in a separate block allows linearizing the model (for frequency analysis, for example) by simply setting a constant temperature, or, more drastically, by opening the nonlinear feedback.

The thermal model is based on the assumption that the motor temperature is affected by the power dissipated in it because of the resistive and mechanical

losses:

$$P_{diss} = P_R + P_M \tag{2.3.6}$$

With reference to Figure 2.3.1, the resistive losses are due to resistances R_a and R_f:

$$P_R = R_a i_1^2 + R_f i_2^2 \tag{2.3.7}$$

The mechanical loss P_M is due to friction in the bearings and winding, it can be modelled as a first approximation considering a braking torque T_{loss} acting on the motor shaft, so that:

$$P_M = \omega T_{loss} = \omega \left(T_0 + T_2 \omega^2\right) \tag{2.3.8}$$

Where torque T_0 includes the contribution of the dry friction losses. As a first approximation it is considered as independent from the angular speed. The second term of equation 2.3.8 includes the contribution of the winding losses, modelled as a quadratic function of the angular speed ω.

The motor temperature is computed under the assumption that 1) the internal thermal conductivity of the motor is infinite, so that the motor temperature is uniform (small Biot's number, less than 0.1). Additionally, it is assumed that 2) the thermal capacity of the surrounding ambient is so large that the dissipated power does not change its temperature. These assumptions lead to the equation of the non steady thermal conduction [16]:

$$\tau_{th} \frac{d\vartheta}{dt} + \vartheta - \vartheta_{amb} = R_{th} P_{diss} \tag{2.3.9}$$

Where: ϑ_{amb} is the surrounding ambient temperature, R_{th} is the thermal resistance between the electric motor and the environment, and τ_{th} is its thermal time constant. They can be obtained from physical principles (first law of thermodynamics, Fourier's law, Biot's number) and material's characteristics or from data fitting of experimental data in transient and steady state conditions. The thermal typical response of the electric motor as function of the time for a step input current is reported in Figure 2.3.2.
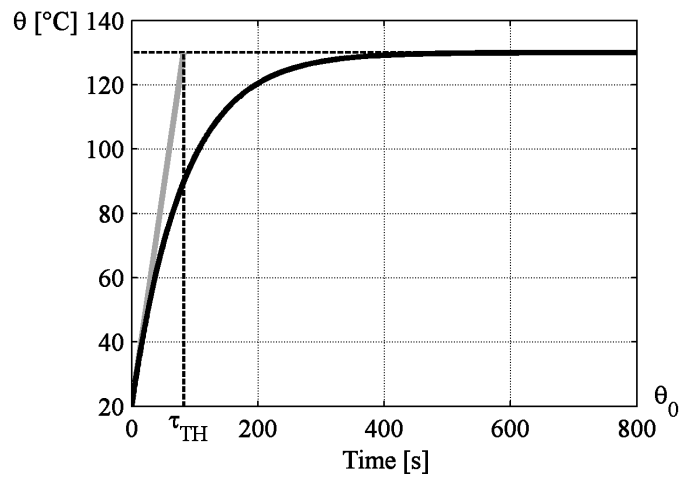
Figure 2.3.2: Example of thermal response of the ETEL TMK 0175-100 electric motor (Table 2.6.1) with a constant dissipated power P_{diss}=3125 W (solid line). The ratio R_{th}/τ_{th} determines the slope of the temperature curve in the origin. The initial temperature of the motor is 20° C.
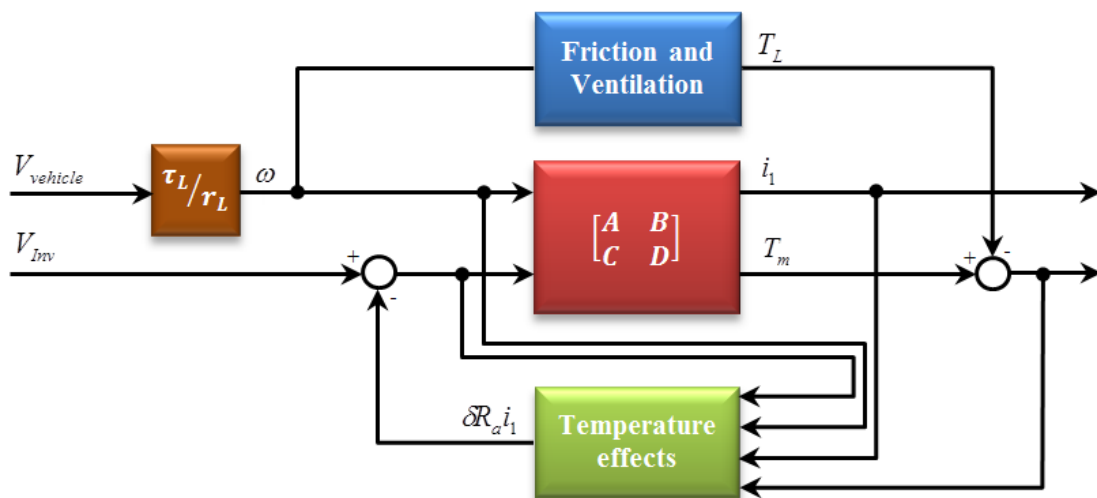
Figure 2.3.3: Model of the electric motor including temperature effects, friction and ventilation losses

Figure 2.3.4 shows the typical motor characterization obtained in steady state conditions with the model of Figure 2.3.3. The grey solid line in the left diagram (Figure 2.3.4a) represents the maximum torque to angular speed characteristic, while the contour lines indicate the efficiency.

Considering a given combination of torque and angular speed, the temperature

of the motor increases from the initial condition to reach a steady state. This is evidenced in the diagram at the right of the same figure for three representative operating points. The solid curves on the same diagram show the temperature, on the associated scale at left. The dotted ones represent the efficiency (scale at right). The final value reached by these curves is the same reported in the efficiency map of the Figure 2.3.4a).

Point A of the torque map (164 Nm, 500 rpm, triangle marker), leads to a steady state temperature as high as 230° C with a final efficiency lower than 60%. Point B (74 Nm, 2150 rpm, black dot marker) stabilizes at about 63° C The efficiency of about 90% represented in the left figure corresponds to the value reached after the transient. Point C (80 Nm, 3700 rpm, circle marker) is on the constant power part of the torque speed characteristic. The temperature after the transient reaches the maximum operating value of 130° C. This temperature is almost common to all points of the constant power portion of the diagram.

High efficiency points (B and C, for example) are characterized by a smaller temperature rise and a rather constant efficiency compared to low efficiency ones (point A of Figure 2.3.4).
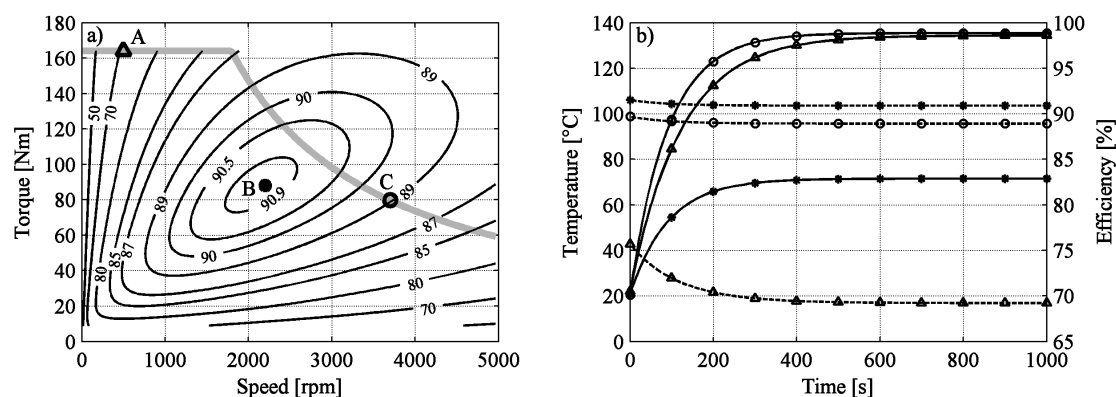
Figure 2.3.4: ETEL TMK 0175-100 characterization. a) Torque (solid grey) and efficiency (contour) map in steady state conditions. b) Temperature (solid line, left scale) and efficiency (dotted, right scale) as function of the time. The different lines represent the operating points A, B, C evidenced in the efficiency map (a). Same markers indicate corresponding conditions. Initial temperature of the motor: 20° C.

2.4 Control system

Each electric motor is driven by a power electronics (inverter), driven by a control logic that manages different aspects from low level functions such as the current

feedback loop and the motor thermal and electrical safety, to high level ones such as the torque splitting between different motors. These control functions are implemented in the simulator as represented Figure 2.4.1. They will be described in the following starting from the inner loops.

Current controller This control loop includes the current controller. It computes the driving voltage as function of the error between reference and measured current with a classical PI. Two saturations are added to this block: the voltage output from the power stage is saturated to that of the DC bus, while the reference current is saturated to the peak current, as specified by the motor manufacturer.

Temperature controller Overheating of the electric motor could cause loss of insulation of the copper wire (short circuit) and/or demagnetisation of the permanent magnets. This occurs when the motor temperature overcomes a maximum value (ϑ_{max}) allowed by the motor construction. The aim of the temperature controller is to prevent such damages by saturating the reference current signal. As reported in Figure 2.4.2, this is done by means of a temperature margin $\Delta\vartheta$ depending on the temperature dynamics.

If ($\vartheta < \vartheta_{max} - \Delta\vartheta$), no saturation occurs. If ($\vartheta_{max} - \Delta\vartheta < \vartheta < \vartheta_{max}$), the current saturation is decreased linearly with the temperature, as represented in Figure 2.4.2. If the maximum temperature is exceeded ($\vartheta > \vartheta_{max}$) the reference current is saturated to zero to allow the motor to cool down with its natural thermal dynamics.

The selection of the temperature margin ($\Delta\vartheta$) is a matter of compromise depending from the application. Increasing the temperature margin ($\Delta\vartheta$) allows coping with faster temperature gradients, but this comes at the cost of reducing the maximum torque that can be obtained from the motor.
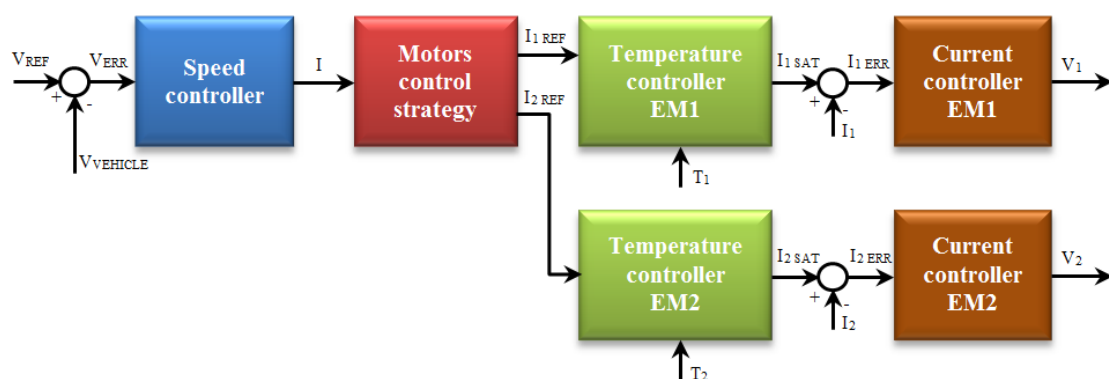
Figure 2.4.1: EV control system

Torque split strategy It is well known that the highest efficiency is reached by an electric motor in a relatively narrow region of the torque speed map. This region is usually located in a relatively high speed, high power range. Because of this characteristic, it may be convenient to have two or more relatively smaller electric motors (split motors) working in parallel on the same shaft and powered only when necessary instead of a bigger one. The potential advantage of this solution could be to exploit the active motor in a high efficiency region even when the driving cycle requires a small torque and power, instead of having just large one working all the time. By converse, the higher temperatures that would be reached in smaller motors could have negative effects on the efficiency and so jeopardise the potential benefits in terms of efficiency. In any case, even a demonstrated better efficiency should be carefully evaluated against the higher costs of a larger number of motors and power electronics.

As the potential benefits of having more electric motors is largely dependent by the driving cycle, it is not obvious to say if and when this benefit could be present and in what conditions.

The aim of the present section is therefore to investigate the potential benefits of a split motors configuration relative to one with a single motor.

Despite the large number of design choices in splitting the motor and in deciding the control strategies, the analysis has been performed on three rather basic configurations. The aim is to quantify the potential benefits in a relatively simplified, and to extend the analysis exploring a more thorough set of parameters only in case of a real advantage. To this end, a configuration with two electric motors in parallel on the same shaft is compared to one with only one motor. The two configurations share the same rated power and motor design i.e. the total torque and maximum power of the two smaller motors working in parallel is the same as the larger one. Table 2.6.1 shows the main characteristics of the off the shelf electric motors adopted for the study.

The control strategy for the split configuration is based on the saturation of the torque (or current) reference (Figure 2.4.2). This is done by means of two different logic:

1. Saturate EM1 first, then activate EM2. The aim of this strategy is to reach high efficiency points for one motor and exploit the second one only when necessary.

2. Torque split proportional to maximum torque of each motor: with this strategy the electric motors works in the same working point relative to their maximum power. This control strategy does not differ from using a single electric motor with same total power, except that the single motor would have a better efficiency because, among the others, the smaller end turn resistance. This case is therefore used as reference to assess the advantages of the motor split logic.
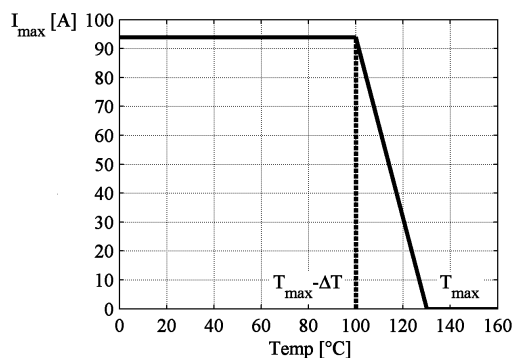
Figure 2.4.2: EM driving current saturation in function of motor temperature

Speed controller The aim of the vehicle speed controller is to follow a driving cycle. It computes the total current (or torque) request to be sent to the inverters as function of the error between the reference speed and the measured speed of the vehicle. This controller represents what the driver does acting on the accelerator and brake pedal. A rather low bandwidth PI controller is used to this end, defined by the transfer function:

$$\frac{I}{V_{ERR}}(s) = K_p + \frac{K_I}{s} \tag{2.4.1}$$

The adopted gains for the proportional and integral terms are:

- $K_p = 400\ \frac{As}{m}$

- $K_I = 0.25\ \frac{A}{m}$

2.5 Powertrain optimisation - Mission profile

The mission profile for the present study is that typical of a small urban, full-electric vehicle. For this reason a set of different driving cycles have been considered, as summarized in Table 2.5.1. ECE15 is an urban driving cycle characterized by low speed and low motor load. New European Driving Cycle (NEDC) contains four repeated ECE15 cycles and an extra-urban cycle (EUDC). It is commonly adopted for vehicle emissions homologation and fuel consumption measurements. In the U.S. New York City Cycle (NYCC) and Federal Test Procedure 75 (FTP 75) have been developed for light-duty vehicles and it is characterized by low speed urban driving with frequent starts and stops. Similarly, in Japan for urban driving cycle JPN 15.

The capability to follow certain driving cycles is only one part of the problem. Additional requests such as the hill start and hill traveling capability are essential

for insuring a real functionality to the vehicle. A vehicle optimized for following certain driving cycles but not capable of overcoming a steep garage ramp, or of traveling uphill, would be, in fact, useless. The same matter applies for hill traveling. Similarly some performances such as a large enough maximum speed and acceleration should be guaranteed even if not present in the driving cycle. The following functional requirements have then been considered in the powertrain optimization:

- Hill start: max ground slope that the vehicle must be able to overcome in transient conditions. The vehicle must be able to start with 25% ground slope it must be able to reach a minimum speed of 30 km/h and maintain it for at least 60 s.

- Hill traveling: max ground slope that the vehicle must be able to overcome in steady-state conditions, also with temperature limitation. The ground slope considered is 15% with a minimum speed of 50 km/h.

- Maximum speed: the vehicle must be able to travel at more than 100 km/h in steady-state conditions.

- Maximum acceleration: the acceleration time on 0-60 km/h must be less than 8s.

The previous performances are considered in the present study as functional requirements and, as such, they are not included in the evaluation of the energy consumption.

CYCLE		NEDC	NYCC	FTP 75	JPN 15
Duration	$[s]$	1200	600	1874	231
Length	$[km]$	10.7	1.9	17.8	2.2
Max speed	$[km/h]$	120	45	91	70
Average speed	$[km/h]$	32	11	34	33.7

Table 2.5.1: Main characteristics of the driving cycles considered for the present study

2.6 Powertrain - Optimisation procedure and results

The aim of the powertrain design procedure is to find the configuration that best matches the functional requirements (hill start, hill traveling, max speed and acceleration) and minimizes the average energy consumption when following the driving
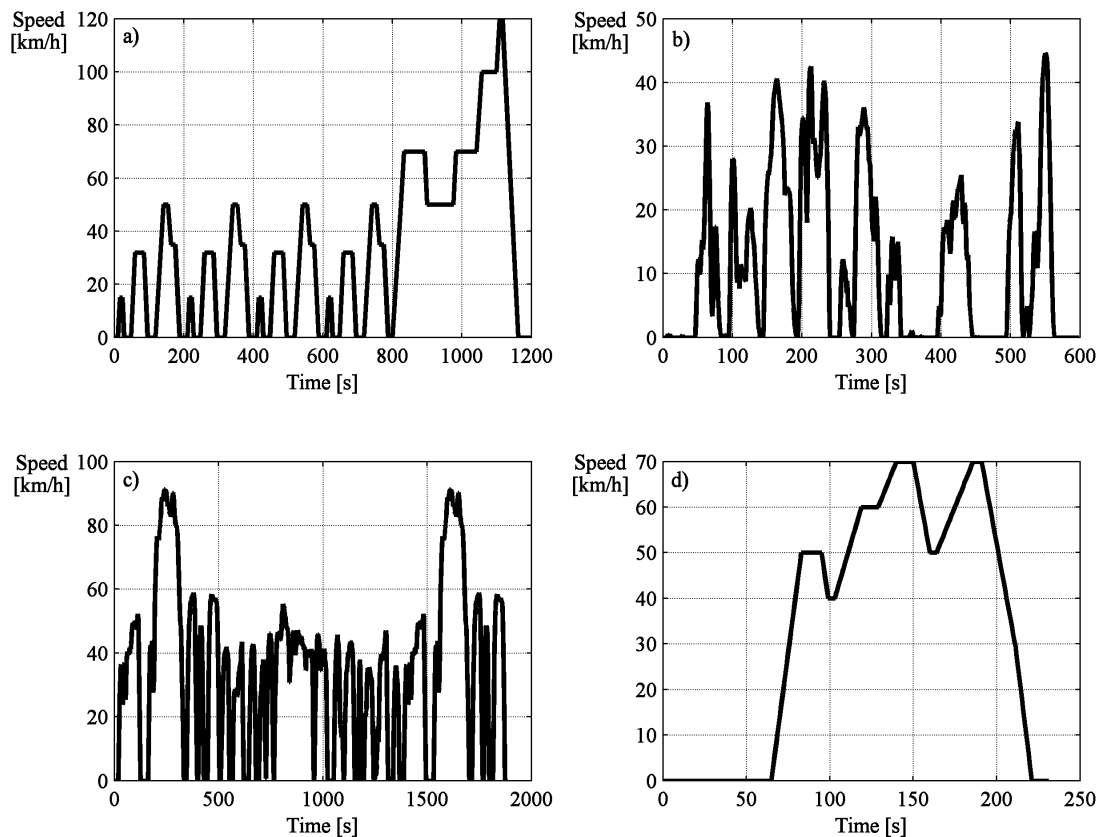
Figure 2.5.1: Example of driving cycles speed profiles: a) NEDC – b) NYCC – c) FTP 75 – d) JPN 15

cycles. The parameters considered for the design of the electric powertrain and torque-split strategy are:

- Types of electric motor: two electric motors with different maximum power rating have been considered. Their characteristics are reported in Table 2.6.1.

- Number of electric motors (one or two in parallel on the same shaft).

- Torque-split strategy between the electric motors.

- Transmission ratio between electric motor shaft (angular speed ω_{EM}) and wheels (ω_{wheel}):

$$\tau_T = \frac{\omega_{EM}}{\omega_{wheel}} \tag{2.6.1}$$

The mass of the electric motors affects that of the vehicle, so that changing their size the vehicle mass changes. The mass of the the batteries is kept constant.

21

It is included in that of the vehicle (whose parameters are summarized in Table 2.2.1). A better energy efficiency of the powertrain allows then increasing the range rather than reducing the size of the battery pack (with corresponding cost reduction). This choice is motivated by the need to limit the number of design parameters.

The procedure adopted for powertrain optimization is the following:

- Choose the electric motors configuration (one motor, two motors, what size)

- Choose the torque split strategy

- Perform following driving missions, for different transmission ratios

  - hill start
  - hill traveling
  - driving cycles

- Verify acceleration performance

- Verify max speed performances

	PARAMETERS		ETEL TMK0175-050	ETEL TMK0175-100
P_{max}	Max mechanical power (steady-state)	$[kW]$	15.9	30.9
T_{max}	Max torque	$[Nm]$	80	164
I_{ss}	Max current (steady-state)	$[A_{rms}]$	26.8	52.8
I_p	Max current (peak DC=5%)	$[A_{rms}]$	49.1	93.9
k_T	Torque constant	$[Nm/A_{rms}]$	3.86	4.04
R_s	Stator resistance	$[\Omega]$	1.08	0.483
L_s	Stator inductance	$[mH]$	7.62	4.15
R_i	Iron losses equivalent resistance	$[\Omega]$	1750	972
L_i	Iron losses equivalent inductance	$[\mu H]$	7.62	0.415
P_w	Max windings losses	$[W]$	1660	2910
τ_{th}	Thermal time constant	$[s]$	100	82
R_{th}	Thermal resistance	$[K/W]$	0.0643	0.0352
J_{EM}	Rotor inertia	$[kgm^2]$	$7.8 \cdot 10^{-3}$	$1.4 \cdot 10^{-2}$
m_{EM}	Mass	$[kg]$	15	24
ω_{max}	Max speed	$[rpm]$	5170	4960

Table 2.6.1: Electric motors data

The optimal configuration is that satisfies all requirements and minimizing the energy consumption.

As the results are strongly affected by the driving cycle, the study has been repeated for each of them (Table 2.5.1). The energy consumption per unit distance has then been averaged among all driving cycles to obtain a sort of overall minimum. This corresponds to making a weighed average where each cycle has the same weight. Although questionable, this choice may reduce the distance between real and standard driving cycles by simply averaging between different driving styles.

If electric motors are used also for braking, some energy could be regenerated. To evaluate the potentialities of an ideal regeneration on urban driving cycles, maximum and minimum energy consumption have been computed with: a) no regeneration of braking energy, or b) 100% regeneration. This means that all energy that is output from the electric motors during braking is stored in the batteries with no dissipations. If the braking torque that can be generated by the motors is not enough to follow the driving cycle, the gap is filled by the mechanical brakes. In this case only the power managed by the electric motors is regenerated.

The results obtained for different driving missions are described in the following. The different results are usually plotted as function of the transmission ratio that is considered as the main design parameter to adapt a given motor configuration to the mission profile.

2.6.1 Hill start

Hill start tests are performed with a ramp speed saturated at 30 km/h. The acceleration along the ramp is a rather low 1 km/h/s. The results obtained with EM1=ETEL100 – EM2=ETEL50 and torque proportional to maximum torque of each motor (torque split strategy 2) are summarized in Figure 2.6.1. Figure 2.6.1 a) is relative to a transmission ratio $\tau = 3.5$ and shows that the reference speed of 30 km/h (grey dotted line) can be maintained (black solid line) only for 60 s. After about 100 s from the beginning of the test (and about 60 s at 30 km/h) the motor temperature reaches the limit of 130° C, the current controller detects approaching overtemperature conditions and starts decreasing the current (grey solid line). Even if the temperature stabilizes at the maximum allowed, the vehicle speed (black solid line) start decreasing until it stops and eventually the vehicle begins backing.
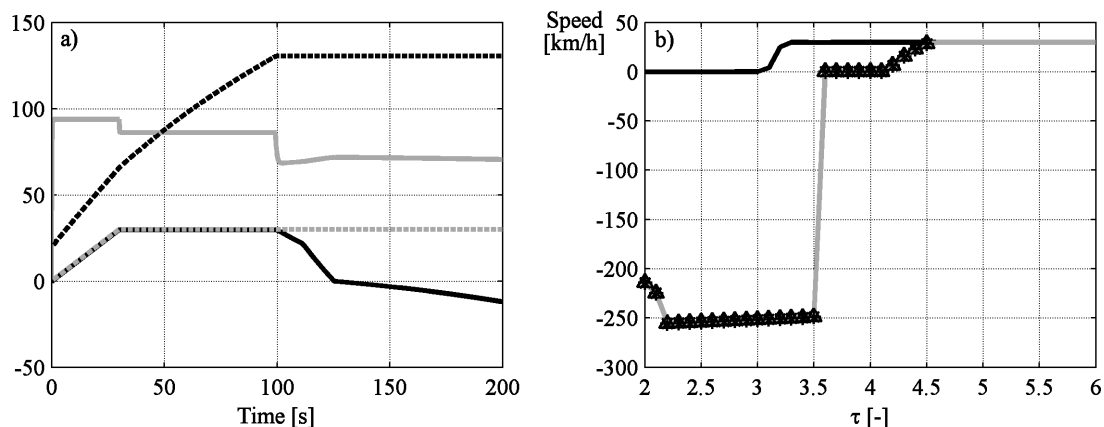
Figure 2.6.1: Hill start. Electric motors: EM1=ETEL100 + EM2=ETEL50; Torque split strategy #2 (proportional to maximum torque of each motor). Diagram a): $\tau = 3.5$, Vehicle speed (black), vehicle reference speed (grey dotted), EM1 current (grey), EM1 temperature (black dotted). Diagram b) Max vehicle speed during transient (black) and steady-state (grey). Limitations due to max temperature of the EM1 (*) and EM2 (Δ) occurs in steady-state conditions.

This means that the torque produced by the electric motors is not enough to balance the gravity with that slope. In any case, with that transmission ratio the reference speed of 30 km/h is held for a time (60 s) long enough to satisfy the minimum requirement. With transmission ratios τ smaller than 3.5, the speed of 30 km/h can not be maintained for 60 s or even it could not be reachable at all. For this reason, the minimum serviceable transmission ratio is 3.5 for this motors configuration.

Figure 2.6.1 b) shows the maximum during transient (solid black line) and steady state speed (grey line) as function of the transmission ratio. The black solid line shows that 30 km/h can be reached in transient conditions only for transmission ratios larger than 3.3. At steady state, a minimum transmission ratio of 3.6 is necessary to held the vehicle still relying on the motor torque only, a minimum of $\tau = 4.2$ is necessary to let it move uphill, and transmission ratios larger than $\tau = 4.5$ are necessary to move at 30 km/h.

2.6.2 Hill traveling

Hill traveling tests are performed with a ramp reference speed saturated at 50 km/h. The acceleration is the same as for hill start: 1 km/h/s. Figure 2.6.2 shows the results obtained with the same powertrain configuration as Figure 2.6.1. The requirements specify that when traveling along a 15% slope, the vehicle should allow a minimum steady state speed of 50 km/h. Figure 2.6.1 a) shows the results

for a transmission ratio $\tau = 2.8$. After 230 s from the start, the temperature grows at the limit of 130° C, the motor controller cuts the current and the vehicle slows down from 50 km/h to 30 km/h. This means that the transmission ratio should be larger than 2.8 to comply to the requirements.
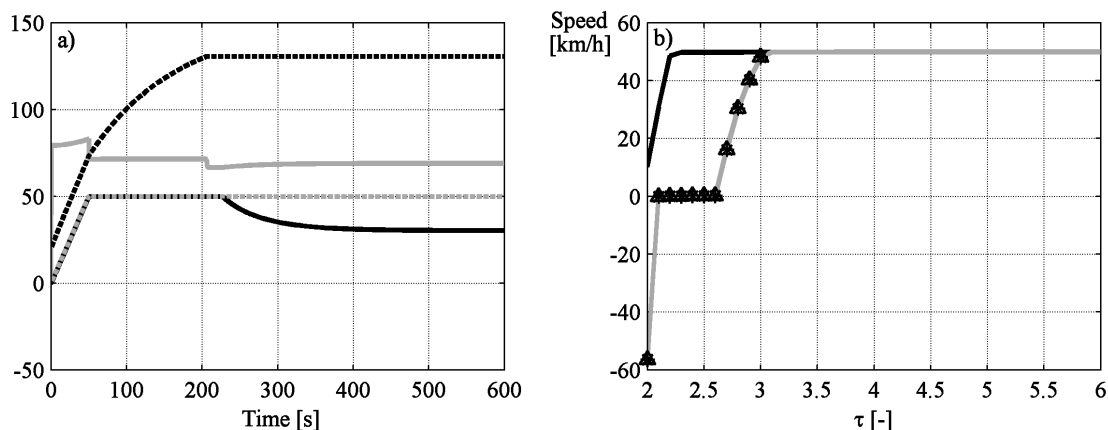
Figure 2.6.2: Hill start results with EM1=ETEL100 – EM2=ETEL50 – Torque split strategy 2 (proportional to maximum torque of each motor). Diagram a): $\tau = 2.8$, Vehicle speed (black), vehicle reference speed (grey dotted), EM1 current (grey), EM1 temperature (black dotted). Diagram b) Max vehicle speed during transient (black) and steady-state (grey). Limitations due to max temperature of the EM1 (*) and EM2 (Δ) occurs in steady-state conditions when the requests cannot be satisfied.

Figure 2.6.2 b) shows the maximum speed in transient conditions (solid black line) and steady state speed (grey line) as function of the transmission ratio. For short time intervals the required hill traveling speed of 50 km/h is reached for $\tau = 2.3$, nevertheless to travel at steady state at that speed the transmission ratio should be larger than 3.1. For $2.3 \leq \tau \leq 2.6$ after reaching 50 km/h, the vehicle must slow down to complete stop to avoid overtemperature conditions. For $2.6 < \tau < 3$ the vehicle keeps going but at a slower speed.

2.6.3 Maximum vehicle speed

The previous analysis shows, on one hand that the minimum transmission ratio is set by thermal issues during hill start and hill traveling conditions. The maximum rotating speed allowed by the electric motor (ω_{max}), together with the maximum required speed (V_{max}) and tire rolling radius (r_L) set, on the other hand, the

maximum transmission ratio (τ_{max}):

$$\tau_{max} = r_L \frac{\omega_{max}}{V_{max}}. \tag{2.6.2}$$

The above equation is just a kinematic constraint and it is valid provided that the motors are powerful enough to win rolling resistance, aerodynamic drag and other mechanical losses. For a given transmission ratio, the maximum speed that can be actually reached can be verified taking into account of the vehicle longitudinal dynamics together with the electric motor model and controller, as represented in Figure 2.1.1.

Figure 2.6.3 shows the maximum vehicle speed as function of the transmission ratio corresponding to a maximum motor speed of 4960 rpm (Table 2.6.1). The powertrain is the same as for Figures 2.6.1 and 2.6.2. Assuming a max speed of 100 km/h the transmission ratio must be less than 6.2.
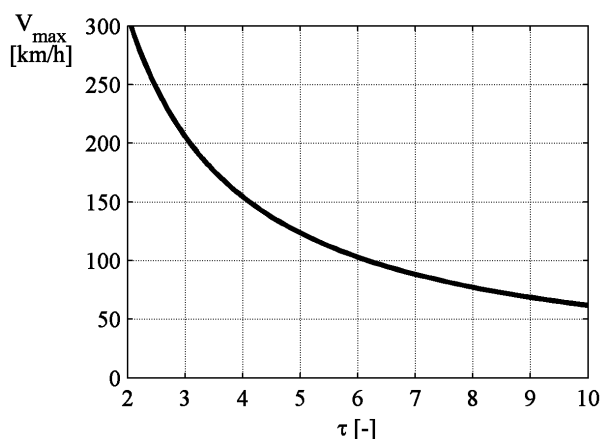
Figure 2.6.3: Max traveling speed. EM1=ETEL100 – EM2=ETEL50 – Torque split strategy 2 (proportional to maximum torque of each motor).

2.6.4 Driving cycles

The mission of this small electric vehicle is to minimize the energy consumption in urban context. For this reason, the optimisation procedure was based on the driving cycles summarized in Table 2. For a given combination of motors and torque split strategy, simulations of a driving cycle can be performed to evaluate the energy consumption per unit distance. The transmission ratio is a free parameter that can be varied in the range previously set by hill start/traveling and max speed analysis. Modifying the transmission ratio is then possible to find the value that minimizes the fuel consumption. That minimum is linked to a given driving

cycle and powertrain configuration. Once the optimal transmission ratio is found, the maximum speed and acceleration of the vehicle must be verified, including temperature limitation.
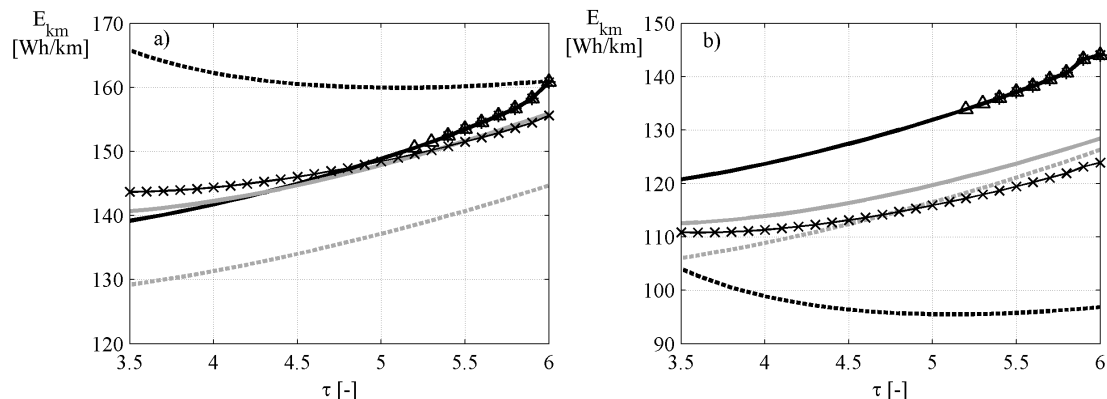
Figure 2.6.4: Energy consumption per km with EM1=ETEL100 – EM2=ETEL50 – Torque split strategy 2: a) Driving cycles without regeneration of braking energy. NEDC (black), NYCC (black dotted), FTP (grey), JPN15 (grey dotted), Average of all cycles (black x) – b) Driving cycles with 100% regeneration of braking energy. Limitations due to max temperature of the EM1 (*) and EM2 (Δ) occurs when the requests cannot be satisfied.

As shown in Figure 2.6.4, the results are strongly affected by the driving cycle, not only in terms of energy per unit traveled distance but also in the transmission ratio that optimizes the energy consumption. The diagrams reported in the figure do not show a minimum in the range of transmission ratios adopted for the plot. This is because this range is bound by the already mentioned hill start/traveling and by max speed considerations.

Comparison of diagrams 2.6.4 a) and b) shows that the energy saving allowed by regenerative braking is largely dependent on the adopted driving cycle. The largest saving is obtained in the NYCC driving cycle that is characterized by low speed but high accelerations and decelerations that are compatible with braking using the electric motors.

Each driving cycle has a different optimal transmission ratio, the average of the energy per unit distance of the four cycles of Table 2.5.1 has been added to the present analysis. The aim is to obtain a result not too specific of a given driving cycle. Even if questionable, the idea behind this choice is to take the different driving cycles into account as due to different urban context and different driving styles. Averaging them together allows to take these differences into account. The results of this analysis are reported in the same Figure 2.6.4 where black x line indicates the average energy consumption with regenerative braking (b) and

without (a). In this case the optimum transmission ratio ($\tau = 3.6$) falls within the range of transmission ratios allowed by the other constraints.

		1	**2**	**3**	**4**	**5**	**6**
EM1 (ETEL)	[-]	100	50	100	100	100	100
EM2 (ETEL)	[-]	-	100	50	100	50	100
Torque split strategy	[-]	-	1	1	1	2	2
τ	[-]	5.1	4.3	3.9	3.6	3.6	3.0
Average energy consumption (no regeneration)	[Wh/km]	141.7	159.3	147.8	154.6	143.7	145.8
Average energy consumption (regeneration)	[Wh/km]	108.6	130.3	115.8	123.6	110.8	112.9
Acceleration time (0-60 km/h)	[s]	6.7	5.2	5.7	4.7	6.2	5.7
Max steady-state speed	[km/h]	96	115	125	134	132	153
Temp max EM1	[°C]	125	131.6	94.6	90.9	79.5	64.7
Temp max EM2	[°C]	-	90.7	69.6	72	70.4	64.7

Table 2.6.2: Optimal results for each powertrain configuration

What done in Figures 2.6.4 for a given combination of motors and torque split strategy (EM1=ETEL100 – EM2=ETEL50 – Torque split strategy 2) has been repeated for all combination of motors and torque split strategies, as summarized in the first three rows of Table 2.6.2. Even if the solution that minimizes the energy consumption is #1, with only one electric motor ETEL100, this configuration is able to follow NEDC with a maximum EM temperature of 125°C, very close to the maximum temperature allowed (130°C). The configuration with better performances, strongly lower maximum motor temperature and only slightly higher energy consumption is the #5, with two electric motors working in parallel and torque split strategy 2. The results show that the best torque split strategy is the #2, with better performances and less energy consumption with respect to strategy 1. In Figure 2.6.5 is reported a comparison between the configurations #3 and #5 (EM1=ETEL100 - EM2=ETEL50, respectively with torque split strategy 1 and 2). The temperature taken into account is the average between the two motors and the whole efficiency of the powertrain system (Mechanical power output / Electric power input) is considered. In order to evaluate a quasi steady state thermal condition, NEDC driving cycle was repeated for three consecutive times (obtaining a bigger cycle with threee equal NEDC sub-cycles) and only the last

one was taken into account. Strategy 2 leads to the lowest energy consumption, probably because the highest efficiency and the lowest average temperature of the electric motors at each time of the driving cycle, as can be seen in the same Figure 2.6.5.

Torque strategy #2 involves the use of the two electric motors in parallel all the time, with torque request proportional to their maximum rating. This indicates that a powertrain with two motors, installed on the same shaft and driven independently from each other do not lead to energy savings, at least with the torque split strategies that have been considered in the present study. This suggests the adoption of only one motor rated as the two optimal ones. Using one bigger motor instead of two smaller ones would improve the efficiency because, among the others, to the smaller electrical resistance of the end windings and to the reduced aerodynamic drag.

A detailed cost analysis is out of the scope of the present study, nevertheless the use of only one motor would lead to additional benefits related to the cost saving in the electric machines (one bigger motor costs less than two smaller ones with same cross section) and, above all, of the inverter (one bigger inverter costs much less than two smaller ones of about half size).
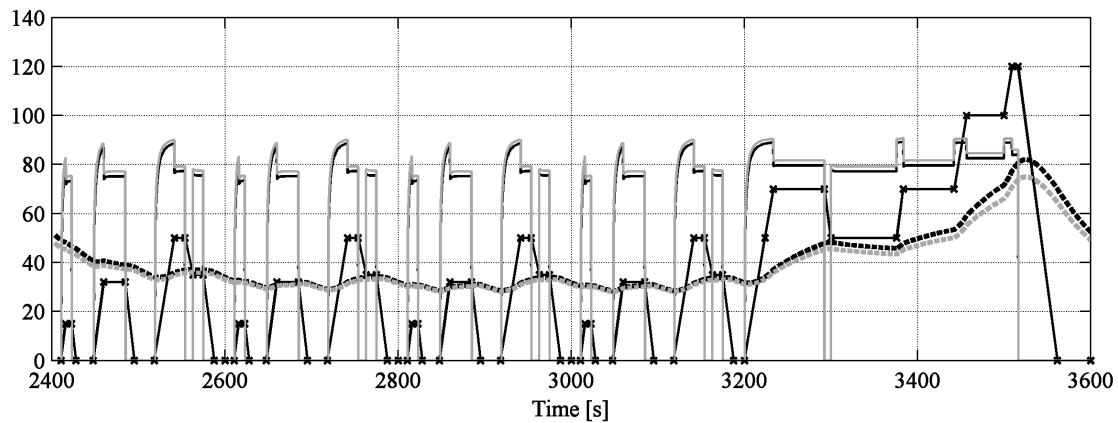
Figure 2.6.5: Comparison between the configuration #3 and #5 of Table 2.6.2 (EM1=ETEL100 – EM2=ETEL50 with torque split strategy 1 and 2) during the third part of NEDC driving cycle (black x) – Torque split strategy 1 (configuration #3): EM efficiency (black), EM Temperature (black dot) – Torque split strategy 2 (#5): EM efficiency (gray), EM Temperature (gray dot) – Are considered the global efficiencies of the powertrain (EM1+EM2) without regeneration of braking energy and the average temperatures between EM1 and EM2. A bigger cycle formed by three consecutive NEDC sub-cycles was considered and only the third NEDC cycle is reported, in order to consider a quasi steady state thermal condition with repeated driving cycles.

Chapter 3

Modeling and Torque-split strategies for a sustainable city hybrid vehicle

3.1 Overview and modeling

The aim of the analysis is to evaluate the feasibility and the performance of an hybrid vehicle having a really limited amount of mechanical modifications with respect to the related traditional pure-ICE vehicle. Furthermore, an investigation about the performance and the need of a micro-hybrid or a full-hybrid vehicle driving strategies (allowing the full-electric driving mode with the same hardware, considering the classification reported into the introduction 1.1) is reported. Finally, possible improvements to the proposed initial configuration, based on the results of the simulations, are proposed. Particularly considering the energy flows between the hybrid powertrain components.

The functional scheme of the initial proposed vehicle configuration is reported in Figure 3.1.1.

The idea is to match the advantages of a full-electric vehicle, in terms of efficiency and fuel consumption, minimizing the mechanical modifications and thus the hybridization costs of the related traditional ICE vehicle.

A simulation model was built in Matlab/Simulink environment. The general structure of the model is reported in Figure 3.1.2 and the related overview of the Matlab/Simulink model in Figure 3.1.3.

As the model of the full-electric vehicle described in paragraph 2.1, also in this case the input is the reference longitudinal speed profile the vehicle has to follow, for example the typical NEDC homologation driving cycle, commonly used in automotive field. The controllers drive the electric motor, the ICE and the
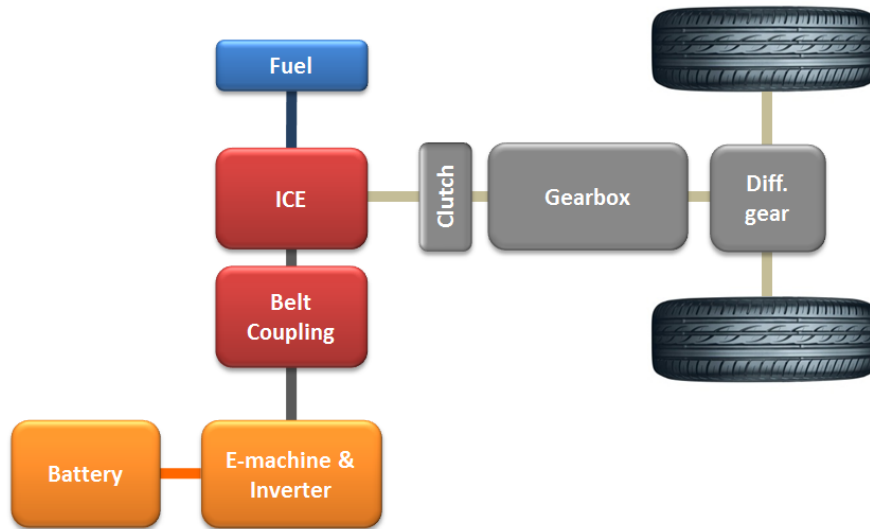
Figure 3.1.1: Topology of the proposed hybrid vehicle

brakes in order to minimize the difference between the reference and the actual vehicle speed. Within the controller subsystem are also located the torque-split strategies and a more complete longitudinal driver, not only demanded to drive the throttle and the brakes, but the gear change and the clutch command too.

In the following will be reported the main differences and improvements with respect to the model of the full electric vehicle described in chapter 2. The aim of the first phase of the project was to build a modular vehicle model, in which different level of detail of some powertrain components can be easily chosen. This is in order to allow the user to perform different types of simulations during the progress of the project, mainly related to the longitudinal dynamics, considering at the beginning just the fuel consumption but successively to allow the first analysis of the driver longitudinal comfort too. The aim can be achieved improving the degrees of freedom of the driveline. Particularly, are implemented the polar inertia of the wheels, connected to the ground by means of a tire (modeled with the hugely known Pacejka's Magic Formula), and the Engine inertia, connected to the driveline by means of the angular stiffness of the clutch. Therefore, two additional degrees of freedom can be easily and independently chosen and taken into account. The details are reported in paragraph 3.2 and the number of degrees of freedom was not further increased due to different reasons:

- More detailed models of the different subsystems (ICE, EM, driveline with gearbox, differential and so on) can be obtained in a more reliable way with specific and dedicated software.
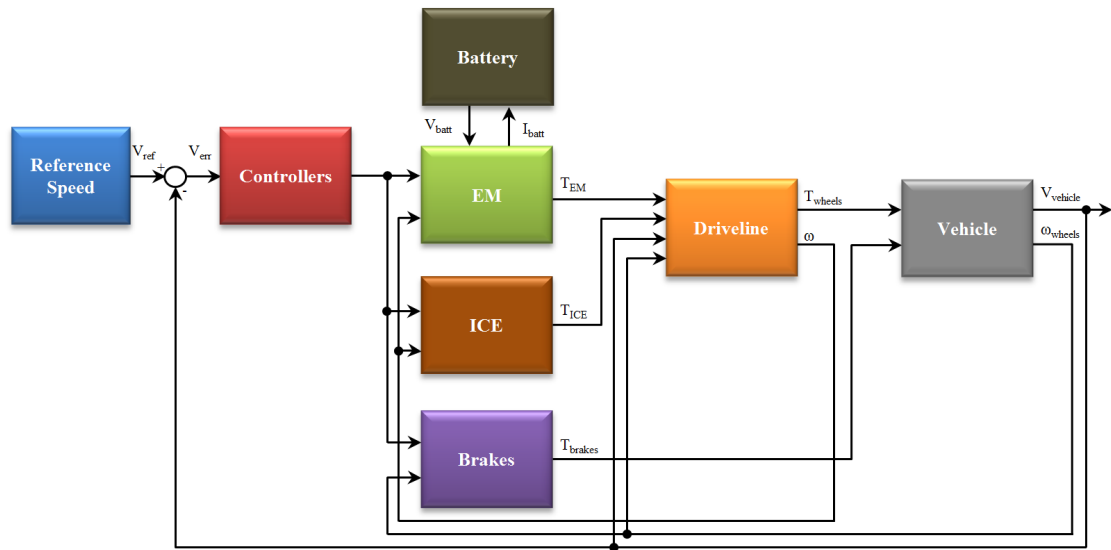
Figure 3.1.2: Model structure of the whole hybrid vehicle

- Increasing the DOFs of the system, higher integration frequency are required, both for the numerical stability of the whole model and to be able to represent effects at increasing frequency. Simulation of the whole vehicle model with a too many degrees of freedom can be excessively computation time consuming, especially considering the commonly used driving cycles, with durations of hundreds or thousands of seconds.

3.2 Vehicle and driveline models

As described in paragraph 2.1, to achieve performance analysis of the whole hybrid system on driving cycles, a simple longitudinal dynamic model of the vehicle, with just one degree of freedom, is sufficient. Due to the low longitudinal accelerations and longitudinal forces between tires and ground, the maximum capabilities and the related longitudinal slip of the tires can be neglected. Therefore, for these purposes, the vehicle can be simply represented like an equivalent inertia at the ICE crankshaft, as reported in equations 2.2.1 and 2.2.2. The main parameters of the hybrid vehicle are listed in Table 3.2.1 along with the associated symbols.
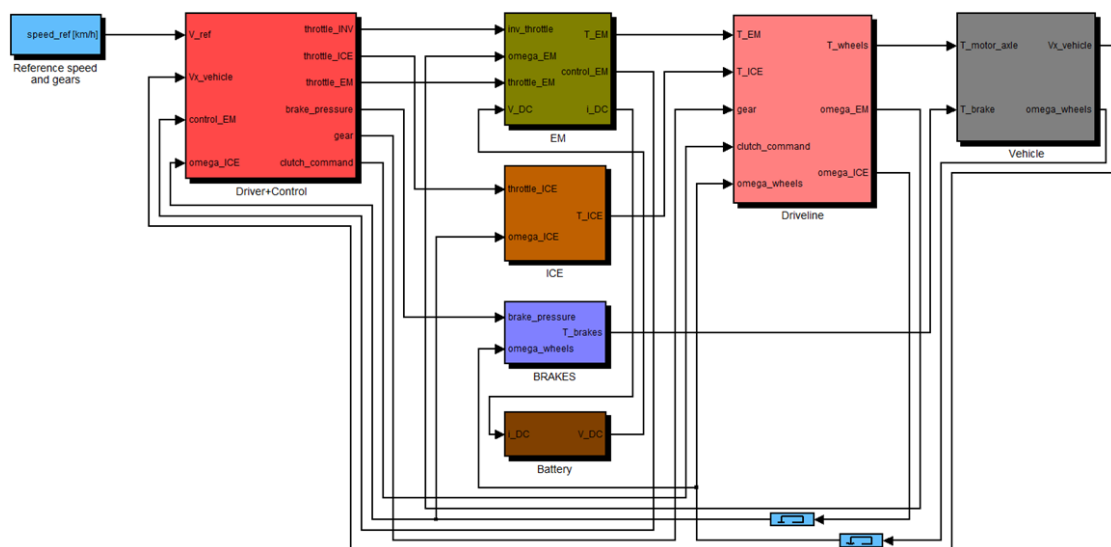
Figure 3.1.3: Overview of the Matlab/Simulink model of the whole hybrid vehicle

	Parameter		Value
M	Whole vehicle mass (with 3 passengers)	$[kg]$	
J_W	Wheel inertia	$[kgm^2]$	
J_{ICE}	Engine inertia	$[kgm^2]$	
r_L	Wheel loaded rolling radius	$[m]$	
f_0	Constant coast-down coefficient	$[N]$	
f_2	Quadratic coast-down coefficient	$\left[\frac{N}{(km/h)^2}\right]$	

Table 3.2.1: Hybrid vehicle parameters

On the other hand, more detailed simulations of start&stop maneuvers might be useful in a second phase of the project, in order to identify the critical aspect for a better optimization of the whole system, especially a more detailed optimization of the torque-split strategy taking into account the longitudinal comfort of the vehicle. For this reason, one or two additional degrees of freedom are implemented and can be easily chosen by the user, as schematized in Figure 3.2.1.

In each case, the driveline input torque T_p is that at the crankshaft, due to the whole powertrain (ICE+EM).

The equivalent inertia of the powertrain due to the ICE, electric motor and belt transmission ($J_{p,eq}$), that of the wheels and gearbox ($J_{w,eq}$) and the equivalent rotational inertia of the vehicle ($J_{v,eq}$) are taken into account, as suggested by Genta [37]. These parameters can be calculated similarly as reported in equation
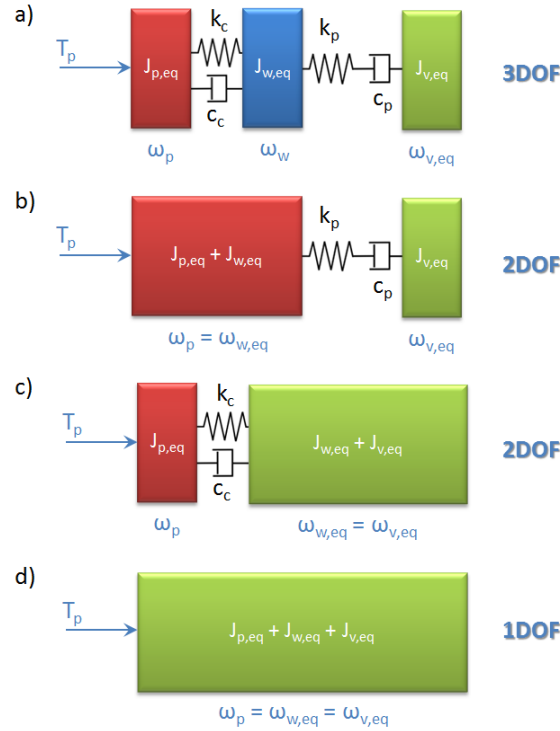
Figure 3.2.1: Implemented possible configuration of the driveline model, that can be chosen by the user.

2.2.2:

$$J_{p,eq} = J_{ICE} + J_{ME} \frac{1}{\tau_{belt}^2} \tag{3.2.1}$$

$$J_{w,eq} = 4J_W \frac{1}{\left(\tau_{gear}\tau_{final}\right)^2} \tag{3.2.2}$$

$$J_{v,eq} = M \left(\frac{r_L}{\tau_{gear}\tau_{final}}\right)^2 \tag{3.2.3}$$

At this phase of the project, the belt transmission between the electric motor and the ICE crankshaft is simply modeled as a transmission ratio $\tau_{belt} = \frac{\omega_{ICE}}{\omega_{EM}}$ and an efficiency. Due to the potentially high torques involved, an efficiency $\eta_{belt} = 95\%$ was taken into account and the whole torque at the ICE crankshaft is:

$$T_p = T_{ICE} + T_{EM} \frac{1}{\tau_{belt}} \eta_{belt} \tag{3.2.4}$$

Each wheel is considered as a rigid body, with its own polar inertia $J_{w,eq}$ and the wheel-ground contact can be characterized by the curve of the longitudinal force coefficient versus the longitudinal slip $\mu_x = f(\sigma)$ reported in Figure 3.2.2.
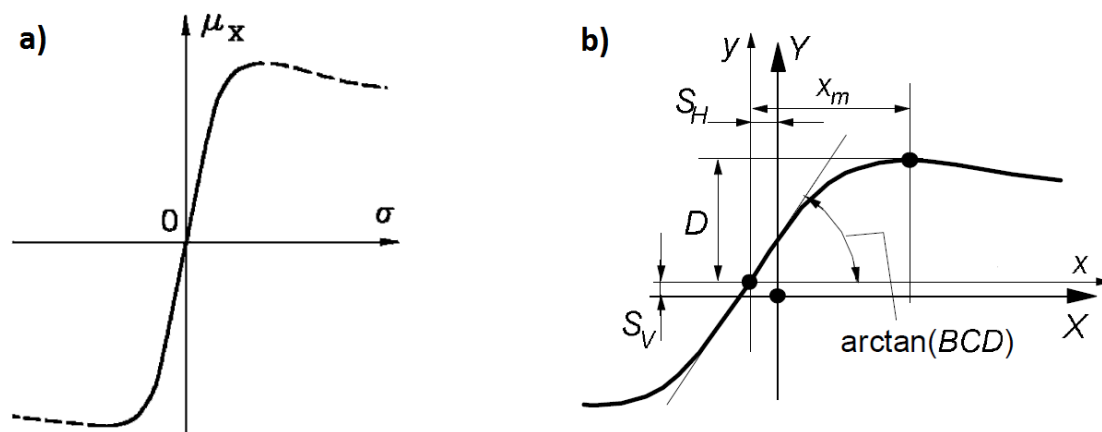
Figure 3.2.2: Longitudinal characteristics of a tire

Often, only the first linear part of the curve is used and its slope can be easily obtained from the coefficients of the Pacejka's Magic Formula by the product $B_x C_x D_x$. Otherwise, the whole longitudinal Magic Formula can be used, representing the whole curve. In the vehicle model, both the solutions are used and can be chosen.

Considering the pure longitudinal Magic Formula, it is reported in equation 3.2.5 (a complete set of all the tire parameters can be found in [38]).

$$F_{x0} = D_x \sin \left[C_x \arctan \left\{ B_x \sigma - E_x \left(B_x \sigma - \arctan \left(B_x \sigma \right) \right) \right\} \right] + S_{Vx} \qquad (3.2.5)$$

With the longitudinal slip σ linked to the ratio between the angular speed of the wheel ω_W and the speed of the moment of inertia simulating the vehicle ω_v:

$$\sigma = \frac{\omega_W}{\omega_v} - 1 \qquad (3.2.6)$$

where:

$$\omega_v = \frac{V}{r_L} \qquad (3.2.7)$$

Instead, considering only the first linear part of the curve, the longitudinal force generated between tires and ground can be:

$$F_x = F_z \mu_x = F_z \left(B_x C_x D_x \right) \sigma \qquad (3.2.8)$$

The wheel-ground contact can be modeled as a viscous damper with damping coefficient, as presented by Genta [37]:

$$c_p = F_x r_L = \frac{F_z \left(B_x C_x D_x \right) r_L^2}{V} \qquad (3.2.9)$$

36

Usually the tire model is complemented by adding a spring in series with the damper, with a stiffness:

$$k_p = F_x r_L = \frac{F_z \left(B_x C_x D_x\right) r_L^2}{a} \tag{3.2.10}$$

Where a is a length equal to half the length of the contact zone. It can be modified to take into account the longitudinal compliance of the tires and the suspension.

The additional degree of freedom can be taken into account considering the equivalent inertia of the powertrain (EM+ICE) connected to the primary shaft of the gearbox by means of the stiffness (k_c) and damping (c_c) of the clutch.

Locking the wheels and the clutch degrees of freedom, the inertia can be simply added to obtain the equivalent inertia at the crankshaft of the whole vehicle.

The part of the matlab model that allows the choice of the wheels degree of freedom is reported in Figure 3.2.3, while the driveline model is in Figure 3.2.4.
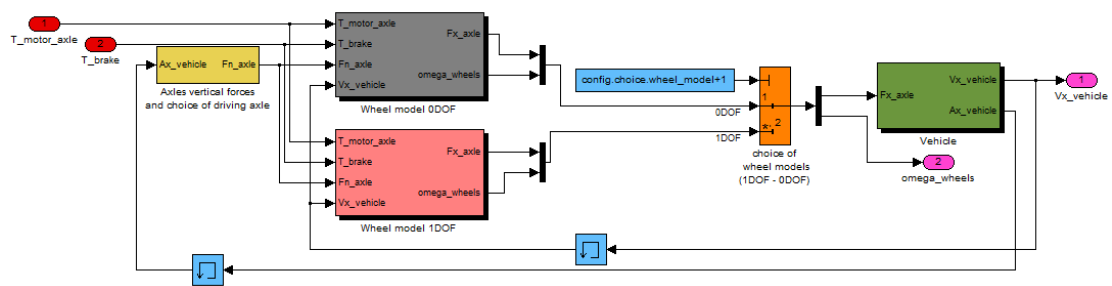
Figure 3.2.3: Matlab/Simulink model of the vehicle subsystem
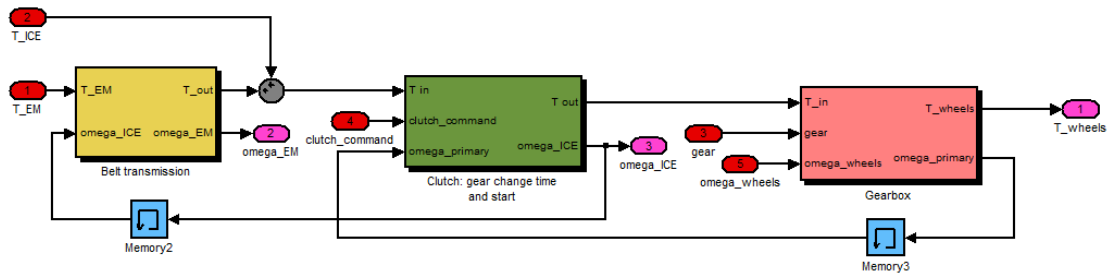
Figure 3.2.4: Matlab/Simulink model of the driveline

The gearbox and the final drive are modeled as simple transmission ratios, related to the engaged gear, and an efficiency. The available experimental data relates its efficiency to:

- Gearbox temperature

- Input torque

- Angular speed of the input shaft

- Engaged gear

With a 3D linear interpolation for each engaged gear, the whole efficiency of the gearbox can be calculated at each time step of the simulation. Consequently, the output torque and the dissipated power can be obtained at each time step in function of the the input torque and efficiency. Furthermore, knowing the dissipated power, the thermal resistance and the thermal time constant of the gearbox, its temperature can be evaluated by means of a 1DOF thermal model, as that used for the electric motor reported in equation 2.3.9.
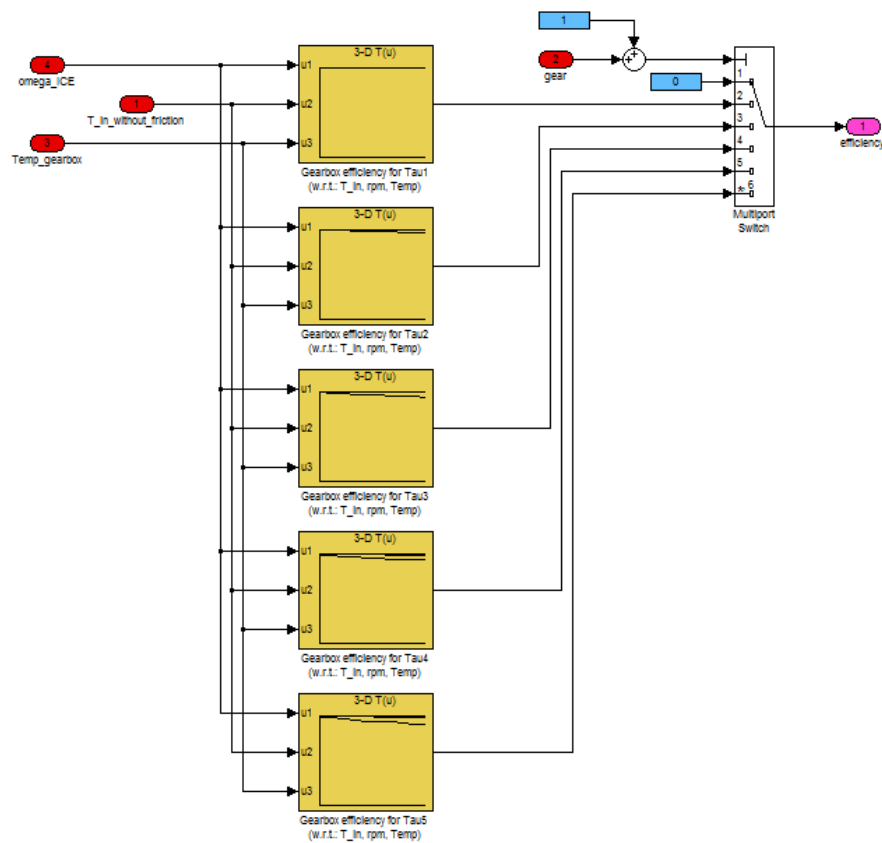
Figure 3.2.5: Gearbox efficiency evaluation by means of a 3D linear interpolation for each engaged gear

3.3   Battery model

In chapter 2, an investigation about a possible optimal solution, in terms of energy consumption, using one or two electric motors in a full-electric vehicle is presented. In that case, a battery model was not taken into account but just an infinite capacity battery was considered. This is in order to evaluate only the capabilities and the maximum performances of the different configurations of the electric motors. Furthermore, the differences in energy consumption and battery currents required to drive the car are due to the difference in efficiency only, therefore they are of the same order of magnitude with all the electric motor configurations.

Instead, considering an hybrid vehicle, key factors in the determination of the torque-split strategy between the ICE and the electric motor (presented in paragraph 3.6.2) are the characteristics of the battery at each time step. Particularly, the capacity and the state of charge (SOC) of the battery are the most important limitations in the possible usage of the electric motor because, for example, it cannot be used in driving or braking mode if the battery is empty or fully recharged respectively. In addition, its efficiency must be evaluated and taken into account because the amount of energy dissipated into the battery determines its temperature and can be an important part of the energy dissipated by the whole hybrid powertrain.

For this reason, a reliable evaluation of the state of charge of the battery must be implemented. The most simple electric model of a battery consists of an ideal voltage source in series with an internal resistance, but this model does not take into account the battery SOC. An easy-to-use battery model, presented and experimentally validated by Tremblay [35] (schematized in Figure 3.3.1) was taken into account. It uses just the state of charge (SOC) of the battery as a state variable and it is composed by a controlled voltage source in series with a resistance that represents the internal resistance of the battery.

The presented model is able to accurately reproduce the battery manufacturer's charge and discharge curves for a huge number of battery chemistry, like Lead-Acid, Lithium-Ion (Li-Ion), Nickel-Cadmium (NiCd) and Nickel-Metal-Hydride (NiMH). In addition, this model was integrated into the Matlab SimPowerSystem toolbox.

The present research is conducted in an early phase of the project and for this reason, a small amount of experimental data about the components of the hybrid vehicle was available. Related to the battery characteristics, just the type (Li-Ion), nominal capacity (Ah) and nominal voltage (V) were known. The first estimation of reasonable numerical value of the battery model parameters was carried out from the SimPowerSystem in function of the available data. That toolbox was used just to obtain the parameters values, but it was not implemented within the hybrid vehicle model, where just the model equations are used.

The battery is modeled using a simple controlled voltage source in series with
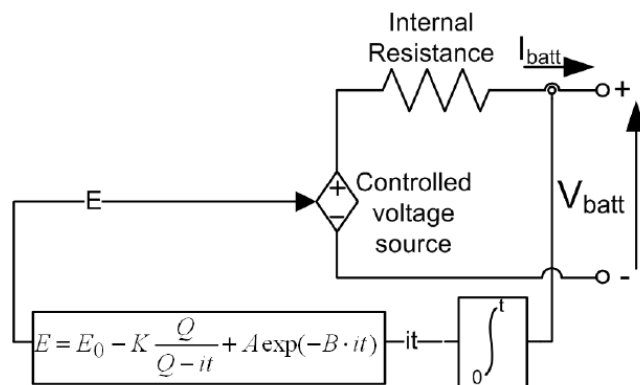
Figure 3.3.1: Battery model

a constant resistance, as shown in Figure 3.3.1. The battery voltage is calculated in function of its nominal capacity, voltage and instant current. For this reason, the model presents the same characteristics for charge and discharge cycles. The open-circuit voltage of the controlled voltage source is calculated with a non-linear equation, based on the actual SOC of the battery:

$$E = E_0 - K \frac{Q_{nom}}{Q_{nom} - \int_0^t i \, dt} + A e^{-B \int_0^t i \, dt} \tag{3.3.1}$$

Where

Parameter			Value
E	No load voltage	$[V]$	–
i	Battery current	$[A]$	–
E_0	Battery constant voltage when fully-recharged	$[V]$	
K	Polarization voltage	$[V]$	
Q_{nom}	Battery nominal capacity	$[Ah]$	
A	Exponential zone amplitude	$[V]$	
B	Exponential zone time constant inverse	$[Ah^{-1}]$	
R_{batt}	Internal resistance	$[\Omega]$	

Table 3.3.1: Battery parameters

Consequently, the closed-circuit battery voltage is:

$$V_{batt} = E - R_{batt} i \tag{3.3.2}$$

If an initial battery state of charge SOC_0 has to be considered, an initial value of the integral of the battery current can be taken into account:

$$i_{t,0} = (1 - SOC_0) \, Q_{nom} \tag{3.3.3}$$

that represents the amount of electric charge that has to be extracted from the fully charged battery to have the desired initial state of charge SOC_0.

The equation 3.3.1 becomes:

$$E = E_0 - K\frac{Q_{nom}}{Q_{nom}SOC_0 - \int_0^t i\,dt} + Ae^{-B\left[(1-SOC_0)Q_{nom}+\int_0^t i\,dt\right]} \qquad (3.3.4)$$

And the battery actual state of charge:

$$SOC = \frac{Q_{nom}SOC_0 - \int_0^t i\,dt}{Q_{nom}} \qquad (3.3.5)$$

The battery model is based on the following assumption:

- Constant internal resistance during charge and discharge and it does not vary with respect to the current amplitude.

- Model's parameters identified from discharge characteristics and assumed to be the same for charging.

- Capacity independent from the amplitude of the current.

- The temperature does not have effect on the model.

- Self-discharge effect neglected.

- No memory effect of the battery.

And has the following limitations:

- The minimum no-load battery voltage is 0 V and the maximum one is not limited.

- The minimum capacity is 0 Ah and the maximum one is not limited. Therefore a $SOC > 1$ can occur if the battery is overcharged.

These are the limitations of the battery model itself. To avoid the unreasonable conditions of $SOC > 1$, the control system of the torque split strategy, reported in paragraph 3.6, is based on the SOC and it is demanded to maintain the battery SOC within a reasonable (and tunable) range, for example between 0.5 and 0.9 to avoid under and over-charging conditions.

The battery model might be easily improved introducing the effect of the battery temperature on the internal resistance. The battery temperature can be estimated by means of a single degree of freedom thermal model (characterized by its thermal resistance and thermal time constant) and the internal resistance

dissipated power, analogous to that used for the electric motors and reported in equation 2.3.7 and 2.3.9. Furthermore, the torque-split strategy was built taking into account the battery temperature too. At the actual state of the project, due to the lack of the battery experimental data, that improvement was implemented but still not used because it could not be extensively validated.

3.4   ICE model

The Internal Combustion Engine is simply modeled as a torque generator in function of its angular speed and throttle aperture. The maximum torque and the specific fuel consumption (and its related efficiency) were experimentally measured by the manufacturer and reported in Figure 3.4.1.
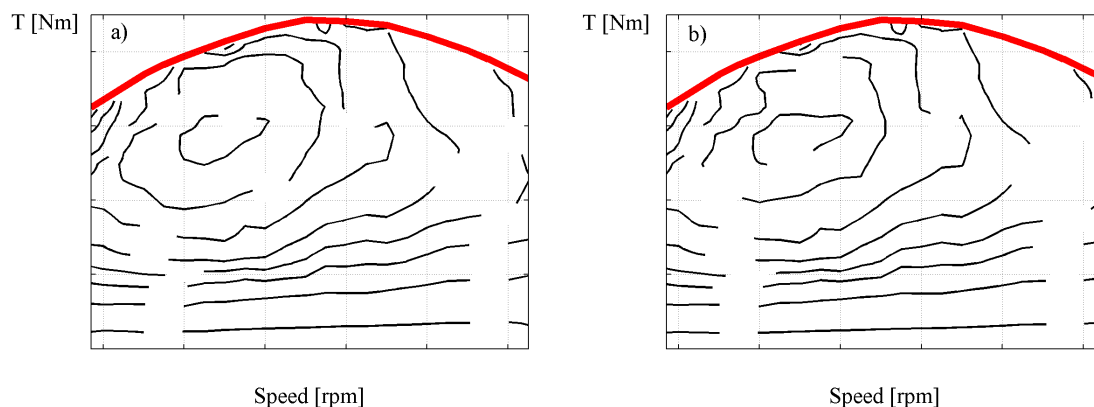
Figure 3.4.1: ICE maximum available driving torque (red) in function of the rotation speed, a) the contour plot of the specific fuel consumption [g/Hph] map for each working point and b) the related engine efficiency

The specific fuel consumption q [g/Hph] of the engine relates the amount of consumed fuel to the generated mechanical energy, so it is an equivalent formulation of the engine efficiency and it is usually defined in function of the mean effective pressure instead of the torque:

$$pme = \frac{2\pi i T}{V} \tag{3.4.1}$$

where T is the engine torque, V the total capacity of the engine and i is a coefficient related to the stroke number of the engine (i=1 for a 2 strokes engine and i=2 for a 4 strokes one).

The vehicle longitudinal controller drives the gear change and the engine throttle to follow the desired longitudinal speed of the vehicle, for example the NEDC

vehicle homologation driving cycle. Therefore, at each time step of the cycle, the working point of the engine on the torque-speed plane is determined, in terms of needed engine torque, pme and angular speed. With a double linear interpolation between the available points of the specific fuel consumption plane, it is possible to determine the instant specific fuel consumption (when it does not match exactly the available data of the engine fuel consumption map). It can be multiplied by the instant engine power to obtain the fuel mass flow:

$$\dot{m}_{fuel}(t) = P(t)\, q(T, \omega) \tag{3.4.2}$$

Finally, integrating in time the fuel mass flow, the total consumed fuel mass is obtained:

$$m_{fuel} = \int_0^T \dot{m}_{fuel}(t)\, dt \tag{3.4.3}$$

In idle conditions, the mechanical power generated by the engine is zero, so this leads to a null fuel rate. By means of a switch in the simulation model, the idle fuel mass flow and a start&stop strategy can be taken into account. Considering the longitudinal distance traveled by the car, the traditional fuel consumption in $[^l/_{100km}]$ or $[^{km}/_l]$ can be easily computed.

The equivalent efficiency of the engine can be computed from the specific fuel consumption, considering its lower heating value $H_{L\,fuel}$:

$$\eta_{ICE} = \frac{1}{H_{L\,fuel}q} \tag{3.4.4}$$

Of course, this leads to correct results just considering the right units for q because the $H_{L\,fuel}$ is generally expressed in $[^{kJ}/_{kg}]$.

In addition, the resistant torque of the engine in over-running mode, when it is driven by the electric motor or in case of engine braking, is introduced. One of the aim of the present work is to explore the effects of the resistant torque of the engine on the potentialities of the hybrid powertrain schematized in Figure 3.1.1, in terms of fuel consumption, dissipated energy, regenerable braking energy and maximum temperatures and performance of its components, determining the best torque-split strategies between the ICE and electric motor.

3.5   Electric motor model

Two different models of the electric motor are implemented within the whole vehicle model. The first one is the analytic model described in paragraph 2.3, that quantifies the stator and rotor losses by means of their mono-phase equivalent impedance. In addition it can take into account the temperature effect on the motor efficiency, varying the stator resistance in function of the copper temperature.

Due to the small amount of available data at this early phase of the project, also a traditional empiric model of the motor is implemented because an experimental steady-state maximum torque curve and the related efficiency map, reported in Figure 3.5.1, was available. The static efficiency map takes into account both the driving and the braking working condition of the electric motor, but it cannot consider the efficiency variation in function of the motor temperature.

In both cases, evaluating the dissipated power from the efficiency map, the motor temperature can be estimated by means of the one degree of freedom thermal model described in equation 2.3.9.
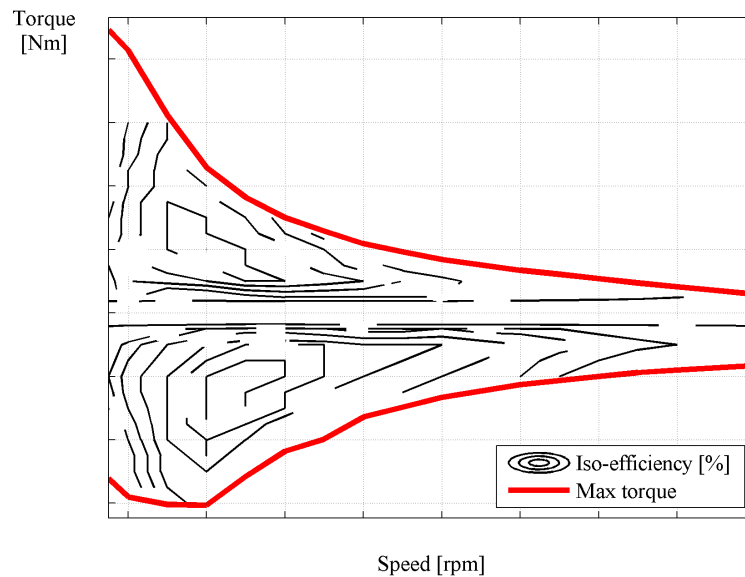
Figure 3.5.1: Electric motor maximum available driving (red, positive) and braking (red, negative) torque in function of the rotation speed, and the contour plot of the efficiency map for each working point.

3.6 Controllers and torque-split strategies

3.6.1 Driver

In order to follow the desired vehicle longitudinal speed, a model of a longitudinal driver is needed. The same low bandwidth PI controller implemented for the full-electric citycar model, reported in Paragraph 2.4, is used. Differently from the previous one, the hybrid vehicle is based on a traditional ICE vehicle, so the driver does not have to simply drive the throttle, but also the clutch and the gear change. A gear change duration of 0.5s is implemented and a maximum (2500 rpm) and

minimum (1000 rpm) engine rotational speed is taken into account for gear up-shift and down-shift respectively.

3.6.2 Torque-split strategies

In the present sustainable city hybrid vehicle, the internal combustion engine is the main prime mover, like the traditional vehicles. In addition, an electric motor can be used braking or helping the traditional ICE to maximize the global efficiency of the whole hybrid powertrain. This aim can be reached defining the proper torque-split strategy between the ICE and the electric motor. The strategy must be able, at each time step and using the input signals measured on the vehicle, to decide the amount of torque that has to be generated by the ICE, the electric motor and the passive brakes in order to follow the desired speed profile, minimizing the energy consumption of the vehicle.
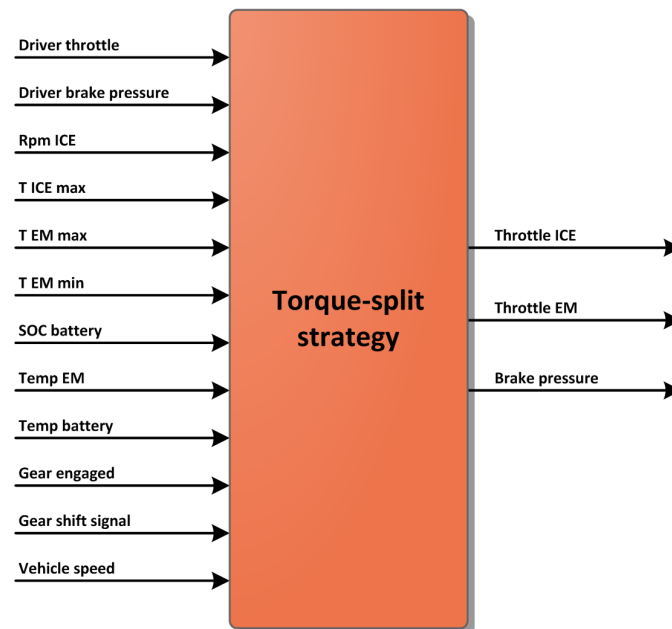
Figure 3.6.1: Torque-split strategy - Overview of inputs and outputs

For this purpose, the strategy schematized in Figure 3.6.1 is proposed, taking into account the input signals:

- Driver throttle: the throttle position command of the driver. It is needed to understand the desired torque that must be generated by the whole powertrain.

- Driver brake pressure

- ICE angular speed

- Maximum ICE torque: in function of the ICE angular speed.

- Maximum electric motor torque: the maximum nominal torque of the electric motor in driving mode, provided by the motor manufacturer. The torque is positive when it has the same direction of the ICE angular speed. Thus, a negative torque occurs in braking condition.

- Minimum electric motor torque: the maximum absolute value of the electric motor torque in braking mode.

- Battery State of Charge (SOC)

- Electric motor temperature

- Battery temperature

- Engaged gear

- Gear shift signal: it is equal to 1 during a gear shift maneuver, otherwise 0.

- Vehicle longitudinal speed

At the beginning, the whole torque requested by the driver have to be calculated. Using a traditional ICE vehicle, the torque at the crankshaft is uniquely generated by the ICE. In case of a parallel hybrid vehicle, the same torque can be generated by an infinite number of combinations between engine and motor torques:

$$T = T_{ICE} + \frac{T_{EM}}{\tau_{belt}}\eta_{belt} \tag{3.6.1}$$

Where τ_{belt} is the transmission ratio of the belt transmission between the crankshaft and the electric motor and η_{belt} is its average efficiency. The strategy must be able to choose the "best" couple to guarantee the desired torque at the crankshaft, maximizing the efficiency of the powertrain. Of course, the torque-split must be feasible, so it must take into account the maximum performance of the electric motor at each time step. In an hybrid vehicle, it can be determined by a number of parameters, like the size of the motor that determines the maximum nominal steady-state driving and braking torques, the motor angular speed, the battery state of charge, the motor and battery temperatures. Once the electric motor maximum performance is known, the best torque-split can be determined, using a strategy based on the working conditions of every component of the hybrid powertrain, estimated by means of the input signal measured on the vehicle.

Summarizing, the strategy consists of the three main parts schematized in Figure 3.6.2:

- Definition of the driver requested torque: knowing the maximum ICE torque curve in function of its angular speed, the requested torque can be calculated as:

$$T_{req} = T_{ICE\,max} * \frac{\alpha_{driver}}{100} \tag{3.6.2}$$

  where α_{driver} is the driver throttle percentage aperture (100% means wide open throttle). In this case, the requested torque is calculated with the throttle percentage aperture with respect to the maximum ICE torque. Further strategies can be added to use the electric motor in addition to the ICE, in order to have an temporary electrical boost when full power is requested by the driver (paragraph 3.6.2.2). Furthermore, instead of a simple product, a non linear look-up table between the throttle aperture α_{driver} and the requested torque T_{req} can be used, in order to better set the transfer function between the throttle and the longitudinal dynamics of the vehicle.

- Definition of the electric motor usage limitations at each time step, based on the conditions of each hybrid powertrain component.

- ICE, electric motor and braking torques definition, in function of the electric motor limitations and the input signals.
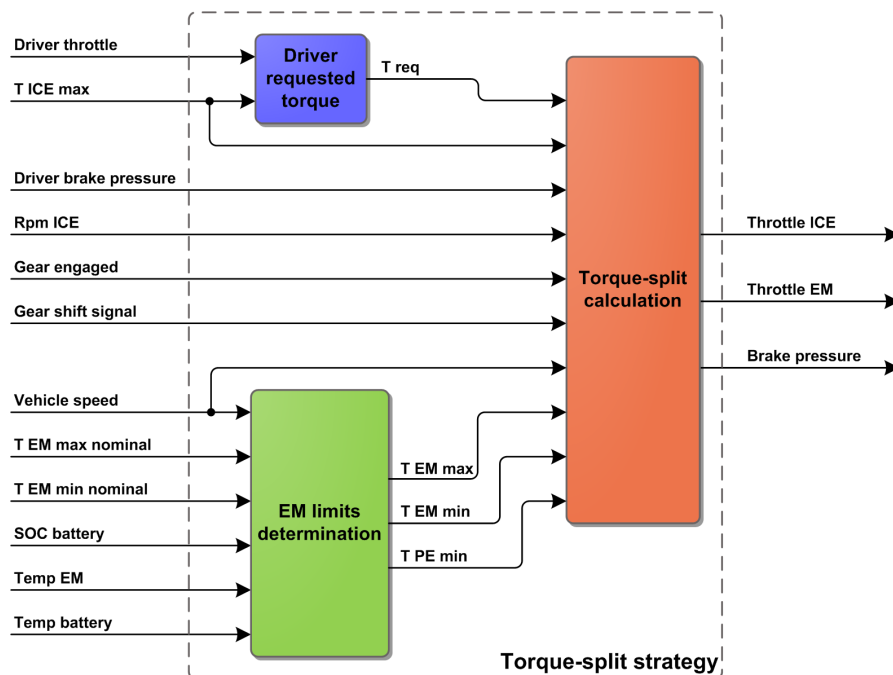
Figure 3.6.2: Torque-split strategy - Main subsystems

3.6.2.1   Electric motor usage limitations

During the run of the vehicle, at each time step the strategy is demanded to calculate the torque that must be generated by the ICE, the electric motor and the passive brakes. The ICE remains the main prime mover of the vehicle and the electric motor can be used at the same time, braking or accelerating the ICE to improve the efficiency of the whole hybrid powertrain. In addition, it can be used to start the vehicle in full-electric mode too. For this purpose, the maximum braking ($T_{EM\,min}$) and driving ($T_{EM\,max}$) torques that can be generated by the electric motor must be calculated, taking into account all the constraints due to the hybrid powertrain components:

- Battery state of charge (SOC): it must stay within an acceptable range to guarantee its functionality, reliability and duration, avoiding under and over-charging. The electric motor cannot generate a braking torque when the battery is fully recharged or similarly, it can not generate a driving torque when the battery reaches the minimum acceptable SOC.

- Battery and EM temperature: the driving strategy must guarantee that the temperature of each component remains lower than the maximum allowable.

In order to satisfy these requirements in a progressive way, a fuzzy-logic strategy with very simple membership functions is implemented. The membership functions, reported in Figure 3.6.3, ranges between 0 and 1 and are used as multiply factors of the steady-state torques of the electric motor. When all the limitations do not occur, all the nominal torque of the electric motor can be used. Therefore, all the membership functions must be equal to 1 and both its maximum and minimum torques are equal to the EM nominal steady-state torques. But when one of the limitations is approaching, at least one of the membership functions decreases, because the maximum driving or braking electric motor torque has to be reduced to guarantee that all the limits are never exceeded. When one of the limits is reached, the related membership function falls to 0 and the electric motor cannot be used any more. The membership functions reported in Figure 3.6.3 are built to guarantee the following acceptable ranges:

- Battery SOC: from 50 to 90 %. The membership function (a) is multiplied to the max EM driving torque, therefore the limitation starts with a SOC less than 60%. When the battery SOC is 50%, the max allowable EM driving torque falls to 0. Similarly, the function (b) multiplies the max EM braking torque, thus the limitation starts with a SOC higher than 80% and when the SOC reaches 90%, the battery cannot be charged any more and the available EM braking torque decreases to 0.
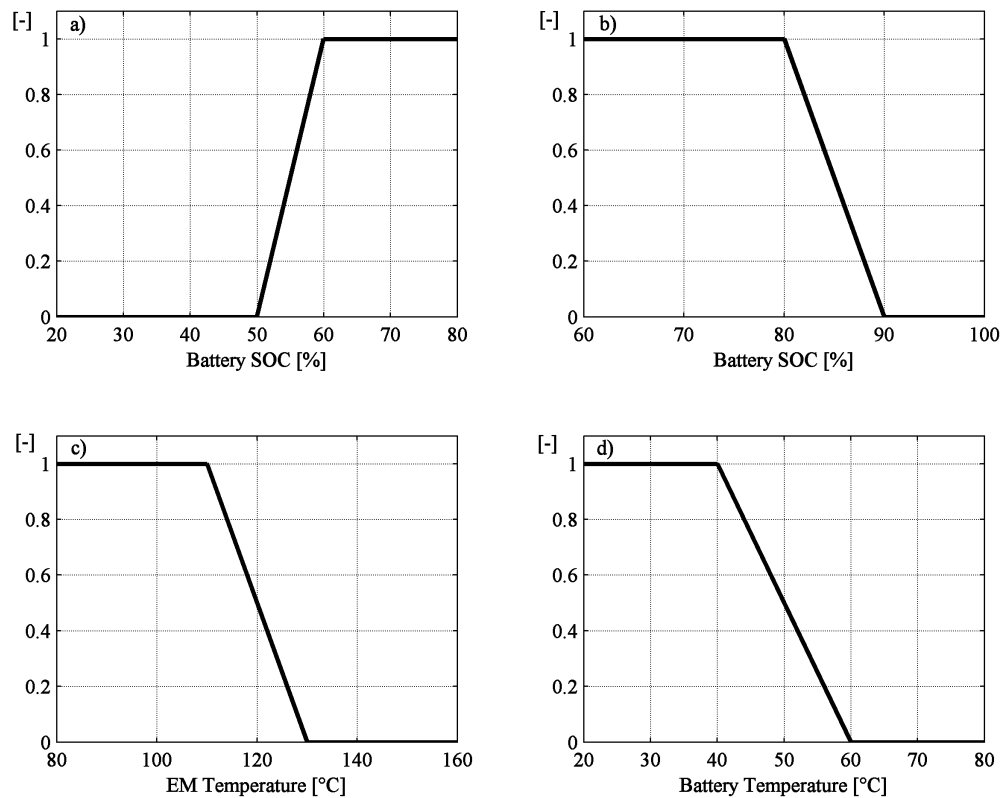
Figure 3.6.3: EM limitations by means of fuzzy logic membership functions: multiply factors of the nominal steady-state EM a) driving torque, b) braking torque, c) - d) both driving and braking torques.

- EM temperature: less than 130°C. When the EM temperature reaches 110°C the limitation starts acting, both on driving and braking torque (membership function c), because the efficiency of the EM (of course less than 1) increases its temperature both in driving and braking phases. When the EM temperature reaches 130 °C, the membership function (c) falls to 0 and the electric motor cannot be used any more.

- Battery temperature: less than 60°C. Similarly to the previous EM temperature limitation, the function (d) limits the battery maximum temperature to 60 °C and starts acting at 50°C, reducing the EM max torque both in driving and braking phases. This is because the battery temperature rise is due to the current flow from and to the battery, due to the electric motor.

The implementation of the fuzzy logic EM limitation within the Simulink model is reported in Figure 3.6.4.

With this approach, additional limitations can be easily added, once additional characteristics of each component of the hybrid powertrain are available during the development of the project.
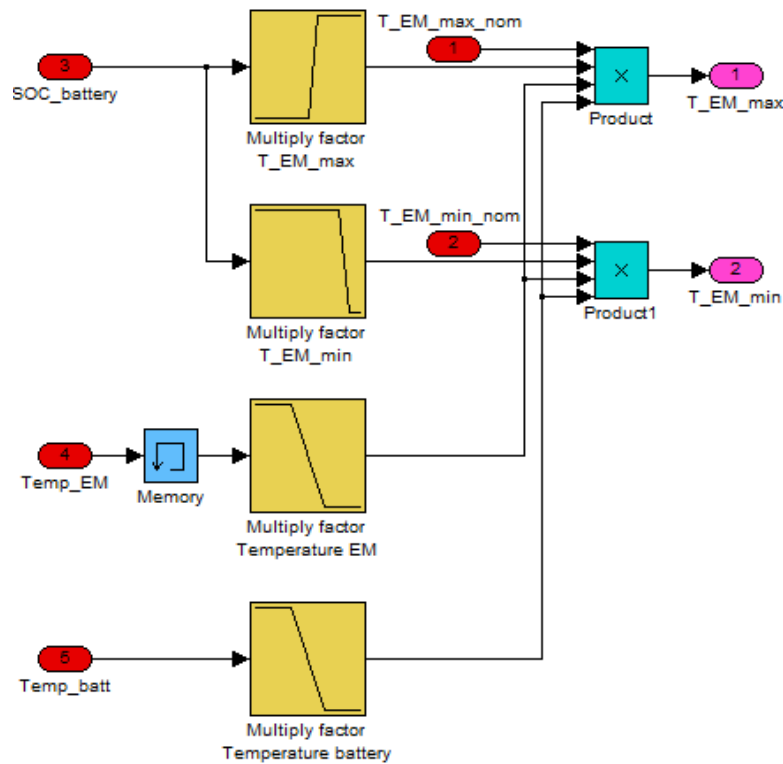
Figure 3.6.4: Torque-split strategy - Implementation of Fuzzy logic EM limitations in Simulink

3.6.2.2 Torque-split calculation

For a better understanding of the hybrid powertrain performance, energy flows and dissipation, different torque-split strategies are implemented and their results are compared:

1. Pure ICE: the reference fuel consumption for each simulation, it is the initial vehicle configuration that has to be improved.

2. Pure ICE with start&stop strategy: the engine is stopped during idle phases.

3. Full-hybrid: the main target is to drive the electric motor to maximize the engine efficiency, but also additional features are implemented:

- Maximize the ICE efficiency by means of the electric motor torque.

- Start&stop strategy: it stops the engine when the car is stationary and would run in idle condition.

- Regenerative braking: to recover the maximum amount of the vehicle kinetic energy, the electric motor can generate a braking torque, using it as an alternator to recharge the battery.

- The possibility to start and run the vehicle in full-electric mode: in order to allow an additional usage of the energy recovered or generated by the electric motor .

4. Simple-hybrid: just start&stop, regenerative braking and full-electric start.

5. Full-hybrid without regenerative braking

ICE and hybrid components dissipated energies

In order to explore the performance and the effectiveness of the different torque-split strategies, all the dissipation in every component of the hybrid powertrain must be evaluated, comparing the fuel consumptions obtained with the full-hybrid and the simple-hybrid strategies. This allows to understand if, using the full-hybrid strategy, the energy saved due to the improvement of the engine average efficiency is bigger with respect to the additional dissipation into the hybrid components (motor, battery, belt transmission) that occur when the energy flow between the ICE, belt, electric motor and battery improves. Or to evaluate the importance of the regenerative braking or the usage of a full-electric driving mode. For this purpose, the energy consumption of different strategies are compared.

The energy dissipated by the battery can be obtained from the battery current, requested or provided by the electric motor, and its internal resistance:

$$E_{diss\,batt} = \int_0^T R_{batt} i_{EM}^2\,(t)\ dt \tag{3.6.3}$$

The mechanical energy dissipated by the belt transmission, between the electric motor and the engine crankshaft, can be calculated from the electric motor torque, with two different definitions when the electric motor is driving ($P_{EM,mec} > 0$) or braking ($P_{EM,mec} < 0$) respectively:

$$\begin{cases} E_{diss\,belt,\,EM\,drive} = \int_0^T (1 - \eta_{belt})\,P_{EM,mec}\,(t)\ dt & (P_{EM,mec} > 0) \\ E_{diss\,belt,\,EM\,brake} = \int_0^T \frac{1-\eta_{belt}}{\eta_{belt}} |P_{EM,mec}\,(t)|\ dt & (P_{EM,mec} < 0) \end{cases} \tag{3.6.4}$$

The whole belt dissipated energy is the sum of the previous energies dissipated in the different conditions:

$$E_{diss\,belt} = E_{diss\,belt,\,EM\,drive} + E_{diss\,belt,\,EM\,brake} \qquad (3.6.5)$$

The energy dissipated by the electric motor can be calculated from the mechanical energy and its efficiency, calculated by means of the static efficiency maps or the analytic model in function of the torque and the angular speed of the motor. Also in this case, the whole electric motor dissipated energy $E_{diss\,EM}$ can be calculated adding the energies dissipated in braking and driving conditions:

$$\begin{cases} E_{diss\,EM,\,drive} = \int_0^T \left(1 - \eta_{EM}\left(T_{EM}, \omega_{EM}\right)\right) P_{EM,\,mec}\left(t\right) dt & \left(P_{EM,\,mec} > 0\right) \\ E_{diss\,EM,\,brake} = \int_0^T \frac{1 - \eta_{EM}\left(T_{EM}, \omega_{EM}\right)}{\eta_{EM}\left(T_{EM}, \omega_{EM}\right)} \left|P_{EM,\,mec}\left(t\right)\right| dt & \left(P_{EM,\,mec} < 0\right) \end{cases}$$
$$(3.6.6)$$

Finally, the energy dissipated by the engine in driving mode can be calculated from the mass fuel rate $(\dot{m}_{fuel})$ consumed on the driving cycle, the lower heating value $(H_{L\,fuel})$ of the gasoline and the resultant positive mechanical energy generated by the engine. The energy dissipated in engine-brake conditions can be calculated simply integrating the braking power, due to the resistant torque of the engine in over-running mode:

$$\begin{cases} E_{diss\,ICE,\,drive} = \int_0^T \frac{P_{EM,\,mec}(t)}{\dot{m}_{fuel}(t)\,H_{L\,fuel}} dt & \left(P_{ICE,\,mec} > 0\right) \\ E_{diss\,ICE,\,brake} = \int_0^T \left|T_{ICE,\,over-running}\left(t\right)\right| \omega_{ICE}\left(t\right) dt & \left(P_{ICE,\,mec} < 0\right) \end{cases}$$
$$(3.6.7)$$

Therefore, the dissipated energy takes into account both the engine efficiency from the static specific fuel consumption map and the fuel consumed in idle conditions. The whole hybrid powertrain dissipated energy can be calculated easily adding all the dissipation:

$$E_{diss,pwt} = E_{diss\,ICE} + E_{diss\,EM} + E_{diss\,belt} + E_{diss\,batt} \qquad (3.6.8)$$

The whole efficiency of the hybrid powertrain, reported in Figure 3.6.5, can be calculated considering the total energy in input and output involved into the hybrid powertrain. The energy inputs are:

- Fuel chemical energy (E_{fuel}), due to the fuel mass and its low heating value:

$$E_{fuel} = m_{fuel} H_{L\,fuel} \qquad (3.6.9)$$

- Mechanical energy from the clutch $(E_{clutch\,neg})$, flowing into the hybrid powertrain during the braking phases. It is dissipated by the engine due to its over-running resistant torque and the remaining part can be regenerated by the electric motor to recharge the battery.

The energy output is the mechanical energy provided to the clutch in driving conditions $(E_{clutch\,pos})$.

Considering a null variation of the internal energy, having an equal battery SOC at the beginning and at the end of the simulation, the energy balance equation of the hybrid powertrain can be written as:

$$E_{fuel} - E_{clutch\,pos} + |E_{clutch\,neg}| - E_{diss,pwt} = 0 \qquad (3.6.10)$$

The whole efficiency of the hybrid powertrain from tank to wheels, related to the dissipation, can be calculated as:

$$\eta_{hyb\,pwt} = \frac{E_{clutch\,pos}}{E_{fuel}} = \frac{E_{fuel} + |E_{clutch\,neg}| - E_{diss,pwt}}{E_{fuel}} \qquad (3.6.11)$$

Finally, it can be noticed that the positive energy provided to the clutch is the energy demanded to move the vehicle. Therefore, knowing the vehicle characteristics, it is related only to the driving cycle.
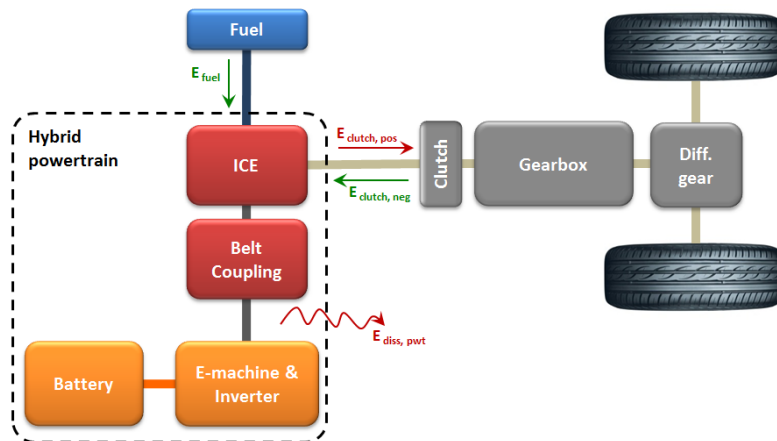
Figure 3.6.5: Hybrid powertrain: the energy inputs are the fuel and the mechanical energy from the clutch, that is the vehicle kinetic energy during the braking phases. The output is the mechanical energy provided to the clutch in driving conditions.

Full-hybrid strategy

Maximization of ICE efficiency After the definition of the electric motor maximum torques, the torque-split strategy has to calculate the amount of torque that must be generated by the ICE, EM and brakes at each time step. The full-hybrid implemented strategy is demanded to use the available electric motor

torque to maximize the ICE efficiency. This idea is based on the assumption that the internal combustion engine is the powertrain component having the lowest global efficiency, while the electrical components generally have higher efficiencies. Furthermore, looking at the maps in Figure 3.4.1, the engine has a good efficiency in working conditions close to the maximum torque curve, while the efficiency falls down rapidly when the motor is not heavily loaded. Unfortunately, the latter is a typical working condition of the homologation driving cycles (NEDC) and more generally, of driving in urban context. In addition, urban driving is characterized by a low average speed with frequent accelerations and decelerations. For this reason, using traditional vehicles it is reasonable to say that a big amount of energy is dissipated into the passive brakes, because the vehicle kinetic energy must be frequently converted into heat to decelerate the car by means of the brakes. Instead, the extra-urban cycles are characterized by higher speed with less frequent accelerations. In this case, the biggest amount of energy is dissipated by the dissipative forces like aerodynamics and tire rolling resistance. In urban driving, a big reduction in energy consumptions can be obtained with a regeneration of the braking energy, because theoretically all the vehicle kinetic energy not dissipated by dissipative forces can be recovered. The regeneration can be obtained using the electric motor as a generator, providing an electrical braking torque instead of the traditional passive brakes.

At each time step, the engine is characterized by its angular speed. The driver requested torque T_{req} is known from the throttle aperture, as reported in equation 3.6.2. The requested torque can be generated by an infinite number of combination between engine and motor torques:

$$T_{req} = T_{ICE} + \frac{T_{EM}}{\tau_{belt}}\eta_{belt} \tag{3.6.12}$$

If the electric motor is not used ($T_{EM} = 0$), the required torque is generated just by the engine (point R in Figure 3.6.6). The engine working point can be moved within the range $\overline{AB}$ by means of the electric motor torque. Choosing the desired engine torque, the needed EM torque is:

$$T_{EM} = (T_{req} - T_{ICE})\frac{\tau_{belt}}{\eta_{belt}} \tag{3.6.13}$$

In particular, with the maximum electric driving torque, the engine working point lies in A, while with the maximum electrical braking torque, the engine working point moves toward B.

The desired engine torque can be chosen to maximize its efficiency within the feasible range $\overline{AB}$ (point P), and the needed electric motor torque can be calculated so that:

$$T_{EM,\eta\,max} = (T_{req} - T_{ICE,\eta\,max})\frac{\tau_{belt}}{\eta_{belt}} \tag{3.6.14}$$
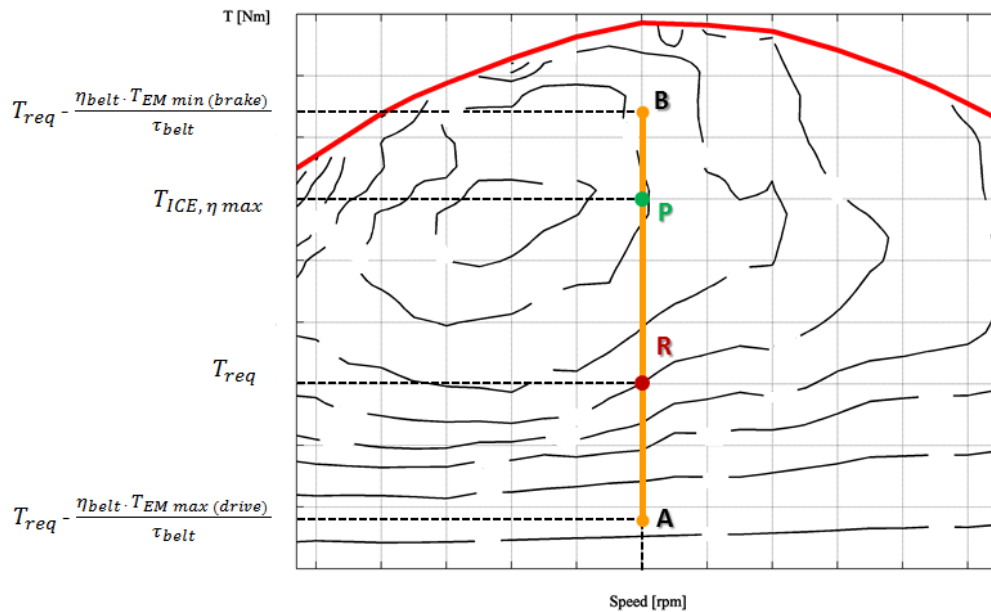
Figure 3.6.6: Torque-split feasible points - R) Required torque T_{req} in pure ICE mode, A) ICE working point with the EM in parallel generating its maximum possible driving torque $T_{EM\,max}$, B) ICE working point with the EM in parallel generating its maximum possible braking torque $T_{EM\,min}$, P) ICE working point with the maximum feasible ICE efficiency. τ_{belt} is the belt transmission ratio between electric motor and the ICE crankshaft and η_{belt} is its average efficiency.

The easiest way to choose the optimal ICE working point is considering its rotational speed and a static engine efficiency map. This method is used in the present analysis but it can be improved considering for example a dynamic efficiency map in function of the engine temperature or other parameters.

In any case, the presented strategy takes into account all the limitations influencing the electric motor available torque, and the ICE can be forced to work in the working point that maximize its efficiency.

Additional features implemented into the full-hybrid strategy are the regenerative braking, start&stop and the possibility to start and to run the vehicle in full-electric mode.

Regenerative braking Theoretically, all the kinetic energy of the vehicle not dissipated by the dissipative forces during the braking phases, can be recovered instead of being dissipated with the passive traditional brakes. Of course, the tires rolling resistance and the aerodynamic forces are present but using the vehicle coast-down coefficients (Table 3.2.1) it is possible to calculate the resistant force

at a typical urban speed of 50 km/h:

$$F_{res} = f_0 + f_2 V_x^2 = \qquad N \tag{3.6.15}$$

Braking the same vehicle with a low deceleration of 0.3g, the module of the braking force is:

$$F_{brake} = ma = \qquad N \tag{3.6.16}$$

It is one order of magnitude higher than the resistant force at 50 km/h. For this reason, it is reasonable to say that the majority of the vehicle kinetic energy is dissipated by the passive brakes during the braking phases.

The implemented strategy brakes the vehicle using the electric motor as much as possible. If the the requested braking torque exceeds the limit of the electric motor (determined by the fuzzy-logic at each time step), the additional requested torque can be generated by the traditional passive brakes. In this way, the amount of regenerated energy is maximized but all the electric motor limitations (due to the battery SOC, temperatures and so on) are taken into account.

The regenerative braking can be very important to reduce the energy consumption of the vehicle, especially in urban driving, taking into account that at low speed the motion resistant forces are small with respect to the requested acceleration and deceleration forces. Furthermore, all the driving cycles representative of urban driving are characterized by frequent accelerations and decelerations, almost without constant speed periods.

For this reason, to have an idea of the amount of the recoverable energy during decelerations, the vehicle kinetic energy is:

$$E_k = \frac{1}{2} m V_x^2 \tag{3.6.17}$$

The resistant motion force can be calculated from the coast-down coefficients of the vehicle (Table 3.2.1) in function of the longitudinal speed:

$$F_{res} = f_0 + f_2 V_x^2 \tag{3.6.18}$$

If all the kinetic energy is recovered and neglecting the efficiency of the electrical powertrain, theoretically all the kinetic energy can be used to move the vehicle at a constant speed equal to the initial V_x, for a longitudinal distance x that equals the work of the resistant forces:

$$E_k = x \, F_{res} \quad \Rightarrow \quad \frac{1}{2} m V_x^2 = x \left(f_0 + f_2 V_x^2 \right) \tag{3.6.19}$$

Therefore, the longitudinal distance that can be traveled using all the recovered kinetic energy is:

$$x = \frac{\frac{m}{2}}{\frac{f_0}{V_x^2} + f_2} \tag{3.6.20}$$

(confidential numerical data are omitted)   56

Plotting the longitudinal distance x in function of the initial speed V_x (Figure 3.6.7) it can be noticed that, for example, the kinetic energy at 50 km/h is equal to the energy needed to travel for more than ....m at a constant speed $V_x = 50\,km/h$. This means that at 50 km/h, the same amount of the kinetic energy of the vehicle, would be dissipated by the resistant forces traveling at the same constant speed for more than ....m. If all the vehicle kinetic energy during just one braking phase from 50km/h could be recovered, the vehicle could travel for additional ....m with the same fuel consumption of the pure-ICE driving mode. Of course, the regeneration efficiency cannot be equal to 1 due to the efficiency of every component of the hybrid powertrain. But this simple example can be useful to understand the importance of the regenerative braking, especially on urban driving cycles with frequent accelerations and decelerations.
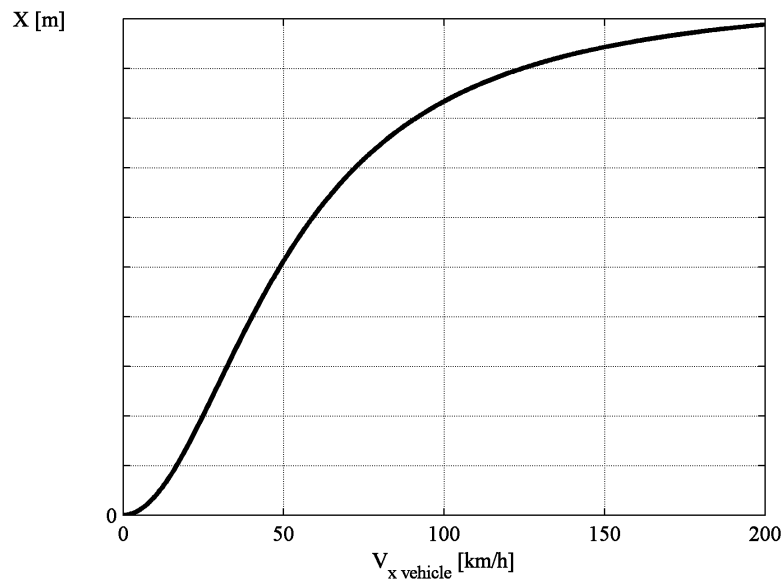
Figure 3.6.7: Longitudinal distance that can be traveled using all the recovered vehicle kinetic energy

Full-electric mode The electric energy stored into the battery can be used, by the electric motor, to generate a driving torque that can help the engine to generate the requested torque T_{req}, as reported in equation 3.6.12. Due to the configuration of the hybrid vehicle, the electric motor is directly coupled with the engine crankshaft by means of a belt transmission, as the alternator on a traditional ICE vehicles. For this reason, when the car is running in full-electric mode, the engine have to rotate too. In this case, in addition to the vehicle resistant force, also the ICE resistant torque in over-running conditions have to be overcome. The

amount of the ICE resistant torque is a key factor that influence the convenience in using the full-electric mode. The effects of different resistant torques are reported in paragraph 3.7.3 and the results of the simulations with the full-hybrid strategy with and without the usage of full-electric driving mode are in paragraph 3.7.4.
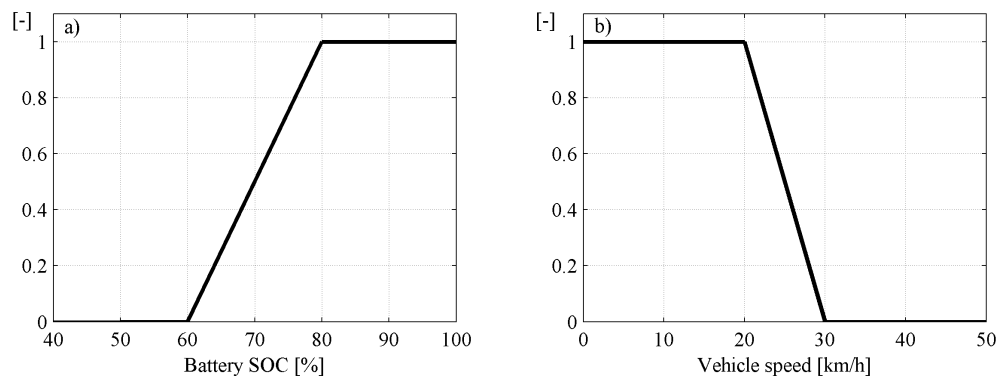
Figure 3.6.8: Fuzzy logic membership functions: multiply factors of the maximum electric motor torque ($T_{EM\,max}$) to define the maximum driver requested torque ($T_{PE\,max}$) to run in full-electric mode.

Defining a maximum driver requested torque ($T_{PE\,max}$) to allow the full-electric run, the control strategy determines that the full-electric mode can occur just if:

$$T_{req} \leq T_{PE\,max} \tag{3.6.21}$$

To have feasible conditions, $T_{PE\,max}$ must be lower than the maximum driving torque of the electric motor ($T_{EM\,max}$ defined in paragraph 3.6.2.1). Further conditions can be added in function of the battery state of charge and the longitudinal vehicle speed. Also in this case a fuzzy-logic can be used: the membership functions are reported in Figure 3.6.8 and the related simulink model in Figure 3.6.9. The maximum driving torque of the electric motor $T_{EM\,max}$ is multiplied by the membership functions to define the full-electric limit torque $T_{PE\,max}$. Using this simple strategy, when:

- $T_{req} \leq T_{PE\,max}$ the torque generated by the engine is $T_{ICE} = 0$ and the vehicle is running in full-electric mode.

- $T_{req} > T_{PE\,max}$ the torque generated by the engine is $T_{ICE} = T_{ICE\,\eta\,max}$, maximizing the engine efficiency.

The electric motor torque is then calculated as in equation 3.6.14.

But when the requested torque T_{req} overcomes the full-electric limit torque $T_{PE\,max}$, the ICE torque would change suddenly from 0 to $T_{ICE\,\eta\,max}$. To avoid
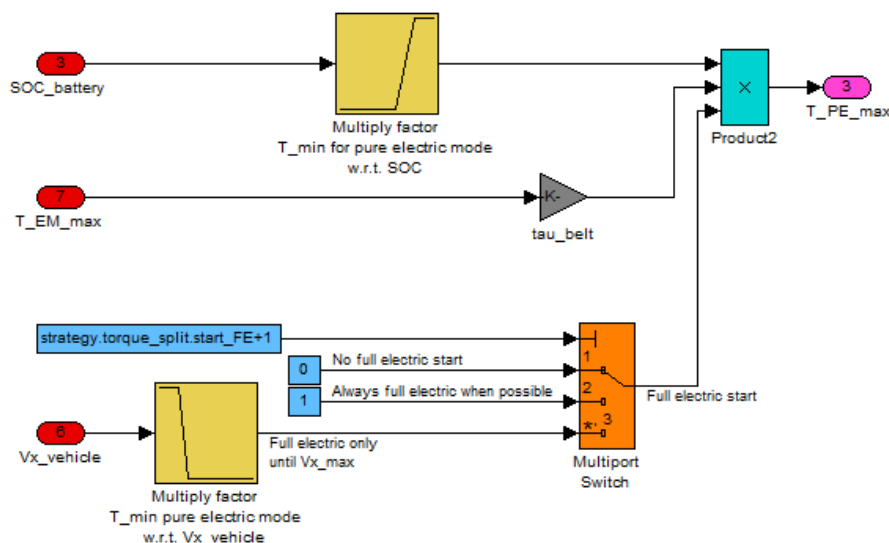
Figure 3.6.9: Simulink implementation of the fuzzy logic membership functions: multiply factors of the maximum electric motor torque ($T_{EM\,max}$) to define the maximum driver requested torque ($T_{PE\,max}$) to run in full-electric mode.

abrupt variations of the ICE driving torque, causing an on-off behavior of the strategy, a linear transition can be introduced to allow a gradual variation of ICE and EM torques. At each time step, the optimal ICE torque $T_{ICE\,\eta\,max}$ is always calculated, also when the car is running in full-electric mode. When the requested torque is approaching the full-electric limit (it can happen both when the T_{req} increases or when the limit torque $T_{PE\,max}$ decreases, for example due to the reduction of the battery SOC), the linear transition can start. The desired amplitude ΔT_{linear} of the linear transition is introduced, so that the engine torque can be calculated as:

- $T_{req} \leq T_{PE\,max} - \Delta T_{linear}$ the torque generated by the engine is $T_{ICE} = 0$.

- $T_{req} > T_{PE\,max}$ the torque generated by the engine is $T_{ICE} = T_{ICE\,\eta\,max}$.

- $T_{PE\,max} - \Delta T_{linear} < T_{req} \leq T_{PE\,max}$ the torque generated by the engine is the linear interpolation between the other conditions, as reported in Equation 3.6.22 and in Figure 3.6.10 (a):

$$T_{ICE} = T_{ICE,\eta\,max}\left(1 - \frac{T_{PE\,max} - T_{req}}{\Delta T_{linear}}\right) \qquad (3.6.22)$$

The same procedure is used with the simple hybrid strategy, changing from the full-electric mode to the pure-ICE condition, reported in Figure 3.6.10 (b).
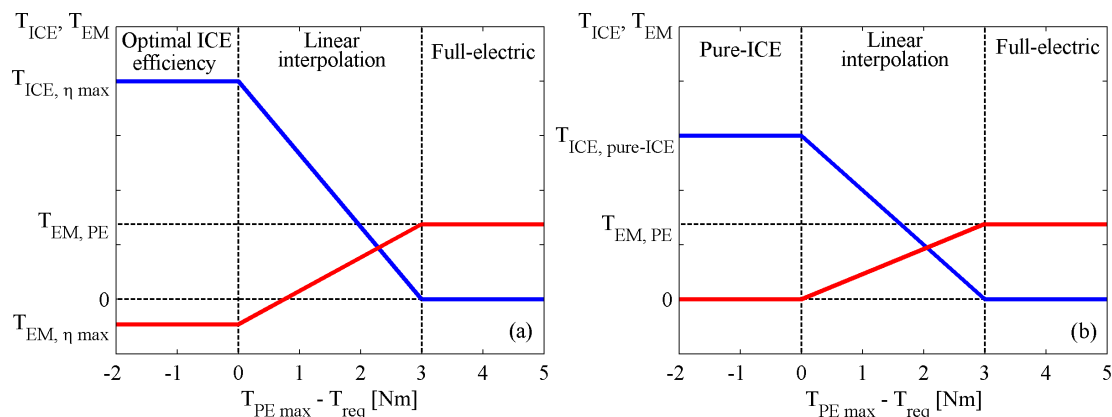
Figure 3.6.10: Linear interpolation between full-electric mode ($T_{EM,PE}$) and (a) optimal ICE efficiency working conditions with full-hybrid strategy ($T_{ICE,\eta max}$; $T_{EM,\eta max}$) or (b) pure-ICE ($T_{ICE,pure-ICE}$) with simple-hybrid strategy. ICE (blue) and EM (red) torques are reported, and an amplitude $\Delta T_{linear} = 3\,Nm$ of the linear transition is considered. Usually when the engine is low loaded, to maximize the ICE efficiency ($T_{ICE,\eta max}$) a braking torque of the electric motor is needed ($T_{EM,\eta max}$), as showed in Figure 3.6.6 too.

Electric boost The electric motor can be used not only to improve the efficiency of the internal combustion engine, but it can provide additional torque, in parallel with the engine, to improve the maximum vehicle performance when the driver requests the full power. Also in this case, a gradual and linear rise of the electric motor torque is necessary. For this reason, an additional condition to calculate the driver requested torque can be added to the equation 3.6.2: when the throttle aperture (α_{driver}) is higher than the throttle aperture for electric boost activation (α_{boost}, for example 90%), the requested torque is calculated adding to the engine maximum torque the contribution of the electric motor torque:

$$\begin{cases} T_{req} = T_{ICE\,max} * \frac{\alpha_{driver}}{100} & (\alpha_{driver} \leq \alpha_{boost}) \\ T_{req} = \left[T_{ICE\,max} + \frac{\eta_{belt}}{\tau_{belt}} T_{EM\,max} \frac{\alpha_{driver}-\alpha_{boost}}{100-\alpha_{boost}} \right] * \frac{\alpha_{driver}}{100} & (\alpha_{driver} > \alpha_{boost}) \end{cases}$$

$$(3.6.23)$$

The contribution of the electric motor torque starts to be positive when the throttle aperture $\alpha_{driver} > \alpha_{boost}$ and grows linearly until $\alpha_{driver} = 100\%$ when the maximum electric motor torque is added to the maximum engine torque. Of course, $T_{EM\,max}$ takes into account all the electric motor limitations reported in paragraph 3.6.2.1.

3.7   Test procedure and results

The aim of the present thesis is to evaluate, by means of a simulation model, the performance of a parallel hybrid vehicle having the configuration proposed in Figure 3.1.1. The reference driving cycle is the NEDC, commonly used by the car manufacturers as reference for fuel consumption homologation of their vehicles. Simulating the vehicle running along the NEDC, the effects of the main parameters that characterize the hybrid powertrain can be evaluated, and the results are commonly considered as representative of the typical average usage of the vehicles. In any case, the effects are then quantified more in detail considering not only the NEDC but also other cycles (like the NYCC, FTP 75, JPN 15, reported in Figure 2.5.1 and in Table 2.5.1), representative of additional different usage of the vehicles. They are commonly used by the manufacturers, in parallel with the NEDC, to evaluate more in detail the real-world fuel consumptions and performance of their vehicles, considering a wider amount of vehicle usage conditions. The effects of the more critical parameters can be evaluated, leading to the possible modification to the proposed initial configuration.

First of all, a validation of the model, based on the experimental results is needed. The fuel consumption obtained with the model on the NEDC driving cycle, can be compared with the fuel consumption declared by the car manufacturers in combined conditions, or with specific data provided in case of a prototype is analyzed.

Once the model is validated and it is representative of the real vehicle, different simulations are performed to evaluate, mainly on fuel consumption and energy dissipation, the effects on the NEDC of:

1. Different torque-split hybrid strategies

2. ICE resistant torque in over-running mode and regenerative braking

3. Usage of full electric driving mode

4. Thermal behavior of the electric motor and environment temperature

5. Additional driving cycles

The effects of the parameters in points 1, 2, 3, 4 are evaluated on NEDC driving cycle, because it is the reference driving cycle used for vehicle homologation. In the last point (5), the effectiveness of the different torque-split strategies is evaluated on the other commonly used driving cycles ECE, NYCC, FTP75, JPN15.

3.7.1 Pure-ICE Validation on the NEDC

First of all, a validation of the vehicle model based on experimental results is needed, to guarantee the correct correspondence between the model and the real vehicle.
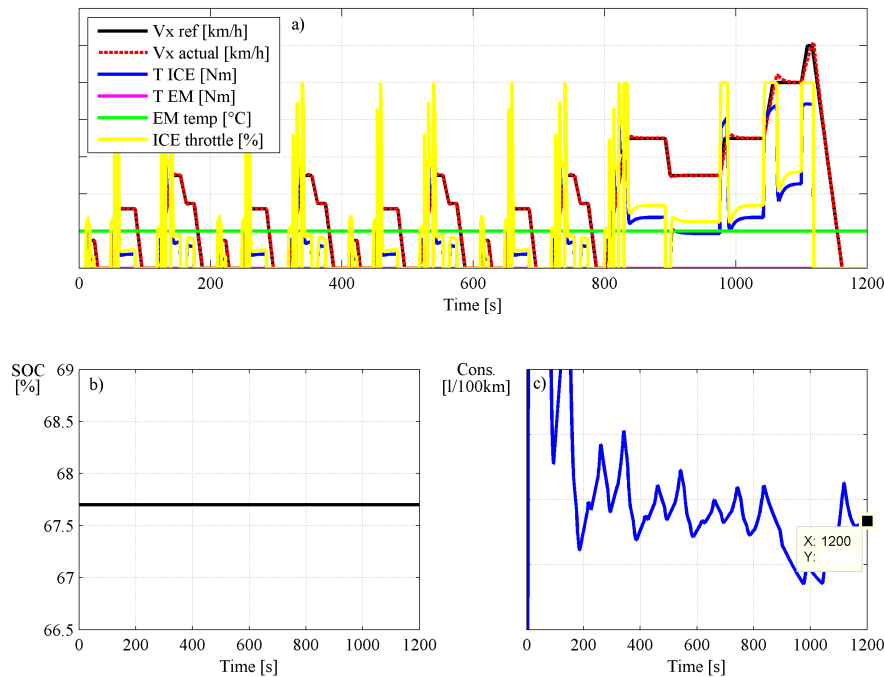
Figure 3.7.1: Pure-ICE fuel consumption validation on NEDC - a) Reference (black) and actual (red) vehicle speeds, ICE (blue) and EM (magenta) torques, EM temperature (green) and ICE throttle command (yellow) - b) Battery state of charge (SOC) - c) ICE average fuel consumption: the average fuel consumption on the whole NEDC driving cycle is calculated at the end of the cycle. The calculated vehicle fuel consumption on the NEDC is   l/100km, comparable with the reference   l/100km, declared by the vehicle manufacturer.

The vehicle parameters in table 2.2.1 are taken into account and the declared fuel consumption on the NEDC of   l/100km is considered as a reference. The fuel consumption was obtained by the car manufacturer without a start&stop strategy and, of course, driving the car in pure-ICE mode. The results of the simulation model are reported in Figure 3.7.1 and the resultant fuel consumption is   l/100km, comparable with the declared one. Of course, the electric motor is not used, therefore the battery state of charge (b) does not vary, as well as its temperature (a).

3.7.2 Effects of the different control strategies on the NEDC

The fuel consumption on the NEDC driving cycle is calculated using the different driving strategies reported in paragraph 3.6.2.2:

1. Pure ICE

2. Pure ICE with start&stop strategy

3. Simple hybrid

4. Full-hybrid

5. Full-hybrid without regenerative braking
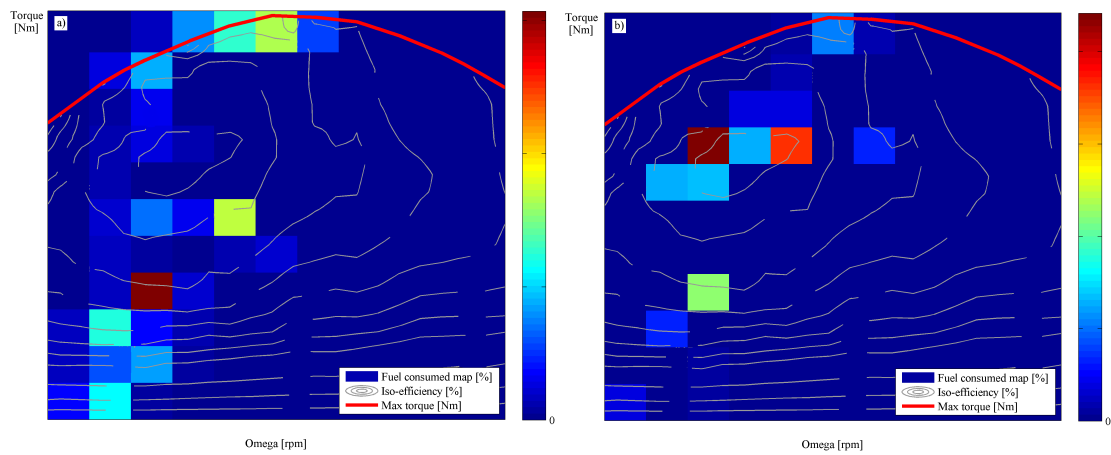
Figure 3.7.2: ICE fuel consumed map on NEDC, with the ICE resistant torques in over-running mode $T_{res} = 10\% \, T_{ICE\,max}$: for each working zone, the percentage of fuel consumed with respect to the total one is superimposed to the iso-efficiency contour curves of the internal combustion engine, for pure-ICE (a) and full-hybrid (b) strategies. The ICE average efficiency rises from   % (a) to   % (b).

In order to better visualize the engine most used working zones and the effectiveness of the hybrid strategies, a map showing the percentage of the consumed energy (linearly proportional to the fuel, by means of its lower heating value) in each zone can be superimposed to the engine efficiency map. In Figure 3.7.2 are compared the results related to the pure-ICE mode (a) and the full-hybrid strategy (b) on the NEDC driving cycle. In the latter case, the usage of the electric motor is demanded to force the internal combustion engine to work in high efficiency working points. The biggest amount of energy is consumed in very high efficiency
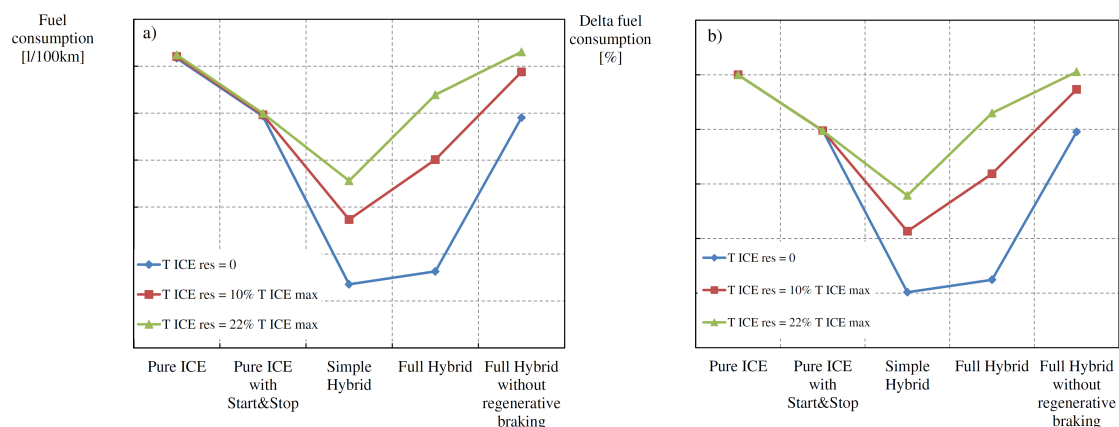
Figure 3.7.3: a) ICE fuel consumption on NEDC driving cycle and b) percentage difference with respect to the pure-ICE driving mode, with ICE resistant torques in over-running mode $T_{res} = 0$ (blue), $T_{res} = 10\% \, T_{ICE\,max}$ (red), $T_{res} = 22\% \, T_{ICE\,max}$ (green).

working zones (red squares) and the average engine efficiency rises from   % to   %, with a maximum possible engine efficiency of about   %.

The fuel consumption on the NEDC in function of the torque split strategy, reported in Figure 3.7.3, show that a fuel consumption reduction of about   % can be obtained just with a start&stop strategy on the traditional pure-ICE vehicle. Experimentally, a reduction between   % and   % was measured by the manufacturer. The difference is due to the additional fuel consumption at each engine start, not considered at the moment within the vehicle model. The ICE resistant torque has no effects, as expected, on the fuel consumptions in pure-ICE mode with and without the start&stop strategy, because the engine works in over-running conditions just during the braking phases and the vehicle kinetic energy would be dissipated in any case by the passive brakes.

The lowest fuel consumption is obtained using the simple-hybrid torque-split strategy, with every ICE resistant torque in over-running mode. Improving the ICE resistant torque, the fuel consumption increases because the electric motor needs to generate an additional torque to drive the car during the full-electric driving phases. In addition, part of the vehicle kinetic energy is dissipated by the ICE resistant torque and it can not be regenerated by the electric motor.

A slightly higher fuel consumption is obtained with the full-hybrid strategy (with respect to the simple-hybrid) with $T_{res} = 0$ and furthermore, it is more influenced by the ICE resistant torque. This is due to the additional energy dissipation because of the bigger energy flow between engine, belt, electric motor, battery and vice-versa.
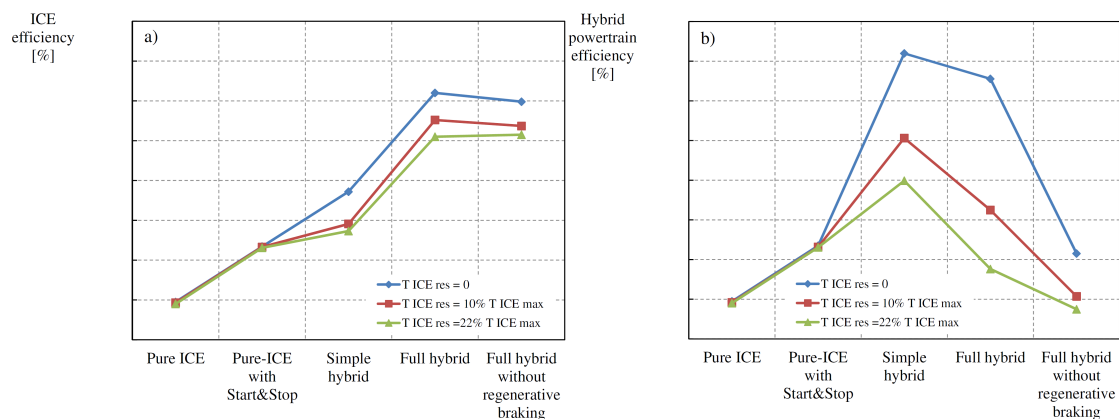
Figure 3.7.4: Average efficiency of the ICE (a) and of the whole hybrid powertrain (b) on the NEDC driving cycle, with the ICE resistant torques in over-running mode $T_{res} = 0$ (blue), $T_{res} = 10\% \, T_{ICE\,max}$ (red), $T_{res} = 22\% \, T_{ICE\,max}$ (green).

Figure 3.7.4 shows the ICE and the whole hybrid powertrain average efficiencies calculated in equation 3.6.11, on the NEDC. Despite the engine efficiency using the full-hybrid strategy is close to the maximum, as shown in Figure 3.7.2 too, the global efficiency of the hybrid powertrain is maximized with the simple-hybrid strategy.

This effect can be explained inspecting in Figure 3.7.5 the energy dissipated by the engine (a), by the hybrid components (b) and the total one (c). The energies are calculated with equations 3.6.3-3.6.8 and normalized with respect to the ICE dissipated energy in pure-ICE driving mode.

With the pure-ICE driving modes (with and without the start&stop strategy), the hybrid components are not used, therefore all the energy is dissipated by the engine. Having the same driving cycle, the mechanical energy needed to move the vehicle is the same in all cases ($E_{clutch\,pos}$ in equations 3.6.10-3.6.11) and the input energy from the clutch ($E_{clutch\,neg}$) is related to the engine resistant torque and to the usage of regenerative braking. Therefore a reduction of the whole dissipated energy (ICE+Hybrid components) means a reduction in fuel consumption, as can be noticed comparing the fuel consumption in Figure 3.7.3 (a) and the total energy dissipation in Figure 3.7.5 (c).

With the full-hybrid strategy and $T_{res} = 0$, the energy dissipated by the engine is slightly lower than that dissipated with the simple-hybrid strategy, due to the bigger efficiency of the ICE. But the total dissipated energy is higher due to the additional dissipation in hybrid components.

The full-hybrid strategy without regenerative braking is not effective and a slight reduction in fuel consumption with respect to the pure-ICE mode can be
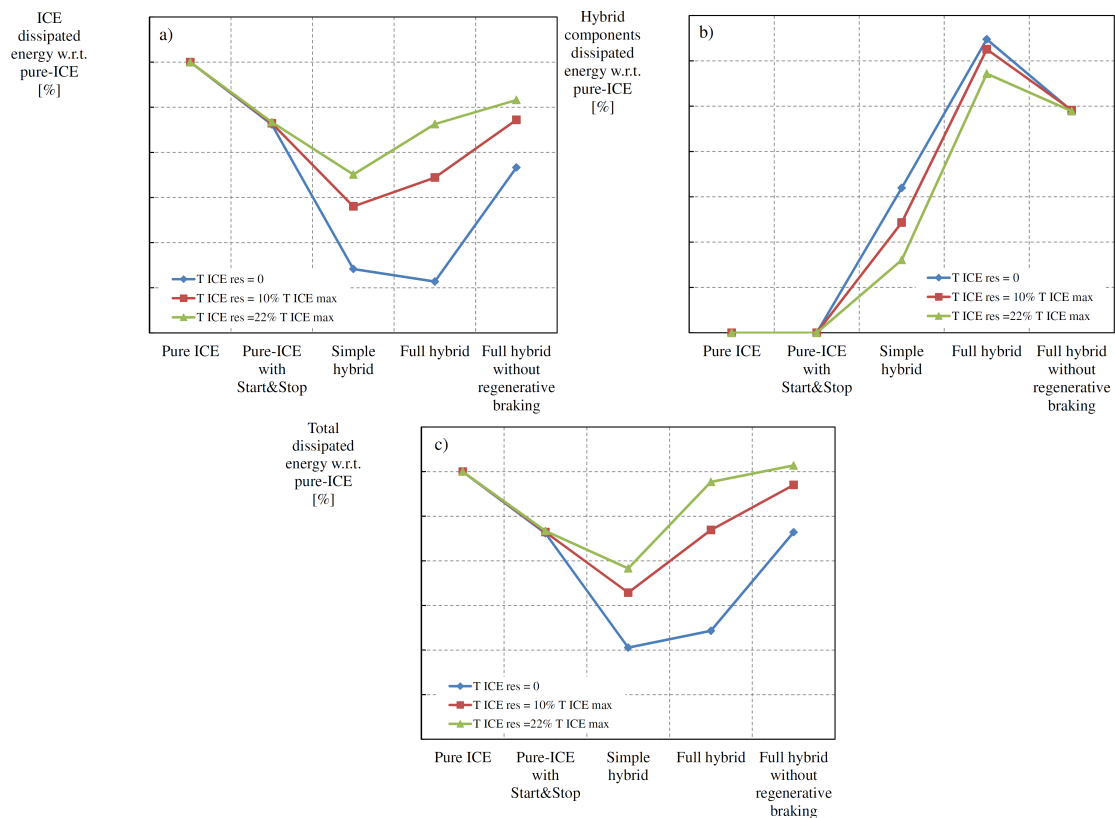
Figure 3.7.5: Dissipated energies on NEDC driving cycle, normalized with respect to the whole energy dissipated by the engine in pure-ICE driving mode. Energy dissipated by the engine (a), by the hybrid components (b) and the total (c), with ICE resistant torques in over-running mode $T_{res} = 0$ (blue), $T_{res} = 10\% \, T_{ICE\,max}$ (red), $T_{res} = 22\% \, T_{ICE\,max}$ (green).

obtained just with low ICE resistant torque. But also without engine resistant torque, the advantage is lower than using a simple start&stop strategy. The NEDC driving cycle is characterized by a very low speed in the first urban section, with frequent acceleration and decelerations. In this conditions, the vehicle energy dissipation is mainly due to the passive brakes, that dissipates the vehicle kinetic energy to decelerate the vehicle. Instead, in case of high and constant speed, the energy is mainly dissipated by the dissipative forces acting on the vehicle, like aerodynamics and rolling resistant forces. For this reason, the most effective feature of a hybrid vehicle on urban driving cycle is the regenerative braking.

Therefore, the best solution seems to be the simple hybrid strategy because it implements the regenerative braking and uses the regenerated energy to drive the car in full-electric mode, minimizing at the same time the usage of the hybrid

components, reducing the dissipation and increasing the global efficiency of the powertrain. The effectiveness of the full-hybrid strategy seems to be slightly lower with low engine resistant torque and decreases rapidly when the resistant torque rises. But probably it is related to the specific configuration of the hybrid powertrain and to the specific efficiencies of each component of the hybrid powertrain, from the electric hardware to the engine efficiency map. In this case, a small and high-efficiency engine is considered, specifically designed for small urban vehicles and the difference in ICE average efficiency between the pure-ICE and the full-hybrid strategies is just about   %. Furthermore, the full-hybrid strategy might be the best one, using better batteries and electric motors, a worst engine and the electric motor directly connected to the gearbox, allowing to avoid the engine resistant torque simply disengaging the clutch.

3.7.3 Effects on the NEDC of the ICE resistant torque in over-running mode and the regenerative braking

Using the powertrain configuration schematized in Figure 3.1.1, with the electric motor in parallel with the engine by means of a belt transmission, the engine and the electric motor cannot be decoupled. For this reason, when the engine is in over-running condition, during braking phases or when it is driven by the electric motor, it dissipates energy due to its resistant torque. As already anticipated in paragraph 3.7.2, an increase of the engine resistant torque causes an increase of the dissipation within the hybrid powertrain, thus an increase of fuel consumption and a fall of the effectiveness of the hybrid strategies. On the other hand, it has no effects on the pure-ICE driving mode, both with and without the start&stop strategy.

The effects of the engine resistant torque on the effectiveness of each torque-split strategy can be analyzed observing the fuel consumptions in function of the resistant torques, reported in Figure 3.7.6. The pure-ICE strategies are not influenced when the resistant torque increases, having almost constant fuel consumptions, while the hybrid strategies performance decrease. The best strategy for this vehicle is the simple-hybrid because it always generates the lowest fuel consumptions, with a reduction of about   % with respect to the pure-ICE mode with the maximum engine resistant torque (Figures 3.7.3, 3.7.6). Furthermore, it is less influenced by the resistant torque, with respect to the full-hybrid. In addition, with the maximum considered resistant torque, the latter has a slightly higher fuel consumption than the pure-ICE with a simple start&stop strategy.

Finally, the electrical energy regenerated by means of the electric motor decreases when the resistant torque increase, as reported in Figure 3.7.7 (c-d).

The vehicle kinetic energy variation (ΔE_c) can be dissipated or regenerated
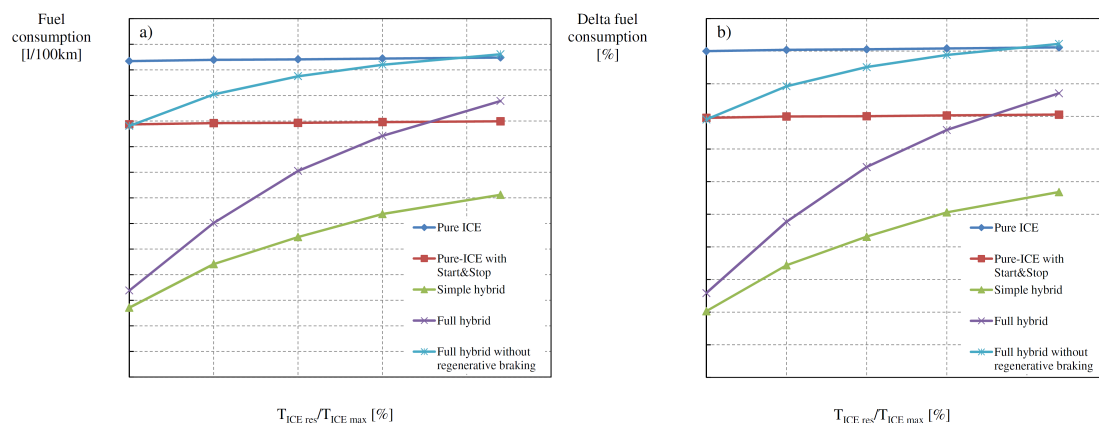
Figure 3.7.6: Fuel consumption on the NEDC driving cycle (a) and the difference with respect to the pure-ICE driving mode (b) in function of the ICE resistant torque in over-running mode.

during the braking phases:

$$\Delta E_c = \tfrac{1}{2}m\left(V_{x,i}^2 - V_{x,f}^2\right) = E_{diss}|_{F_{res,\,brake}} + E_{diss}|_{T_{ICE\,res}} + E_{diss}|_{T_{brake}} + E_{reg}|_{T_{EM\,res}} \tag{3.7.1}$$

Where:

$$\begin{cases} E_{diss}|_{F_{res,\,brake}} & = \int_0^T F_{res,\,brake}\left(V_x\right) \cdot V_x\left(t\right) dt \\ E_{diss}|_{T_{ICE\,res}} & = \int_0^T T_{ICE\,res} \cdot \omega_{ICE}\left(V_x, \tau_{gear}\right) dt \\ E_{diss}|_{T_{brake}} & = \int_0^T T_{brake}\omega_{wheels}\left(V_x\right) dt \\ E_{reg}|_{T_{EM\,res}} & = \int_0^T T_{reg}\omega_{EM}\left(V_x, \tau_{gear}, \tau_{belt}\right) dt \end{cases} \tag{3.7.2}$$

The dissipative resistant force (F_{res}) both during the braking ($F_{res,\,brake}$) and driving phases ($F_{res,\,drive}$), are due to aerodynamics, rolling resistance, gearbox resistance and all the frictions within the components downstream of the clutch. Additional dissipation are due to the traditional passive brakes ($E_{diss}|_{T_{brake}}$) if used, and the engine resistant torques ($E_{diss}|_{T_{ICE\,res}}$). F_{res} can be calculated from the coast-down coefficients of the vehicle in function of the vehicle longitudinal speed V_x:

$$F_{res} = f_0 + f_2 V_x^2 \tag{3.7.3}$$

The longitudinal vehicle speed is defined by the driving cycle (for example the NEDC), as well as the engaged gear. Therefore, the energy dissipated by the dissipative resistant forces during braking phases ($E_{diss}|_{F_{res,\,brake}}$) is imposed by the driving cycle and the vehicle characteristics. For this reason, knowing the initial ($V_{x,i}$) and final ($V_{x,f}$) vehicle speed, for each braking phase of the driving cycle the sum

$$E_{diss}|_{T_{ICE\,res}} + E_{diss}|_{T_{brake}} + E_{reg}|_{T_{EM\,res}} = k \tag{3.7.4}$$

is constant, defining the amount of energy that can be theoretically regenerated. For this reason, if the passive brakes are not used, the amount of possible regenerable energy decreases when the engine resistant torque increases.

Furthermore, the sum of the ICE dissipated energy in over-running mode ($E_{diss}|_{T_{ICE\,res}}$) and the regenerable energy ($E_{reg}|_{T_{EM\,res}}$) is the total energy incoming into the hybrid powertrain ($E_{clutch\,neg}$) from the clutch, reported in Figure 3.6.5:

$$E_{diss}|_{T_{ICE\,res}} + E_{reg}|_{T_{EM\,res}} = |E_{clutch\,neg}| \tag{3.7.5}$$

It is the maximum energy that might be theoretically regenerated with no engine resistant torque and if the passive brakes are not used.
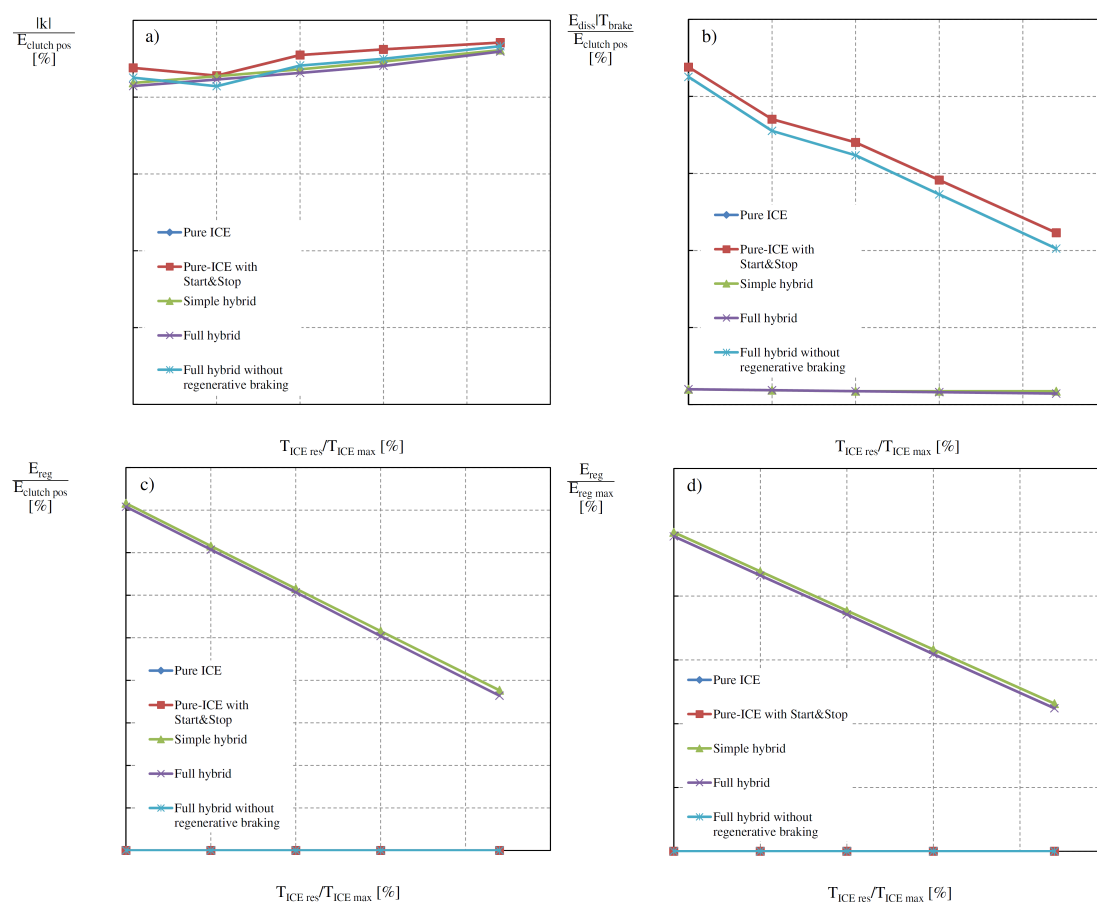
Figure 3.7.7: Regenerative braking on the NEDC: (a) Maximum percentage of the energy needed to move the car ($E_{clutch\,pos}$) that can be regenerated. (b) Energy dissipated by the passive brakes, normalized with respect to $E_{clutch\,pos}$. Regenerated electrical energy on the NEDC driving cycle, normalized with respect to $E_{clutch\,pos}$ (c) and the maximum obtained with the simple-hybrid strategy with no engine resistant torque in over-running mode (d).

The energy outgoing from the hybrid powertrain ($E_{clutch\,pos}$) is exactly the energy needed to move the car during accelerations and constant speed parts. The ratio between the incoming ($E_{clutch\,neg}$) and outgoing ($E_{clutch\,pos}$) mechanical energy to and from the hybrid powertrain represents the percentage of the maximum theoretical energy regenerable on the driving cycle, without engine resistant torque and passive brake usage. It is not influenced by the ICE resistant torque and, for the NEDC, it is reported in Figure 3.7.7 (a).

The percentage of the energy dissipated with the passive brakes is reported in Figure 3.7.7 (b): it is positive just using the strategies without the regenerative braking and decreases when the ICE resistant torque grows up. A small amount of braking usage is present also with the regenerative braking, because the passive brakes are used when the electric motor cannot brake the vehicle enough, due to its limitations in function of the battery SOC or when its temperature grows up too much. But the amount of dissipated energy is small, about   % of the total mechanical energy needed to move the car along the driving cycle.

Another limitation to the possible regenerable energy for each braking phase is due to the maximum electric motor braking torque (called $T_{EM\,min}$, because for sign convention, braking torques are negative). For this reason $T_{res} \leq |T_{EM\,min}|$ and for high decelerations, an additional braking force must be generated with the passive brakes. In this case, increasing the engine resistant torque, the passive brake force can be reduced maintaining constant the maximum regenerable energy. But with low decelerations, typical of the NEDC, the passive brakes are never used and an increase of the engine resistant torque reduces linearly the maximum possible regenerable energy, as shown clearly in Figure 3.7.7 (c-d).

3.7.4 Effects of using a full-electric driving mode on the NEDC

Taking into account the hybrid strategies, it is possible to explore their performance with different limits in using the full-electric mode to start the vehicle. The maximum speed to allow the full-electric mode can be set by means of the fuzzy-logic membership function in Figure 3.6.8 (b).

The simple-hybrid fuel consumption variation with respect to the pure-ICE driving mode, in function of the speed limit, is reported in Figure 3.7.8 (a). The fuel reduction of the strategy without the usage of the full-electric driving mode is about   % and it is not affected by the engine resistant torque. This is expected because the simple-hybrid strategy has the start&stop, the regenerative braking and the electric motor can work together with the ICE, "helping" it in during the boost phases. An additional maximum decrease of about   % can be obtained using the full-electric mode with no engine resistant torque, until a longitudinal speed of 120

km/h, while the decrease is just % with $T_{ICE\,res} = 10\%\,T_{ICE\,max}$ and % with $T_{ICE\,res} = 22\%\,T_{ICE\,max}$. The maximum vehicle speed of the NEDC is 120 km/h, therefore it means to use the full-electric mode without speed limitations, whenever possible due to the other limitations. The simulations were made considering the same initial battery state-of-charge $SOC_{init} = 75\%$.
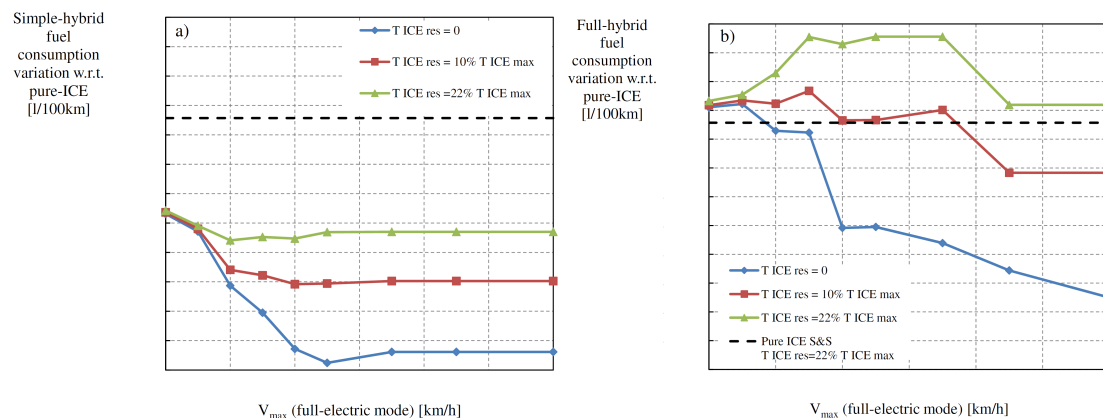
Figure 3.7.8: Fuel consumption variation on the NEDC driving cycle, with respect to the pure-ICE driving mode, in function of the maximum vehicle speed to allow the full-electric driving mode. Related to the simple-hybrid (a) and the full-hybrid strategy (b), with ICE resistant torques in over-running mode $T_{res} = 0$ (blue), $T_{res} = 10\%\,T_{ICE\,max}$ (red), $T_{res} = 22\%\,T_{ICE\,max}$ (green).

The advantage in using the full-electric start of the vehicle falls down when the engine resistant torque increases, because the electric motor has to move the vehicle and, at the same time, to overcome the engine resistance too, dissipating energy. This effect is due to the configuration of the analyzed hybrid powertrain, where the engine, in parallel to the electric motor by means of a belt transmission, cannot be decoupled.

The results of the simple-hybrid strategy on the NEDC in Figure 3.7.9 show that, without the full-electric start, the regenerated energy during the braking phases charges the battery, but that energy remains into the battery reaching a very high state of charge, close to the maximum (90%) allowed by the fuzzy-logic strategy. Therefore, the regenerated energy cannot be used to reduce the fuel consumption during the starting phases and it is used just during the boost phases, mainly for the high speed acceleration in the extra-urban part of the NEDC driving cycle, when the driver requests the maximum power. But to increase the powertrain efficiency, the full-electric start at low speed is more effective because in these conditions, the engine has the lowest efficiency. Instead, during the boost phases the engine is heavily loaded and generally it has high efficiency.

Figure 3.7.9: Simple hybrid results on the NEDC with no full-electric driving mode. a) Reference (black) and actual (red) vehicle speeds, ICE (blue) and EM (magenta) torques, EM temperature (green) and ICE throttle command (yellow). b) Battery state of charge (SOC). c) ICE average fuel consumption: the average fuel consumption on the whole NEDC driving cycle is calculated at the end of the cycle.

The full hybrid strategy, reported in Figure 3.7.8 (b), is more influenced by the engine resistant torque and the usage of the full-electric mode. The energy to recharge the battery comes not only from the vehicle kinetic energy by means of the regenerative braking, but also from the engine. This is because on the NEDC driving cycle, the engine is generally low-loaded and to improve its efficiency, the electric motor has to provide a braking torque, recharging the battery. For this reason, the battery is recharged faster (Figure 3.7.10) and once it reaches the maximum SOC, both the maximum ICE efficiency and the regenerative braking cannot be used any more. If the battery energy cannot be used by means of the full-electric mode, the strategy moves to the pure-ICE mode with start&stop and the fuel consumption difference from the pure-ICE with start&stop is due to the SOC variation between the beginning and the end of the driving cycle, that improve the internal energy of the powertrain system.

In addition, comparable fuel consumptions with respect to the simple-hybrid strategy are obtained only with no full-electric speed limitations and with low

engine resistant torque. This is because, to be effective, the full-hybrid strategy has to use more electrical energy, stored by the regenerative braking and braking the engine, than the simple-hybrid. For this reason, there is a bigger energy flow to and from the battery through the hybrid powertrain and it means bigger dissipation, both of the electrical components and the engine due to its resistant torque.
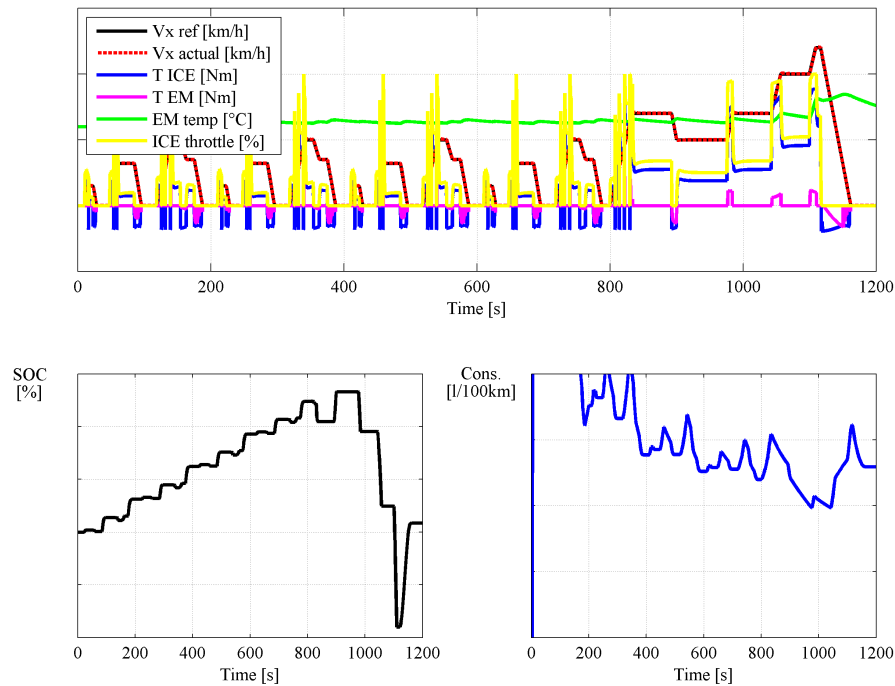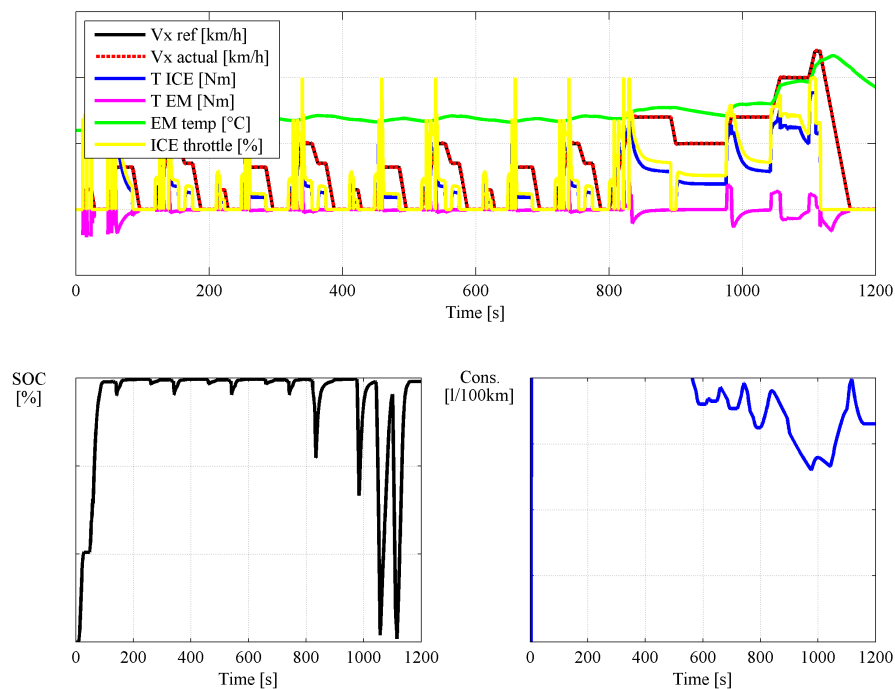

Figure 3.7.10: Full hybrid results on the NEDC with no full-electric driving mode. a) Reference (black) and actual (red) vehicle speeds, ICE (blue) and EM (magenta) torques, EM temperature (green) and ICE throttle command (yellow). b) Battery state of charge (SOC). c) ICE average fuel consumption: the average fuel consumption on the whole NEDC driving cycle is calculated at the end of the cycle.

3.7.5 Effects of the thermal behavior of the electric motor and the environment temperature on the NEDC

As reported in paragraph 3.5, at this early phase of the project, a limited amount of electric motor data were available, just the maximum nominal power $P_{EM} = \quad kW$ and a static efficiency map in function of the angular speed and the torque. The electric motor thermal resistance (R_{th}) and time constant (τ_{th}), parameters of the single degree of freedom thermal model of equation 2.3.9, were initially estimated from the known ETEL TMK 0175-050 electric motor (table 2.6.1), previously used

for the full-electric vehicle project, because its similar size. From equation 2.3.9, the motor temperature becomes:

$$\vartheta = \vartheta_{amb} + R_{th}P_{diss} - \tau_{th}\frac{d\vartheta}{dt} \tag{3.7.6}$$

The motor temperature can be calculated solving the differential equation:

$$\vartheta = (R_{th}P_{diss} + \vartheta_{amb})\left(1 - \frac{R_{th}P_{diss} + \vartheta_{amb} - \vartheta_0}{R_{th}P_{diss} + \vartheta_{amb}}e^{-\frac{t}{\tau_{th}}}\right) \tag{3.7.7}$$

Where ϑ_{amb} is the ambient temperature and ϑ_0 is the initial temperature of the motor. With a step of dissipated power (P_{diss}), an example of the electric motor temperature in time is reported in Figure 3.7.11. Knowing the dissipated power (P_{diss}), due to the efficiency of the electric motor, in steady state condition ($t \to \infty$) the motor temperature is related to its thermal resistance (R_{th}), while the temperature slope in the origin is related to its thermal capacity (R_{th}/τ_{th}), the ambient (ϑ_{amb}) and the initial (ϑ_0) temperatures:

$$\begin{cases} \vartheta|_{t\to\infty} = & R_{th}P_{diss} + \vartheta_{amb} \\ \frac{d\vartheta}{dt}|_{t=0} = & \frac{R_{th}P_{diss}+\vartheta_{amb}-\vartheta_0}{\tau_{th}} \end{cases} \tag{3.7.8}$$

With $\vartheta_0 = \vartheta_{amb}$, the slope in the origin is simply related to the thermal capacity of the motor (R_{th}/τ_{th}).
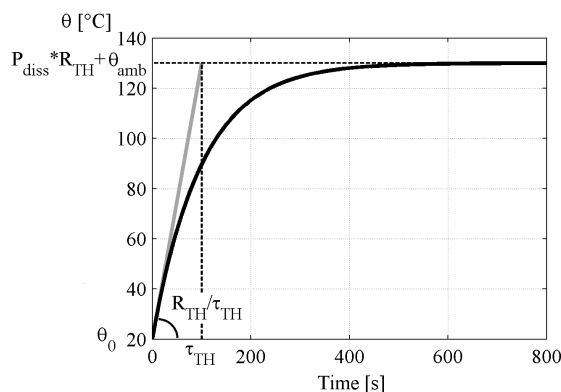
Figure 3.7.11: Example of thermal response of the ETEL TMK 0175-050 electric motor (Table 2.6.1) with a constant dissipated power P_{diss}=1711 W (solid line). The ratio R_{th}/τ_{th} determines the slope of the temperature curve in the origin. The initial temperature of the motor $\vartheta_0 = 20°C$ and the ambient temperature $\vartheta_{amb} = 20°C$.

A sensitivity analysis of the effectiveness of the torque-split strategies can be carried out varying the thermal resistance and the thermal capacity of the electric

motor. This is important to understand the influence of the thermal characteristics of the electric motor to the effectiveness of the strategies, particularly in the early phase of the project when the electric motor characteristics are still not precisely defined. It is possible to vary, with respect to the ETEL TMK 0175-050 reference values:

- The thermal capacity R_{th}/τ_{th} of the motor maintaining constant the thermal resistance R_{th} of the ETEL, varying only the thermal time constant τ_{th}. The effects are reported in Figure 3.7.12 (a).

- The thermal resistance R_{th} maintaining constant the thermal capacity R_{th}/τ_{th} of the ETEL. Therefore it is necessary to vary the thermal time constant at the same time $\tau_{th} = \frac{\tau_{th\,ETEL}}{R_{th\,ETEL}} R_{th}$. The effects are reported in Figure 3.7.12 (b).
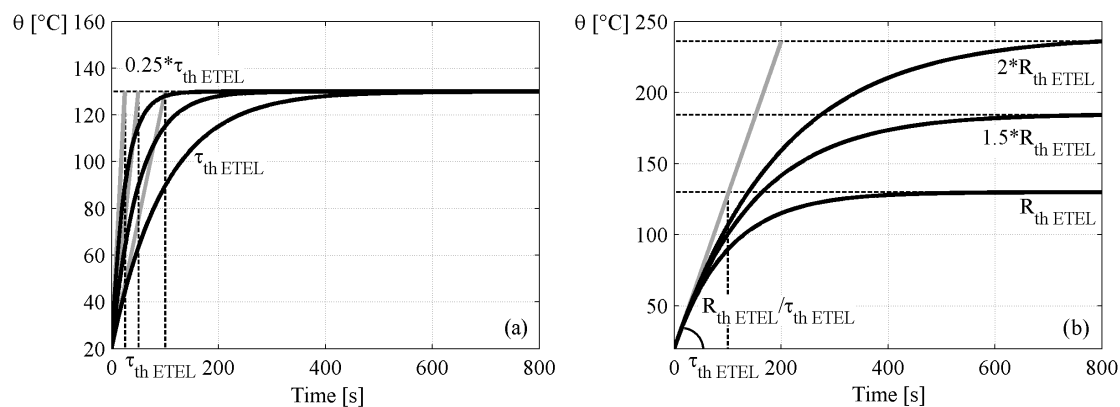
Figure 3.7.12: Example of thermal response of the ETEL TMK 0175-050 electric motor (Table 2.6.1) with a constant dissipated power P_{diss}=1711 W (solid line), varying the ratio R_{th}/τ_{th} (a) and the thermal resistance R_{th}. The initial temperature of the motor $\vartheta_0 = 20°C$ and the ambient temperature $\vartheta_{amb} = 20°C$.

The thermal capacity of the electric motor R_{th}/τ_{th} is modified varying the thermal time constant τ_{th} and maintaining the thermal resistance $R_{th} = R_{th\,ETEL}$. A reasonable under-hood ambient temperature $\vartheta_{amb} = 60\,°C$ is considered.

The fuel consumption variation with respect to the pure-ICE driving mode, reported in Figure 3.7.13 (a), is almost constant in all cases. This is because, reducing the time constant, the electric motor temperature grows more rapidly (Figure 3.7.13 (c)) but the temperature does not reach the maximum tolerable by the electric motor (130°C). For this reason, both the full-hybrid and the simple-hybrid strategies work without limitations, also in the worst case with the thermal capacity of the motor reduced to just   % of the ETEL reference value.

An increase of the thermal resistance R_{th} (Figure 3.7.13 b-d), leads to a decrease of the thermal exchange coefficient of the electric motor toward the environment, increasing the steady-state temperature of the motor. The full-hybrid strategy is more influenced, while on the simple-hybrid no effects are visible in fuel consumptions (Figure 3.7.13 (b)). With the full-hybrid strategy, if the thermal resistance is doubled with respect to the ETEL, the maximum temperature of the electric motor reaches the limit temperature of 130°C, the fuzzy-logic reduces the motor driving current and the strategy reduces its effectiveness. Instead, with the simple-hybrid strategy, the temperature remains in any case lower than the limit. For this reason the strategy is not limited and the fuel consumptions remains constant.
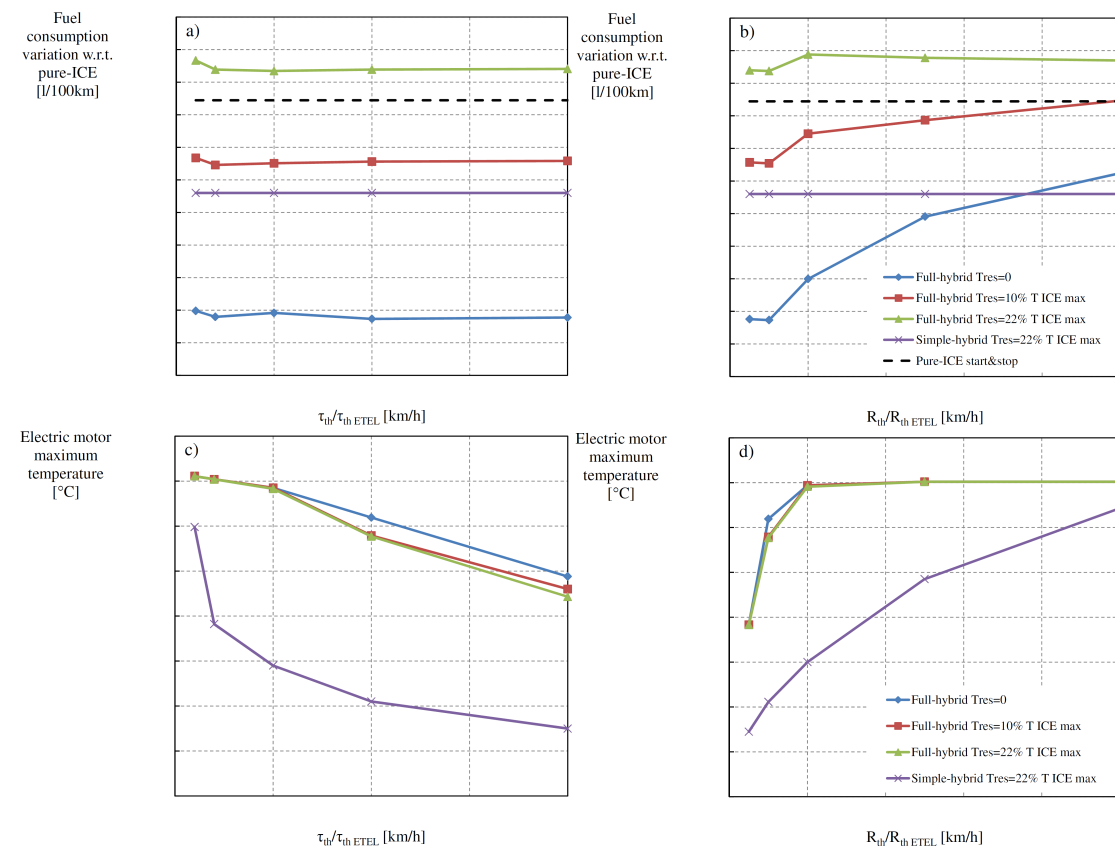
Figure 3.7.13: Effects of the electric motor thermal resistance R_{th} variation, with respect to the ETEL TMK 0175-050, on the fuel consumption (a) and on the maximum electric motor temperature (c). The same effects are reported in function of the thermal capacity R_{th}/τ_{th} variations (b-d). The driving cycle is the NEDC, the initial temperature of the motor $\vartheta_0 = 60°C$ and the ambient temperature $\vartheta_{amb} = 60°C$.

In Figure 3.7.14 are reported the results on the NEDC of the full-hybrid (a) and simple-hybrid (b). In the latter case, the electric motor temperature (green line) grows slower and reaches a lower maximum temperature. Therefore, from the thermal point of view, the simple-hybrid strategy is more robust and it can be effective also using a smaller and less cooled electric motor.

The under-hood ambient temperature can influence the electric motor performance, therefore the effectiveness of the torque-split strategies too. In addition, due to the air temperature, the sun radiation on the vehicle and the presence of the traditional internal combustion engine, the under-hood temperature can grow up significantly, up to 80°C and more, in the worst cases. Since the maximum possible motor temperature is $T_{EM\,max} = 130$°C and the limitations due to the fuzzy-logic (Figure 3.6.3 (c)) start to limit the motor driving current when the motor temperature exceeds 110°C, an increase of the ambient temperature can reasonably limit the possible usage of the electric motor.
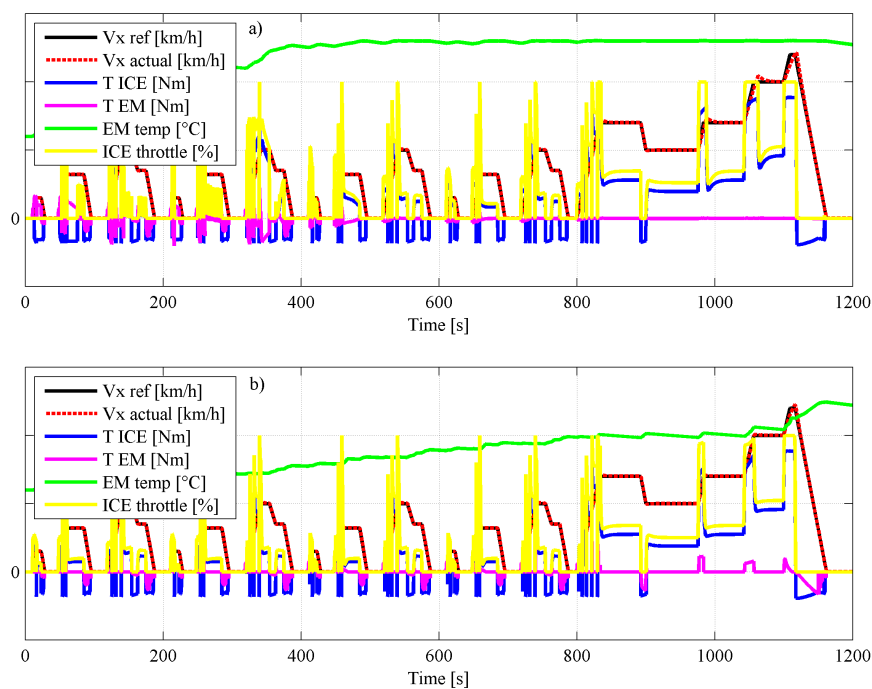
Figure 3.7.14: Full-hybrid (a) and simple-hybrid (b) results on the NEDC with $R_{th} = 10 \cdot R_{th\,ETEL}$ and the engine resistant torque $T_{ICE\,res} = 22\% \, T_{ICE\,max}$. Reference (black) and actual (red) vehicle speeds, ICE (blue) and EM (magenta) torques, EM temperature (green) and ICE throttle command (yellow).

As predictable from the sensitivity analysis of the electric motor thermal characteristics, the maximum motor temperature in function of the ambient tempera-

ture using the simple-hybrid strategy is generally lower than using the full-hybrid strategy, as shown in Figure 3.7.15 (b). For this reason, with the simple-hybrid strategy, the limitations start acting at an higher ambient temperature and the strategy is more effective and less influenced by the environment conditions. Simulations where made until an ambient temperature $T_{amb} = 140$°C, with a maximum possible motor temperature $T_{EM\,max} = 130$°C. When $T_{amb} \geq T_{EM\,max}$, the limitations are always active and the motor cannot be used. For this reason, both the strategies converge to the pure-ICE mode with start&stop.
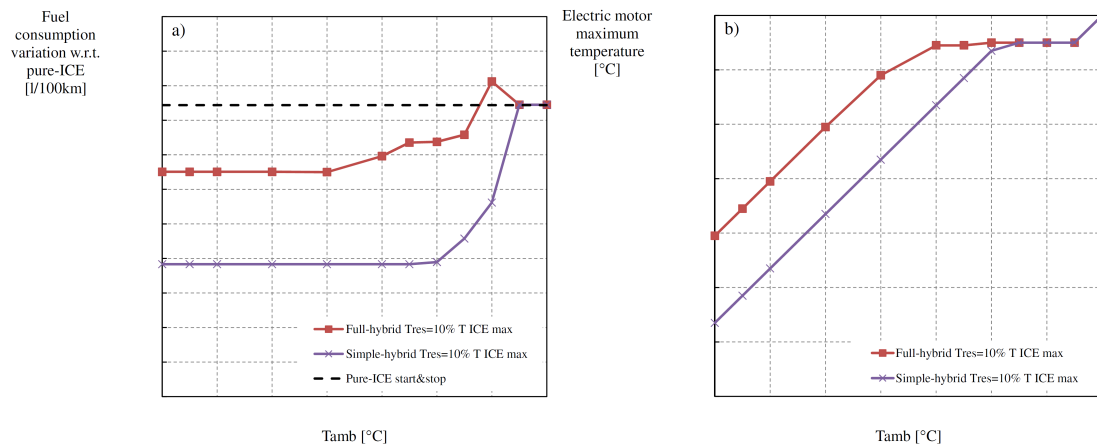
Figure 3.7.15: Effects of the ambient temperature on the fuel consumption (a) and on the maximum electric motor temperature (b). The full-hybrid (red), simple-hybrid (violet) and the reference fuel consumption of the pure-ICE with start&stop (black dotted) are reported. The driving cycle is the NEDC, the engine resistant torque is $T_{res} = 10\%\,T_{ICE\,max}$ and the ETEL TMK 0175-050 electric motor thermal parameters (R_{th} and τ_{th}) are considered.

3.7.6 Effects of the control strategies on different driving cycles

The reference driving cycle generally used for fuel consumption evaluation and vehicle homologation is the NEDC. But also other driving cycles are commonly used to evaluate the vehicle performance and efficiency in a more reliable and robust way, in order to explore a wider range of different vehicle usage. The fuel consumptions with the different torque-split strategies are evaluated on the commonly used driving cycles (described in Figure 2.5.1 and in Table 2.5.1):

- ECE: also known as Urban Driving Cycle (UDC), it is the first urban part of the New European Driving cycle (NEDC)

- New York City Cycle (NYCC)

- FTP75

- JPN15
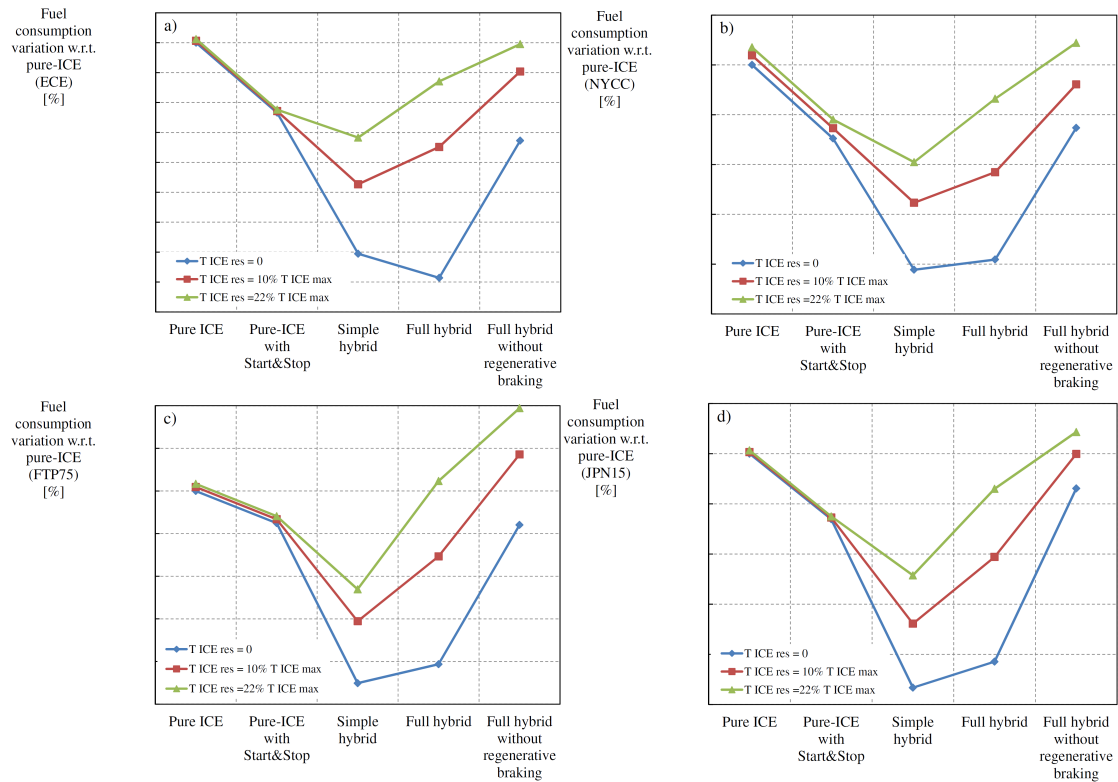
Figure 3.7.16: ICE fuel consumption percentage difference with respect to the pure-ICE driving mode, on ECE (a) NYCC (b) FTP75 (c) JPN15 (d) driving cycles. With ICE resistant torques in over-running mode $T_{res} = 0$ (blue), $T_{res} = 10\% T_{ICEmax}$ (red), $T_{res} = 22\% T_{ICEmax}$ (green), the initial temperature of the motor $\vartheta_0 = 60°$C and the ambient temperature $\vartheta_{amb} = 60°$C.

The percentage variation of the fuel consumption, with respect to the pure-ICE driving mode, are reported for each driving cycle in Figure 3.7.16 and the average fuel consumption in Figure 3.7.17. The results are really similar to the NEDC, both observing each driving cycle and the average values. Especially on the ECE and NYCC the reduction is almost   % considering the best condition, without the engine resistant torque in over-running mode. On the ECE, a cycle with very low average speed and accelerations, the full-hybrid strategy minimizes the consumption but just without engine resistant torque. This is because the low

accelerations and speed lead the engine to very low efficiency working points, also in the constant speed zones, and the full-hybrid strategy can improve the engine efficiency. In fact, the ICE average efficiency in pure-ICE is ___ % and using the full-hybrid strategy it increase to ___ %. It is effective when the engine efficiency improvement allows an energy saving bigger than the additional dissipation within the components of the hybrid powertrain. But this feature is strongly influenced by the engine resistant torque, because is generates additional energy dissipation within the hybrid powertrain.

But globally, with the considered components, the simple-hybrid strategy is the more robust, determines the lowest fuel consumptions, and is less influenced by the engine resistant torque. The presented method can be used for the analysis and optimization of each powertrain configuration, but the choice of the best strategy (for example between the simple and the full hybrid) is strongly influenced by each component of the hybrid powertrain, especially by the engine efficiency map. With a bigger or less efficient engine, it could be possible that the advantage in maximizing its efficiency becomes bigger than the additional dissipation with respect to the simple-hybrid.

Considering the average variations (Figure 3.7.17), with the simple-hybrid strategy a reduction of ___ % can be obtained with the maximum engine resistant torque, that represents a reasonable resistant torque for a modern gasoline engine. But without that resistance, a reduction of about ___ % can be reached, with the same components of the hybrid powertrain but, for example, connecting the electric motor not with the ICE crankshaft but downstream of the clutch, directly to the primary or secondary shaft of the gearbox.
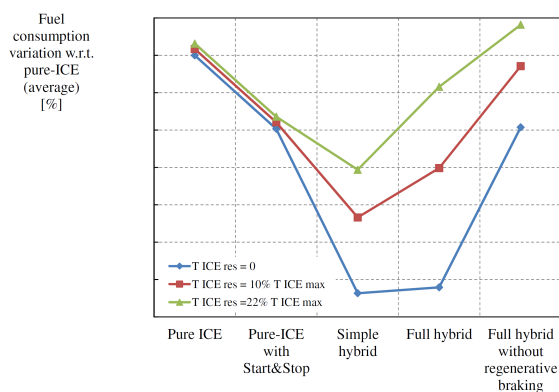
Figure 3.7.17: ICE fuel consumption average percentage difference with respect to the pure-ICE on the ECE, NYCC, FTP75, JPN15. With ICE resistant torques in over-running mode $T_{res} = 0$ (blue), $T_{res} = 10\% \, T_{ICE\,max}$ (red), $T_{res} = 22\% \, T_{ICE\,max}$ (green), the initial temperature of the motor $\vartheta_0 = 60$°C and the ambient temperature $\vartheta_{amb} = 60$°C.

3. Modeling and Torque-split strategies for a sustainable city hybrid vehicle

Both the simple-hybrid and full-hybrid strategies have the regenerative braking and this is the most important feature in urban context, due to the frequent start and stop maneuvers. It allows a huge energy saving because otherwise the kinetic energy of the vehicle would be dissipated with the traditional passive brakes during the frequent start and stop manuevers.

The effectiveness of the regenerative braking decreases in extra-urban context, when the average speed increases and the accelerations and decelerations are less frequent. In this condition, a relevant amount of energy is dissipated by the dissipative forces like aerodynamic and rolling resistance instead by the passive brakes. This is the reason why, using the simple-hybrid strategy, a   % consumption reduction can be obtained on the ECE (Figure 3.7.16 (a)) and only   % on the NEDC, both without the engine resistant torque. The same trend can be observed with $T_{res} = 22\% \, T_{ICE\,max}$ with a reduction of   % and   % respectively.

Chapter 4

Conclusions

4.1 Full-electric vehicle

The study of an electric powertrain composed by two or more electric motors connected in parallel on the same shaft is performed in the present thesis to understand the potentialities in terms of energy consumption in urban cycles. Since the efficiency map of an electric motor is characterized by a maximum in the high power - speed region, the potential advantage of this configuration is to improve the efficiency of the powertrain by exploiting first one motor and to add the contribution of the second one only when necessary, instead of installing a single electric machine of equivalent size. The study is performed considering urban cycles. They could benefit of this solution because of the highly variable speed and torque request that characterizes them. Additional requests, such as hill start/traveling capabilities and max speed/acceleration, are also included in the mission profile in order to guarantee a minimum functionality to the vehicle.

The study is based on a physical model including the longitudinal vehicle dynamics and that of the electric powertrain. The high impact of the thermal aspects on the electric motor performance justifies the adoption of a model including copper, iron, bearings and winding losses. This model is coupled to the thermodynamic equations of the motor to determine its temperature during operation and adapt its parameters. The usual approach based on efficiency maps given at steady state or in peak transient conditions is then overcome by the adopted approach.

The thermodynamic model of the motor allows to control it limiting the current request with a temperature driven logic, to preserve the motor health. The power is limited in this way by the thermodynamic behavior and not by an explicit limitation to the instantaneous torque request as presented in the literature.

The vehicle and powertrain model is used to evaluate powertrains with different combinations of electric motors and control strategies (torque split strategy). The

transmission ratio between electric motors and driving wheels has been optimized for each configuration to minimize the energy consumption, taking into account the hill start/traveling and maximum speed constraints.

Results show that the use of two smaller motors, instead of a bigger one, does not lead to an energy saving, at least with the torque split strategy that saturates a motor first before activating the other.

The reason is the higher temperature of the saturated motor induces higher copper losses. Although exploited in a region of lower efficiency than the smaller one (if compared at same temperature), the bigger motor is much cooler, this leads to less copper losses and a larger overall efficiency on the driving cycle. A more efficient cooling system of the motors, similar of that used on traditional ICE vehicles, could be adopted to improve the performance of the motors.

4.2 Hybrid vehicle

In the second part of the present thesis, a simulation model of an urban Hybrid Electric Vehicle (HEV) was build and validated and an analysis of its potentialities in terms of fuel consumption reduction are presented, based on the simulation results. The idea was to understand the potentialities of an hybrid vehicle, minimizing the amount of modifications and costs for the hybridization of the related traditional pure-ICE vehicle. For this purpose, the traditional alternator was substituted with an electric motor/alternator, coupled in parallel to the engine crankshaft by means of a simple belt transmission and avoiding any other modification. On the other hand, in case of full-electric driving mode, the motor and the engine cannot be decoupled and the electric motor have to drive the engine in over-running mode in addition to the vehicle, dissipating energy.

Different torque-split strategies, using an electric motor in parallel to a traditional combustion engine are implemented. Then, the fuel consumptions of the vehicle, running on the most commonly used driving cycles, are compared to evaluate the the effectiveness of the strategies and the effects of the most important parameters on the fuel consumptions. At each time step of the simulations, the strategies take into account both the maximum performance and the efficiencies of each component of the hybrid powertrain, to maximize the powertrain efficiency and to guarantee the feasibility of the optimization. Particularly, the electric motor limitations due to the motor and battery temperature and state of charge are always taken into account. In addition, all the efficiencies and energy dissipation of every hybrid component are considered to evaluate the global efficiency of the vehicle.

Different torque-split strategies are implemented and compared to evaluate the potential fuel consumption reduction with respect to the traditional pure-ICE

vehicle. At the beginning, a simple start&stop strategy was implemented, to save energy shutting down the engine during idle phases. Successively, a regenerative braking (to recharge the battery by means of the electric motor braking torque) and a full-electric start of the vehicle at low speed were added, leading to a simple-hybrid strategy. The more complex full-hybrid strategy was obtained with a further addition of a "maximum ICE efficiency" strategy, to maximize the ICE efficiency by means of a braking or accelerating torque from the electric motor. To evaluate the importance of the regenerative braking, also a full-hybrid strategy without the regenerative braking was considered.

The effects of the engine resistant torque in over-running mode, the full-electric start at low speed, the regenerative braking and the thermal characteristic of the electric motor and ambient temperature were evaluated with each strategy, because the "best" one should minimize the fuel consumption but, at the same time, to be robust with respect to that parameters.

An average   % fuel consumption reduction can be obtained using the simple start&stop strategy. Experimentally, a reduction of about   -   % was measured and the difference is due to the additional fuel consumption needed for each engine restart, not implemented within the model due to a lack of experimental data at this early phase of the project.

The simple-hybrid strategy showed a minimization of the fuel consumption almost on each driving cycles, especially on the urban ones, and the best robustness with respect to every parameters (engine resistant torque and thermal behavior of the electric motor and ambient temperature). Instead, the full-hybrid strategy showed good performances in terms of fuel consumption only without the engine resistant torque and a bigger sensitivity to the thermal parameters and the engine resistant torque. This is due to the bigger energy flow between the engine and the battery through the electric motor, causing bigger energy dissipation. If the increase of the engine efficiency is not big enough to compensate the additional dissipation within the hybrid components, the global fuel consumption grows up, with respect to the simple-hybrid. Furthermore, on the NEDC the vehicle accelerations are low and to improve the engine efficiency a braking torque of the electric motor is needed, because generally the ICE have good efficiency not so far from the full-throttle zone. Therefore, a lot of electrical energy is generated by the electric motor and it must be used driving the vehicle in full-electric mode. But with high engine resistant torques, a relevant part of the electric energy is dissipated into the engine. Instead, with the simple-hybrid, the energy flow into the hybrid components is small (and the energy dissipation too) and the electrical energy is generated only during the regenerative braking, that otherwise would be dissipated with the passive brakes.

As expected, an increase of the engine resistant torque generally reduces the

advantage of having a regenerative braking because part of the braking force is generated by the engine instead by the electric motor.

The full-electric start at low speed is very important to reduce the fuel consumption because the regenerated energy must be used to move the vehicle, reducing the fuel consumption. Also in this case, with every strategy, a decrease of the engine resistant torque leads to a fuel consumption reduction and the most influenced strategy is the full-hybrid, as expectable.

The full-hybrid without regenerative braking is generally not effective and its maximum advantage is similar to the pure-ICE with start&stop. This is a further indicator of the importance of the regenerative braking, especially on urban driving cycles.

Finally, the simple hybrid strategy is almost not influenced by a variation of the thermal characteristics of the electric motor, within reasonable ranges. This is because the electric motor is used just for full-electric start and regenerative braking, normally with a small duty cycle. Instead, with the full-hybrid strategy, the motor is continuously running, braking the engine and driving the vehicle in full-electric mode to use the produced electrical energy. This leads to a bigger energy dissipation and a bigger increase of the electric motor temperature. If the thermal characteristics of the motor deteriorates, or the ambient temperature increase, it is easy to reach the maximum allowable temperature of the motor, reducing the effectiveness of the strategy.

With the analyzed vehicle configuration, the simple-hybrid strategy is with no doubts the best one, joining the minimization of the fuel consumption on each driving cycle and the robustness with respect to the thermal parameters and the engine resistant torque. The difference with the full-hybrid grows when the engine resistant torque increase, but the difference is very small without the engine resistant torque, with a small advantage of the full-hybrid on the ECE driving cycle.

The best configuration could be obtained coupling the electric motor directly to the gearbox, downstream of the clutch. With this solution, the engine resistant torque could be canceled simply disengaging the clutch and it can double the percentage fuel consumption reduction on the NEDC with the simple-hybrid (from about   % to   %) and more with the full-hybrid strategy (from   % to   %). But of course it requires bigger modifications and higher costs with respect to the traditional pure-ICE vehicle. On the urban driving cycle like the ECE or NYCC, the advantage can be even greater, from   % to   % for the simple-hybrid and from   % to   % for the full-hybrid.

On the other hand, the effectiveness of the simple-hybrid or the full-hybrid strategies are strongly related to the characteristics of each component of the hybrid powertrain, particularly their efficiency. The analyzed vehicle used a small

and high efficiency internal combustion engine, optimized for the urban context and with a high efficiency in a wide range of working conditions. It is possible that, with another engine, the efficiency improvement from the pure-ICE to the full-hybrid strategy can be higher than   % (Figure 3.7.2). Furthermore, the advantages are strongly related to the efficiency of the electrical components too (motor, battery, power electronics). For this reasons, the presented method can be generally used but the choice of the "best" strategy between the simple and the full-hybrid is strongly related to the specific components used into the analyzed hybrid powertrain.

Bibliography

[1] J.Fuglestvedt, T.Berntsen, G.Myhre, K.Rypdal, R.B.Skeie – "Climate Forcing from the Transport Sectors" – Proceedings of the National Academy of Sciences of the United States of America – October 2007

[2] ISTAT – "I Trasporti su Strada e l'Ambiente" – Argomenti n. 20, Roma, Italia – 2001

[3] J.Van Mierlo, G.Maggetto – "Vehicle Simulation Programme" – Presented at Autotech, I Mech E, Birmingham, GB, 1995. [conference paper]

[4] J.Van Mierlo, G.Maggetto – "Multiple Purpose Simulation Programme for Electric and Hybrid Vehicles: Simulation vs. Experimental Results" – Presented EVS 13, Osaka, Japan, 1996. [conference paper]

[5] K.L.Butler, M.Ehsani, P.Kamath – "A Matlab-Based Modeling and Simulation Package for Electric and Hybrid Electric Vehicle Design" – IEEE Transaction on Vehicular Technology, Vol. 48, No. 6 – November 1999

[6] R.Fellini, N.Michelena, P.Papalambros, M.Sasena – "Optimal Design of Automotive Hybrid Powertrain Systems" – Environmentally Conscious Design and Inverse Manufacturing, Proceedings EcoDesign '99: First International Symposium On – 1999

[7] M.A.Kromer and J.B.Heywood – "Electric Powertrains: Opportunities and Challenges in the U.S. Light-Duty Vehicle Fleet" - LFEE 2007-03 RP – May 2007

[8] T.Markel, A.Brooker, T.Hendricks, V.Johnson, K.Kelly, B.Kramer, M.O'Keefe, S.Sprik, K.Wipke – "ADVISOR: a systems analysis tool for advanced vehicle modeling" – Journal of Power Sources, Vol.110, p. 255-266 – 2002

[9] C.Lin, Z.Filipi, Y.Wang, L.Louca, H.Peng, D.Assanis, J.Stein – "Integrated, Feed-Forward Hybrid Electric Vehicle Simulation in SIMULINK and its Use for Power Management Studies" – SAE Paper 2001-01-1334

[10] J.Van Mierlo, G.Maggetto – "Innovative iteration algorithm for a vehicle simulation program" - IEEE Transaction on Vehicular Technology, Vol. 53, No. 2 – March 2004

[11] J. Van Mierlo, P.Van den Bossche, G.Maggetto – "Models of energy sources for EV and HEV: fuel cells, batteries, ultracapacitors, flywheels and engine-generators" – Journal of Power Sources, Vol.128, p. 76-89 – 2004

[12] G.Rizzoni, L.Guzzella, B.M.Baumann – "Unified modeling of hybrid electric vehicle drivetrains" – IEEE/ASME Transaction on Mechatronics, Vol. 4, No. 3 – September 1999

[13] B.M.Baumann, G.Washington, B.C.Glenn, G.Rizzoni, – "Mechatronic design and control of hybrid electric vehicles" – IEEE/ASME Transaction on Mechatronics, Vol. 5, No. 1 – March 2000

[14] C.Musardo, G.Rizzoni, B.Staccia – "A-ECMS: An Adaptive Algorithm for Hybrid Electric Vehicle Energy Management" – Proceedings of the 44th IEEE Conference on Decision and Control, Seville, Spain – 12-15 December 2005

[15] B.N. Chaudhari, B.G. Fernandes – "Equivalent circuit of single phase permanent magnet synchronous motor" – Proceedings of the IEEE Power Engineering Winter Meeting, Columbus, OH, USA - 28 Jan - 01 Feb 2001.

[16] G.V.Fracastoro – "Fondamenti ed applicazioni di termodinamica" – Otto editore, Piazza Vittorio Veneto 14, 10100 Torino – December 2000

[17] G.Genta, L.Morello – "The Automotive Chassis" – Springer – 2009

[18] N.Jalil, N.A.Kheir, M.Salman – "A Rule-Based Energy Management Strategy for a Series Hybrid Vehicle" – Proceedings of the American Control Conference, Albuquerque – June 1997

[19] V.H.Johnson, K.B.Wipke, D.J.Rausen – "HEV Control Strategy for Real-Time Optimization of Fuel Economy and Emissions" – SAE Transaction – 2000

[20] M.Salman, N.J.Schouten, N.A.Kheir – "Control Strategies for Parallel Hybrid Vehicles" – Proceedings of the American Control Conference, Chicago – June 2000

[21] C.C.Chan – "The State of the Art of Electric and Hybrid Vehicles" – Proceedings of the IEEE, Vol. 90 – Feb 2002

[22] K.T.Chau, Y.S.Wong – "Overview of Power Management in Hybrid Electric Vehicles" – Elsevier, Energy conversion and Management, Vol. 43, pp. 1953-1968 – 2002

[23] A.Sciarretta, M.Back, L.Guzzella – "Optimal Control of Parallel Hybrid Electric Vehicles" – IEEE Transactions on Control System Technology, Vol. 12, n.3 – May 2004

[24] Y.Zhu, Y.Chen, G.Tian, H.Wu, Q.Chen – "A Four-Step Method to Design an Energy Management Strategy for Hybrid vehicles" – Proceedings of the 2004 American Control Conference, Boston – 2004

[25] R.Langari – "Intelligent Energy Management Agent for a Parallel Hybrid Vehicle" – IEEE Transactions on Vehicular Technology, Vol. 54, n. 3 – May 2005

[26] C.Musardo, G.Rizzoni, B.Staccia – "A-ECMS: An Adaptive Algorithm for Hybrid Electric Vehicle Energy Management" – Proceedings of the 44th IEEE Conference on Decision and Control and the European Control Conference, Seville, Spain – December 2005

[27] J.Liu, H.Peng – "Control Optimization for a Power-Split Hybrid Vehicle" – Proceedings of the 2006 American Control Conference, Minneapolis, Minnesota, USA – June 2006

[28] P.Pisu, G.Rizzoni – "A Comparative Study Of Supervisory Control Strategies for Hybrid Electric Vehicles" – IEEE Transactions on Control System Technology, Vol. 15, n.3 – May 2007

[29] A.Sciarretta, L.Guzzella – "Control of Hybrid and Electric Vehicles" – IEEE Control Systems Magazine – April 2007

[30] J.Liu, H.Peng – "Modeling and Control of a Power-Split Hybrid Vehicle" – IEEE Transactions on Control System Technology, Vol. 16, n.6 – November 2008

[31] K.C.Bayindir, M.A.Gözükücük, A.Teke – "A Comprehensive Overview of Hybrid Electric Vehicle: Powertrain Configurations, Powertrain Control Techniques and Electronic Control Units" – Elsevier, Energy Conversion and Management, Vol. 52, pp. 1305-1313 – 2011

[32] H.L.Chan, D.Sutanto – "A New Battery Model for use with Battery Energy Storage Systems and Electriv Vehicles Power Systems" – IEEE Power Engineering Society Winter Meeting – 2000

[33] V.H.Johnson – "Battery performance model in ADVISOR" – Journal of Power Sources, Vol. 110, pp. 321-329 – 2002

[34] A.A.Pesaran – "Battery thermal models for hybrid vehicle simulations" – Journal of Power Sources, Vol. 110, pp. 377-382 – 2002

[35] O.Tremblay, L.A.Dessaint, A.I.Dekkiche – "A Generic Battery Model for the Dynamic Simulation of Hybrid Electric Vehicles" – IEEE Vehicle Power and Propulsion Conference – Arlington, TX, 9-12 September 2007

[36] R.C.Kroeze, P.T.Krein – "Electrical Battery Model for Use in Dynamic Electric Vehicle Simulations" – IEEE Power Electronics Specialists Conference – Rhodes, 15-19 June 2008

[37] G.Genta, L.Morello – "The Automotive Chassis" – Springer – 2009

[38] H.B.Pacejka – "Tyre and Vehicle Dynamics" – BH Elsevier – Second edition 2006

[39] A.Emadi, K.Rajashekara, S.Williamson, S.Lukic – "Topological Overview of Hybrid Electric and Fuel Cell Vehicular Power System Architectures and Configurations" – IEEE Transactions on Vehicular Technology, Vol. 54, n.3 – May 2005

[40] C.C.Chan, Y.S.Wong, A.Bouscayrol, K.Chen – "Powering Sustainable Mobility: Roadmaps of Electric, Hybrid and Fuel Cell Vehicles" – Proceedings of the IEEE, Vol. 97, n.4 – April 2009

[41] K.C.Bayindir, M.A.Gözükücük, A.Teke – "A comprehensive overview of hybrid electric vehicle: Powertrain configurations, powertrain control techniques and electronic control units" – Energy Conversion and Management, Vol. 52, pp. 1305-1313 – 2011

[42] H.D.Lee, S.K.Sul – "Fuzzy-logic-based torque control strategy for parallel-type hybrid electric vehicle" – IEEE Transactions on Industrial Electronics – Vol. 45, n. 4, pp625-632 – 1998.

[43] A.Rajagopalan, G.Washington, G.Rizzoni, Y.Guezennec – "Development of fuzzy logic control and advanced emissions modeling for parallel hybrid vehicles" – NREL report SR-540-32919 – 2003.

[44] HILTech Developments Limited (application notes) vehicle hybrid powertrain architectures; 2006.

[45] A.Emadi – "Handbook of automotive power electronics and motor drives" – Taylor & Francis Inc.; 2005.

[46] K.Jonasson – "Control of hybrid electric vehicles with diesel engines" – PhDthesis, Department of Industrial Electrical Engineering and Automation, Lund University, Lund, Sweden – 2005.

[47] M.Ehsani, Y.Gao, S.Gay, A.Emadi – "Modern electric, hybrid electric, and fuel cell vehicles: fundamentals, theory and design" – CRC Press – 2004.

[48] M. Olszewski – "Evaluation of 2004 Toyota Prius Hybrid Electric Drive System" – U.S. Department of Energy – May 2005